Mining Colocation Patterns and Change Detection in Spatiotemporal Data: A Tensor Factorization Approach

Thesis submitted to

Cochin University of Science and Technology

for the award of the degree of

DOCTOR OF PHILOSOPHY

by

SARITHA.S.

under the supervision of

Dr. G. Santhosh Kumar

DEPARTMENT OF COMPUTER SCIENCE

COCHIN UNIVERSITY OF SCIENCE AND TECHNOLOGY

Cochin - 682 022, INDIA

December 2019

Mining Colocation Patterns and Change Detection in Spatiotemporal Data: A Tensor Factorization Approach

Ph.D Thesis in the field of Spatiotemporal Data Mining

Author
Saritha.S.
Department of Computer Science
Cochin University of Science and Technology
Cochin–682 022, Kerala, India.
sarithas@cusat.ac.in

Supervisor
Dr. G. Santhosh Kumar
Department of Computer Science
Cochin University of Science and Technology
Cochin–682 022, Kerala, India
san@cusat.ac.in

December 2019

Dedicated to

my family

CERTIFICATE

Certified that the work presented in this thesis entitled "**Mining Colocation Patterns and Change Detection in Spatiotemporal Data: A Tensor Factorization Approach**" is a bonafide work done by Ms. Saritha. S, under my guidance in the Department of Computer Science, Cochin University of Science and Technology, in partial fulfilment of the requirements for the Degree of Doctor of Philosophy and has not been included in any other thesis submitted previously for the award of any degree.

Kochi
December 2019

Dr. G. Santhosh Kumar
(Supervising Guide)

DECLARATION

I hereby declare that the work presented in this thesis entitled "**Mining Colocation Patterns and Change Detection in Spatiotemporal Data: A Tensor Factorization Approach**" is based on the original work done by me under the guidance of Dr. G. Santhosh Kumar, Professor, Department of Computer Science, Cochin University of Science and Technology and has not been included in any other thesis submitted previously for the award of any degree.

Kochi
December 2019

Saritha.S.

CERTIFICATE

This is to certify that the relevant corrections and modifications suggested by the audience during the pre-synopsis presentation and recommended by the Doctoral Committee of the candidate have been incorporated in the thesis entitled "**Mining Colocation Patterns and Change Detection in Spatiotemporal Data: A Tensor Factorization Approach**."

Kochi
Decemberr 2019

Dr. G. Santhosh Kumar
(Supervising Guide)

Acknowledgements

The work presented in this thesis would not have been possible without the help and support of a large group of people to whom I owe a lot of gratitude.

First and foremost, I express my reverence and heartfelt gratitude to my teacher and supervising guide, Dr. G. Santhosh Kumar, Professor, Department of Computer Science, Cochin University of Science and Technology, for his relentless support, vision, and exemplary guidance. His enthusiasm, wisdom, knowledge and commitment to the highest standards inspired and motivated me. His tailor-made guidance and inexhaustible patience gave me hope during the tough times of this journey. I sincerely acknowledge and thank him for this inspirational mentorship. I treasure the affluent experience of working with him. His motivational attitude paved the successful completion of my dissertation work.

I also thank Dr. Sumam Mary Idicula, Professor, Department of Computer Science, Cochin University of Science and Technology, for her valuable suggestions, and positive thoughts. I express my profound thanks to Dr. Philip Samuel, Professor, Department of Computer Science, Cochin University of Science and Technology and Dr. Madhu S. Nair, Associate Professor, Department of Computer Science, Cochin University of Science and Technology for their for the meaningful interactions during the research phase. I also thank other faculty members and non-teaching staff in the department for their support and cooperation throughout the work.

I am also really grateful to Dr. Gaurav Sharma, Professor, University of Rochester, New York, USA and Chancellor's Chair Professor, Department of Computer Science, Cochin University of Science and Technology. His positive attitude and constructive research implications have steered my dissertation work in the right course.

On lost moments it is great to have the support and words of wisdom from people who can very quickly understand the problems one facing. I thank my friends for the support they had given me in difficult moments. I thank Dr. Sreeraj M for his valuable technical inputs while addressing some challenging problems in my thesis.

I wish to place a record of gratitude to Dr. A. Unnikrishnan, Former Principal, Rajagiri School of Engineering & Technology for the technical ideas, which acted as a catalyst to my thesis.

I thank all my friends at Rajagiri School of Engineering & Technology for their timely support and encouragement. In particular, I remember, Dr. Preetha K. G., Dr. Sminu Izudheen, Dr. Biju Paul, Mr. Binu A., Ms. Shimmi Asokan, Ms. Mary Priya Sebastian, and Mr. Binu R. on this occasion. A special note of thanks to Mr. Shinto Joseph for the lab facilities and support offered at Rajagiri School of Engineering & Technology.

Sharing the research thoughts is a motivating factor throughout this journey. I thank my fellow research scholars, Mr. Muhammed Anees V., Ms. Kochaleema K. H., Ms. Namitha K. and Ms. Athira K. B. for their understanding.

I thank all my teachers who introduced me to the vast expanse of knowledge, throughout my education. I am also grateful to all my students for their wishes and prayers.

I am also blessed to have the support and prayers from my parents Mr. M. Sasikumar and Mrs. R. Saraswathy. A special thanks to my sister Ms. Sumi S. and her family for their relentless encouragement.

Finally, but most importantly, I would like to thank my husband Mr S. Subramanian and our loving kids S. Sivapratap and S. Sivaprasad for their sacrifices, love, prayers and encouragement, without which, this thesis would not have been possible.

All praise and thanks to God Almighty for all the blessings showered on me from time to time.

Saritha.S.

Abstract

Discovery of knowledge from large volume of data is an active research topic in todays world. Mining of conventional data pose many challenges, which are overcome by the research community to a great extent today. The research has now moved to the mining of spatiotemporal data. Large volumes of spatiotemporal data is being generated in todays world in the domains of earth science, epidemiology, human mobility, climate science, transportation and trajectories. Mining spatiotemporal data is important to many real world applications like environment management, urban planning, health care, human mobility understanding, weather prediction and smart transportation. Space and time are the pervasive aspects of the spatiotemporal data. The spatiotemporal data differs from traditional data in different aspects which creates the challenges as well as opportunities for mining the same. The presence of spatial and temporal attributes provide a rich diversity for the formulation of the different types of spatiotemporal data, which can be exploited for mining patterns.

The research contributions of the thesis work is for spatiotemporal data mining approaches like classification, frequent pattern mining and change detection. A novel set of features, namely intra-spectral features and inter-spectral features are proposed for classifying spatiotemporal data, which performs better in comparison with other features for existing classifiers. The combined feature vector of the proposed features is identified as a good discriminant for remote sensing image classification. The features are appropriately represented and are experimented on various classifiers to establish their discriminating capabilities.

Colocation pattern mining of spatiotemporal data is sought in spatial as well as spatiotemporal context. Tensors are used as the underlying data structure and pattern mining algorithms are proposed on the basis of tensor algebra. Decomposition methods of tensors are exploited to find the spatial colocation patterns. The algorithms proposed to find spatial colocation resulted in scalable computation time and less sensitivity in dense environments. The tensorized modeling of image data eliminated the need to

convert the same to traditional transaction type data. The colocation patterns mined yielded patterns with more significance in terms of containment of the number of objects. An algorithm to mine spatiotemporal colocation patterns is proposed, whose underlying principle is based on Boolean Tensor Factorization. An incremental approach for the Boolean Tensor Factorization is proposed for mining spatiotemporal colocation patterns, which made a considerable save in terms of space. The mined colocation patterns helps in understanding a region in spatiotemporal perspective and can be used for urban facility analysis, as well as, detecting the change patterns of a spatial region. Novel interestingness measures are also defined for the proposed algorithms.

A hierarchical spatiotemporal-metric miner model is proposed to perform change detection of urban landscapes. Landscape metrics are incorporated into the miner to obtain more semantics for the change detection. The change detection model helps to identify changes of a region at different granularities. The changes in a region are quantified using two growth indices, namely, Inter-Class Growth Index and Intra-Class Growth Index. Experiments are performed on Indian cities for analyzing the growth over a temporal tag and the results are found to be promising. The proposed change detection model is also conceptualized into a spatiotemporal ontology. The ontology modeled rules which aided to understand the changes which has happened in a region. The axioms provided more spatiotemporal semantics in terms of morphology, shape and texture analysis of a region.

The algorithms proposed in this thesis contributes to applications like urban facility analysis, planning and management.

Preface

Large volumes of spatiotemporal data in the fields of earth science, epidemiology, human mobility, climate science, transportation and trajectories are being produced in today's world. Space and time are the ubiquitous aspects of the spatiotemporal data. Spatiotemporal data mining is the process of discovering interesting and previously unknown, but potentially useful patterns from large spatiotemporal data sets. Due to the enormous quantity and variety of spatiotemporal data produced in the present scenario, the field of spatiotemporal data mining is gaining momentum. Mining spatiotemporal data is important to many real world applications like urban planning, health care, weather prediction, ecology, environment management and smart transportation.

Spatiotemporal data is primarily complex and embedded in continuous space and time. Classical data mining techniques tend to perform poorly when applied to such data due to the inherent autocorrelation and heterogenity. The presence of spatial and temporal attributes provide a rich diversity for the spatiotemporal data which can be exploited for mining patterns. Hence the coupling of spatial and temporal information in the data introduces novel problems, challenges and opportunities in spatiotemporal data mining, with a broad scope of application in various domains. This formed the motivation for the work presented in this thesis.

There are various types of spatiotemporal data that differs in the way in which they are collected and represented. Conventional machine learning and data mining techniques are limited in their ability to process raw spatiotemporal data. Appropriate and suitable representation of spatiotemporal data has to be evolved before applying the data mining techniques. This thesis finds a novel representation of spatiotemporal data using tensors. Subsequently, tensor factorization method is applied to find patterns from spatiotemporal data.

The thesis, presented in eight chapters' deals with the work carried out in mining spatiotemporal data using the concept of tensor factorization.

Chapter 1 introduces spatiotemporal data mining, discusses the motivation behind

the work, states the research problem, enumerates the objectives of the research work and gives an overview of the structure of the thesis.

Chapter 2 presents a systematic survey on the spatiotemporal data, associated data types, representation techniques and data mining problems addressed in spatiotemporal data mining. The properties of different spatiotemporal data types are studied. Common data mining problems like clustering, frequent pattern mining, prediction and change detection are studied from the perspective of spatiotemporal data. An extensive summary of these studies are finally presented in the chapter.

A novel set of features termed as intra-spectral features and inter-spectral features is proposed in *Chapter 3* for the spatiotemporal raster data. The novel features are appropriately represented and are being fed into different classifiers. Experiments proved that the discriminative capability of the proposed feature is best captured through tensor representation techniques.

Chapter 4 describes a framework for spatial co-location mining using tensor-based approaches. The results of the mining are evaluated in terms of novel interestingness measures called spatial dominance. A detailed analysis of the algorithm against the current state of- the- art is performed on various decisive parameters.

Chapter 5 presents a tensor-based approach to find spatiotemporal colocation patterns in classified images. An algorithm to find change patterns in the time series satellite image data using an incremental approach is also presented. The proposed algorithm is evaluated with the existing ones.

The tensor-based approach for change detection in urban landscapes with the support of landscape metrics is proposed in *Chapter 6*. Growth indices for Indian cities are proposed and evaluated. The semantic growth index proposed in this thesis can become handy for town planning authorities.

The studies conducted in this thesis for change pattern analysis is formalized into a spatiotemporal ontology and is presented in *Chapter 7*. Case studies of Indian cities are analyzed using the proposed ontology.

Chapter 8 recapitulates the thesis and briefs appropriate future directions in this research area.

The results of this thesis are published with international journals and proceedings of the international conferences, whose details are provided.

List of Publications

Papers in International Journals

1. Saritha, S., and G. Santhosh Kumar, *Mining spatial colocations from image-objects: A tensor factorization approach*, Journal of Intelligent & Fuzzy Systems, 37 (5), 6707-6716, 2019, IOS Press.

2. Saritha, S., and G. Santhosh Kumar, *Change detection in urban landscapes: A tensor factorization approach*, Spatial Information Research, 27 (5), 587–600, 2019, Springer.

Papers in International Conferences

1. Saritha.S., and G. Santhosh Kumar, *Change Analysis of Indian Metropolitan Cities through a Spatiotemporal Ontology*, In Int. Conference on Data Science and Engineering, ICDSE, IIT Patna, 2019 (To appear in IEEE Xplore).

2. Saritha, S., and G. Santhosh Kumar, *Spatiotemporal Ontology for Understanding Semantics in Change Patterns of Remote Sensing Images*, In Int. Conference on Innovative Computing and Communications, 307–313, LNNS, Springer, 2019.

3. Saritha, S., and G. Santhosh Kumar, *Analysis of the smart growth of Kochi city through landscape metrics*, IEEE Region 10 Symposium (TENSYMP), Kochi, 2017.

4. Saritha, S., and G. Santhosh Kumar, *Inter-Spectral and Intra-Spectral Features for Effective Classification of Remotely Sensed Images*, Procedia Computer Science 115, 549–555, Elsevier, 2017.

5. Saritha, S., and G. Santhosh Kumar, *A hierarchical framework for the classification of multispectral imagery*, Procedia Computer Science 46, 78–85, Elsevier, 2015.

Contents

List of Publications xvii
List of Figures xxiv
List of Tables xxv
List of Symbols xxvii
List of Abbreviations xxix

1 Introduction **1**
1.1 Overview 1
1.2 Background and Motivation 3
1.3 Problem Statement 5
1.4 Objectives 6
1.5 Contributions of the Thesis 6
1.6 Outline of the Thesis 8

2 Literature Survey **11**
2.1 Introduction 12
2.2 Spatiotemporal Data 13
2.2.1 Properties 14
2.2.2 Data Types 15
2.2.3 Data Instances 19
2.2.4 Data Representations 20
2.3 Spatiotemporal Data Mining Approaches 25
2.3.1 Clustering 25
2.3.2 Predictive Learning 27
2.3.3 Frequent Pattern Mining 28

2.3.4 Anomaly Detection 29
2.3.5 Change Detection 30
2.4 Summary of the Chapter 33

3 Intra-spectral and Inter-spectral Features 35
3.1 Introduction 36
3.2 Related Research 37
3.3 Proposed Features 38
3.4 Results and Discussions 41
3.4.1 Dataset 41
3.4.2 Experiments 42
3.5 Summary of the Chapter 47

4 Spatial Colocation Pattern Mining 49
4.1 Introduction 50
4.2 Related Research 52
4.3 Tensor Model for Pattern Discovery in Image-Objects 53
4.3.1 Tensorization 54
4.3.2 Spatial Pattern Discovery from Tensorized Image-Objects . . . 55
4.4 Spatial Colocation Pattern Mining Framework 57
4.4.1 Pixel Mapping to Image-Objects (PMIO) 58
4.4.2 Spatial Colocation Pattern Mining using Tensor Factorization (SCLP-TF) 60
4.5 Results and Discussions 64
4.5.1 Dataset 64
4.5.2 Experiments 64
4.5.3 Evaluation 66
4.6 Summary of the Chapter 70

5 Spatiotemporal Colocation Pattern Mining 73
5.1 Introduction 74
5.2 Related Research 75
5.3 Spatiotemporal Colocation Pattern Mining Framework 76

5.3.1 Spatiotemporal Colocation Pattern Mining using Boolean Tensor Factorization (STCLP-BTF) . . . 77
5.3.2 Spatiotemporal Colocation Pattern Mining using Incremental Boolean Tensor Factorization (STCLP-ITF) . . . 80
5.4 Results and Discussions . . . 84
5.4.1 Datasets . . . 84
5.4.2 Experiments . . . 84
5.4.3 Evaluation . . . 87
5.5 Summary of the Chapter . . . 93

6 Change Detection in Urban Landscapes 97
6.1 Introduction . . . 98
6.2 Evaluative Study of Landscape Metrics . . . 100
6.2.1 Background on Landscape Metrics . . . 100
6.2.2 Dataset . . . 102
6.2.3 Assessment of Landscape Metrics . . . 104
6.3 Related Research . . . 112
6.4 Design of the Proposed System . . . 112
6.4.1 Tensorization of Image Regions . . . 114
6.4.2 Identification of ROI, TOI and MOI . . . 115
6.4.3 Hierarchical Spatiotemporal-Metric (STM) Miner . . . 115
6.5 Results and Discussions . . . 119
6.5.1 Datasets . . . 119
6.5.2 MOIs associated with Growth Indices . . . 121
6.5.3 Evaluation . . . 124
6.6 Summary of the Chapter . . . 129

7 Spatiotemporal Ontology for Change Detection 133
7.1 Introduction . . . 134
7.2 Related Research . . . 135
7.3 Design and Development of Spatiotemporal Ontology . . . 136
7.3.1 Spatial Information . . . 136
7.3.2 Temporal Information . . . 138
7.3.3 Spatiotemporal Information . . . 138

7.4 Reasoning of Spatiotemporal Ontology 138
7.5 Case Studies 141
7.5.1 Study Area 141
7.5.2 Discussion of results and Contributions 142
7.6 Summary of the Chapter 148

8 Conclusion and Future Perspectives **149**
8.1 Conclusion 149
8.2 Future Perspectives 153

A Satellite Specifications **155**

B Landscape Metrics **157**

C Sampled Indian Cities **159**

References **163**

Index **187**

List of Figures

2.1 Events belonging to three types 16
2.2 Trajectories of three moving bodies 18
2.3 Data types, Data Instances and Data Representation of ST Data 20
2.4 Concepts of Tensors, Fibers and Slices 21
2.5 Matricization of Tensors 23
2.6 Canonical Polyadic Decomposition 25
2.7 Tucker Decomposition 25

3.1 Echoing of (a) Square patch and (b) Rectangular patch in the Sliding window 39
3.2 Intra-spectral Features 40
3.3 Inter-spectral Features 41
3.4 World View-2 Images 42
3.5 ROC Curve for AdaBoost and STM using IASF + IESF 45
3.6 Window Size and Accuracy 48

4.1 Spatial Colocation Mining Framework 58
4.2 Image-Objects from the Dataset after PMIO 65
4.3 Number of SCLP mined vs Number of Image-Objects 68
4.4 Computation Time Vs Size of Images 69

5.1 Optimization of Core Tensor Size 86
5.2 Execution Time as a function of neighbourhood distance threshold for STCLP-BTF 86
5.3 Proportion of class changes over the period of time frame 88

5.4 Overall loss/gain of classes over the period of time frame 88
5.5 Comparison on the effect of time slots on execution time 90
5.6 Comparison of the effect of number of objects on execution time 91
5.7 Reconstruction Error for different Core Tensor Size 92
5.8 Reconstruction Error for different Factor Matrix Densities 94
5.9 Comparison of Convergence Time 95

6.1 Regional Division of Kochi 103
6.2 Mean Patch Size in Different Zones 105
6.3 Comparison of Mean Shape Index and Area Weighted Mean Fractal Dimension 106
6.4 Comparison of Contiguity Index of different zones 108
6.5 Comparison of IJI and Contagion Index 108
6.6 Splitting Index of different zones 110
6.7 SDI and SEI of different zones 111
6.8 Design of Spatiotemporal-Metric Miner 114
6.9 Correlation Matrix of MOIs for Intra-Class Growth Index 123
6.10 Correlation Matrix of MOIs for Inter-Class Growth Index 123
6.11 Growth Indices for Type X cities 125
6.12 Inter-Class Growth Index for top-5 ranked Type Y cities at different TOI 127
6.13 Intra-Class Growth Index for top-5 ranked Type Y cities at different TOI 127
6.14 Comparison of Gini Index for Type Y cities for different TOIs 129
6.15 Comparison of Inter-Class Growth Index, Intra-Class Growth Index and average Gini Index values for Type Y cities for TOIs - 10 years and 7 years 130
6.16 Comparison of Inter-Class Growth Index, Intra-Class Growth Index and average Gini Index values for Type Y cities for TOIs - 5 years and 3 years 131

7.1 Area Weighted Mean Fractal Dimension—Shape Analysis 143
7.2 Contiguity Index—Morphological Analysis 145
7.3 Interspersion and Juxtaposition Index–Texture Analysis 146

List of Tables

2.1 Definition of Tensor Products 24
2.2 Summary of Spatiotemporal Applications, Approaches, and Representation 32

3.1 Accuracy of classifiers for different features 46
3.2 Execution Time in minutes for Feature Extraction, Training and Testing 47

4.1 Sample Spatial Colocation Patterns Mined 66

5.1 Sample Spatiotemporal Colocation Patterns Mined using STCLP-BTF . 87
5.2 Sample Spatiotemporal Colocation Patterns Mined using MDCOP . . . 89

6.1 MOI and their dependencies 116
6.2 Categorization of Indian Cities 120
6.3 MOIs influencing Intra-class Growth Index and Inter-Class Growth Index 124
6.4 Growth Indices - Type Y cities for TOI - 10 years 126

7.1 Object properties, domain and range 137
7.2 SWRL Rules and Inferred Axioms of the Spatiotemporal Ontology . . . 140

List of Symbols

$\mathcal{S}$	:	Spatial Tensor
$\widehat{\mathcal{S}}$	:	Reconstructed Spatial Tensor
W	:	window size
C_j	:	Class label of j^{th} pixel
a_{ir}	:	Spatial colocation pattern
c_{kr}	:	Spatial dominance value
at_{ir}	:	Spatiotemporal colocation pattern
ct_{kr}	:	Spatiotemporal dominance value
t_{CL}	:	Colocation Threshold
t_D	:	Spatial Dominance Threshold
$\mathcal{T}$	:	Spatiotemporal Tensor
$\widehat{\mathcal{T}}$	:	Reconstructed Spatiotemporal Tensor
d_{th}	:	Distance Threshold
st_D	:	Spatiotemporal Dominance Threshold
α	:	Intra-Class Growth Index
β	:	Inter-Class Growth Index
m_i	:	i^{th} metric of interest
$CC(R)$	:	Core Consistency Value of a matrix of R columns
Y_{rref}	:	Reduced Row Echelon of Matrix Y
ROI_α	:	Intra-class Growth Index of region ROI
ROI_β	:	Inter-class Growth Index of region ROI

List of Abbreviations

ALS	:	Alternating Least Squares
BTF	:	Boolean Tensor Factorization
CPD	:	Canonical Polyadic Decomposition
CWED	:	Contrast Weighted Edge Density
EMF	:	Echoed Mean Features
IASF	:	Intra-spectral Features
IESF	:	Inter-spectral Features
IJI	:	Interspersion and Juxtaposition Index
K-NN	:	k Nearest Neighbors
MDCOP	:	Mixed Drove Co-occurrence Pattern
MOI	:	Metrics of Interest
PACOP	:	Partial Spatiotemporal Co-occurrence Pattern
PMIO	:	Pixel Mapping to Image-Objects
RCP	:	Representative Colocation Pattern
ROC	:	Receiver Operating Characteristics
ROI	:	Region of Interest
SCLP-TF	:	Spatial Colocation Pattern using Tensor Factorization
SDI	:	Shannon's Diversity Index
SEI	:	Shannon's Evenness Index
SGCT	:	Sparse Graph Condensed Tree

SOWL	:	Spatiotemporal Ontology Web Language
ST	:	Spatiotemporal
STCLP-BTF	:	Spatiotemporal Colocation Pattern using
	:	Boolean Tensor Factorization
STCLP-ITF	:	Spatiotemporal Colocation Pattern using Incremental
	:	Tensor Factorization
STES	:	Spatiotemporal Event Sequence
STM	:	Support Tensor Machine
STM-Miner	:	Spatiotemporal Metric Miner
STS	:	Spatiotemporal Sequence
SVM	:	Support Vector Machine
SWRL	:	Semantic Web Rule Language
TKD	:	Tucker Decomposition
TOI	:	Time of Interest

Chapter 1

Introduction

1.1 Overview 1
1.2 Background and Motivation 3
1.3 Problem Statement 5
1.4 Objectives 6
1.5 Contributions of the Thesis 6
1.6 Outline of the Thesis 8

1.1 Overview

The prolific growth of spatial and temporal data, as well as the emergence of new sets of applications coupled with technologies, accentuate the need for automated discovery of spatiotemporal knowledge. Spatiotemporal data mining is the process of discovering interesting and previously unknown, but potentially useful patterns from large spatiotemporal data sets [1, 2, 3]. Space and time are pervasive characteristics of observations in many domains. The domains of such type are climate science, social sciences, epidemiology, criminology, neuroscience, transportation, and earth sciences. A shared reflection about these

domains is that the deluge of data rapidly transforms them. The data acquired from these domains are inherently spatiotemporal.

Mining spatiotemporal data is important to many real-world applications like ecology and environment management [4], urban planning [5], health care [6, 7], weather prediction [8], smart transportation [5] and public safety [9]. In ecology and environment management, spatiotemporal data mining helps to discover knowledge about causal relationships in environmental changes, analysis of forest coverage, and tracking of pollution events. Thus a detailed analysis of the earth's surface is possible through mining the data. The study of a region or a city in terms of all entities present at different timestamps will help the concerned authorities to do a detailed planning and monitoring of urban facilities. Detection of disease outbreak is yet another promising area of spatiotemporal data mining. Climatologists also define predictors for various events by mining the climatology data. Spatiotemporal data mining has made its biggest imprint in transportation through traffic monitoring, tracing vehicle crusade, traffic planning, vehicle navigation, and fuel proficient routes. Crime analysts are interested in discovering hotspot patterns in a city, and the government agency can allocate resources to ensure public safety. These application domains also point to the interdisciplinary nature of spatiotemporal data mining.

The reasons for the motivation for choosing spatiotemporal data mining as the research field is described in Section 1.2. This thesis addresses certain research issues associated with the field of spatiotemporal data mining. Section 1.3 states the research problem addressed in this thesis and Section 1.4 enumerates the research objectives. The research contributions are highlighted

in Section 1.5. The outline of the thesis is given in Section 1.6.

1.2 Background and Motivation

The spatiotemporal data differs from relational and transactional data in different aspects, which creates challenges as well as opportunities for mining the same [10]. The significant differences are (i) traditional data mining techniques work on the assumption that the data is independent and identically distributed (i.i.d.), which is not valid for spatiotemporal data as it is highly auto correlated (ii) classical data is in discrete forms like transactions or graphs, whereas spatiotemporal data is embedded in continuous space and (iii) spatial and temporal properties of the data is more complicated than the conventional attributes and is challenging to be feature-engineered as well as to discover patterns. Classical data mining techniques underperform when applied to spatiotemporal data because of the above-said reasons. The presence of spatial and temporal attributes provides a rich diversity for the spatiotemporal data, which can be exploited for mining patterns. Traditional data mining deals with distinct objects having well-defined features. For spatiotemporal data, there are numerous novel ways of formulating objects and features. As an example, for the spatiotemporal data, one way is to model spatial locations as objects and measurements over time to define the features, and another way is to model time points as objects and measurements collected from all the spatial locations to define features. Therefore, the coupling of spatial and temporal information in the data introduces novel problems, challenges, and opportunities in spatiotemporal data mining, with a broad scope of application in various domains.

Various types of spatiotemporal data differ in the way of data collection and representation. Following the literature [10], it is understood that the spatiotemporal data types are (a) event data, (b) trajectory data, (c) point reference data and (d) raster data. Event data consists of discrete events occurring at point locations and times (eg-crime event). Trajectories denote the paths traced by bodies moving in space over time. This data is collected by the sensors deployed in the moving objects that can periodically transmit the location of the object over time (eg- moving route of a taxi). Point reference data consists of measurements of a continuous spatiotemporal field over a set of moving reference points in space and time. The measurement of meteorological data using weather balloons floating in space is an example of point reference data. Raster data is the measurement of the continuous or discrete spatiotemporal field that is recorded at fixed locations in space and at fixed points (eg- satellite images of a fixed location at definite intervals of time). A noticeable advantage associated with the different data types is that it is possible to transform one data type to another.

Conventional machine learning and data mining techniques are limited in their ability to process raw spatiotemporal data. Appropriate and suitable representation of spatiotemporal data has to be evolved before applying the data mining techniques. For the spatiotemporal data types outlined earlier, the common representation techniques seen in the literature are the sequence, graph, matrix and tensor [11, 12, 13]. *Sequences* are the representation techniques used for event and trajectory data to find sequential and frequent patterns associated with the spatiotemporal data. Point reference data generally uses *graph* or *matrix* representation to model data instances. As the raster data started growing

enormously, the n-way arrays called *tensors* are used for data representation. Dimensions of the tensor can be used to represent spatial locations and time stamps available in the spatiotemporal grid of raster data. An emerging theme in spatiotemporal data mining research is of studying novel representations of spatiotemporal data sets.

Another emerging direction in spatiotemporal data mining is the problem of integrating multimodal data along with the spatiotemporal data. Tensors support the presence of n-dimensional multimodal data, which can be incorporated with spatiotemporal data. However, the choice of the representation for constructing spatiotemporal data instances depends on the nature of the problem being addressed and the set of data mining methods available for the same. Spatiotemporal data mining addresses several commonly studied data mining problems like clustering, predictive learning, frequent pattern mining, anomaly detection, change detection, and relationship mining.

The diversity of data types, challenges, opportunities, and the range of evolving applications in which spatiotemporal data is being gathered is increasing. These make spatiotemporal data mining an exemplary fusion for innovative research studies in the field of data mining.

1.3 Problem Statement

The research problem is formally stated as follows.

To design and develop algorithms for colocation pattern mining and semantic change detection through effective representation of spatiotemporal data.

1.4 Objectives

The main objective of the work reported in this thesis is to design and develop algorithms for mining patterns from spatiotemporal data. The mined patterns contain knowledge of spatial and temporal relationships that exist in the data. Due to its inherent complex nature of spatiotemporal data, an appropriate representation technique has to be evolved. The effective data representation technique can be carried forward to the problems of colocation pattern mining and change detection. The patterns mined are to be semantic in nature, for better comphrension. Hence the objectives for this research work is set as follows.

1. To study the existing methodologies for mining spatiotemporal data and comprehend the challenges and opportunities.

2. To feature engineer spatiotemporal data for effective classification.

3. To investigate and evolve an effective representation technique for spatiotemporal data.

4. To mine spatial and spatiotemporal colocation patterns from spatiotemporal data.

5. To perform semantic change detection in spatiotemporal data and develop an ontology that conceptualizes the process.

1.5 Contributions of the Thesis

Significant findings and contributions of the thesis are summarized as follows.

- A novel set of features termed as *intra-spectral features* and *inter-spectral features* is proposed for the spatiotemporal raster data that measure the variance of the pixels in the same spectral channel and different spectral channels for the different patches of the image. The novel features are appropriately represented and are being fed into different classifiers. Experiments proved that the discriminative capability of the proposed features are best captured through tensor representation techniques.

- The concept of tensor algebra has been brought into the spatiotemporal domain. Algorithms are proposed for colocation pattern mining in images. In spatial colocation pattern mining, the algorithm performed better in two aspects, namely (i) containment of the number of image-objects in colocation patterns and (ii) computational time. In spatiotemporal colocation pattern mining, the proposed algorithm follows an incremental approach to accommodate the time series data, in terms of optimal space and time, and also yielded significant colocation patterns. Mined colocation patterns are useful for urban facility analysis.

- A spatiotemporal-metric miner that detects change patterns in urban landscapes at different granularities is proposed in this thesis. The miner integrates the landscape metrics data to the raster data to produce semantic change patterns. The miner computes, a novel set of growth indices, namely, *Intra-Class Growth Index* and *Inter-Class Growth Index* that quantifies the growth or detainment of a region. A ranking of Indian cities in terms of change is proposed based on the growth indices. The contribution is useful to urban planning and management authorities.

- The landscape metrics contributing to change pattern analysis is conceptualized into an ontology. The ontology can perform spatiotemporal reasoning in the form of rules and axioms. The ontology rules report changes that occurred in a region in terms of the class label and associated properties. The axioms provide semantic information in terms of morphology, shape, position, and texture. The rules and axioms from the ontology helps to understand the growth or detainment of a region. Case studies on Indian cities are attempted using the proposed spatiotemporal ontology.

1.6 Outline of the Thesis

The research work is reported in eight chapters, and the outline of the thesis organization is as follows:

Chapter 1 introduces spatiotemporal data mining, discusses the motivation behind the work, states the research problem, enumerates the objectives of the research work, and gives an overview of the structure of the thesis.

Chapter 2 presents a systematic survey on the spatiotemporal data, associated data types, representation techniques, and data mining problems addressed in the field of spatiotemporal data mining.

Chapter 3 details the proposed novel features called intra-spectral and inter-spectral features, which provide new insights on the classification of remote sensing images.

Chapter 4 describes a framework for spatial colocation mining using tensor-based approaches. The results of the mining are evaluated in terms of novel interestingness measures. A detailed analysis of the algorithm is

performed on various decisive parameters.

Chapter 5 presents a tensor-based approach to find spatiotemporal colocation patterns in classified images. An algorithm to find change patterns in the time series satellite image data using an incremental approach is presented in this chapter.

Chapter 6 applies the tensor-based approach for change detection in urban landscapes with the support of landscape metrics. Growth indices for Indian cities are proposed and evaluated.

Chapter 7 outlines an ontology for change detection in remotely sensed images, which summarizes the studies conducted in this thesis for change pattern analysis.

Chapter 8 recapitulates the thesis and mentions future directions in this research area.

Chapter 2

Literature Survey

2.1 Introduction 12
2.2 Spatiotemporal Data 13
2.2.1 Properties 14
2.2.2 Data Types 15
2.2.3 Data Instances 19
2.2.4 Data Representations 20
2.3 Spatiotemporal Data Mining Approaches 25
2.3.1 Clustering 25
2.3.2 Predictive Learning 27
2.3.3 Frequent Pattern Mining 28
2.3.4 Anomaly Detection 29
2.3.5 Change Detection 30
2.4 Summary of the Chapter 33

This chapter presents the current state of-the-art of the spatiotemporal data mining field. The challenges and opportunities of the spatiotemporal research aspects are discussed. The chapter outlines the different types of spatiotemporal data and the associated data mining problems for each of these data types. The standard data representations for the different data types are also summarized.

A comprehensive study of data mining problems seen in the different application domains of spatiotemporal data is presented. The opportunities and challenges in the field of spatiotemporal data mining, and varieties of problems studied in spatiotemporal applications are summarized towards the end of the chapter.

2.1 Introduction

Spatiotemporal data has become increasingly available these days with the widespread advancement of various positioning techniques like remote sensing and mobile devices. As the number, size, and resolution of spatiotemporal data sets have rapidly increased in this era of big data, conventional data mining approaches are becoming skeptical about dealing with such kind of data. Mining knowledge from spatiotemporal data has become significant to many real-world applications, as detailed in the previous chapter. To advance the state of-the-art in numerous disciplines, the successful study of such increasingly ubiquitous spatiotemporal data holds great promise. Spatiotemporal data and the inherent relationships that exist in the data restrict the utility of data mining methodologies to identify spatiotemporal patterns. This forms the biggest challenge for the research community of spatiotemporal data mining. Another problem inborn with the spatiotemporal data mining approach is that its techniques must be developed with an awareness of the underlying theories in the application domain due to the interdisciplinary nature of the data. Although the efficacy of classical data mining algorithms is minimal in spatiotemporal data mining, the availability of spatial and temporal information also allows for consideration of novel formulations for data analysis. Objects and related features of spatiotemporal data can be described in multiple ways. As an

example, a particular illustration is to consider spatial locations as artifacts and measurements as characteristics over time, while another illustration is to treat time points as objects and measurements obtained as characteristics from all spatial locations. This kind of novel formulations of spatiotemporal data helps to derive knowledge in different forms and granularities of space and time. Hence it is noteworthy that there are ample opportunities available in various application domains of spatiotemporal data. With this context, the chapter is structured as follows.

Section 2.2 of this chapter details the foundation of spatiotemporal data in terms of its properties, data types, and representation methods, which helps to identify any spatiotemporal data encountered in the real-world. A survey of commonly studied data mining problems using the spatiotemporal data mining approach is reviewed in Section 2.3. The data mining problems addressed in this section are clustering, predictive learning, frequent pattern mining, anomaly detection and change detection. A brief summary of the various data types, instances and representations from the perspective of applications in the field of spatiotemporal data mining is drawn towards the end of the chapter. To complete the first objective of this thesis work, Section 2.4 summarizes the novel aspects of spatiotemporal data mining and comprehend the challenges and opportunities, thus paving the way for further studies.

2.2 Spatiotemporal Data

In this section, the generic properties, data types, and representations of spatiotemporal data are described in detail. This study helps to understand the richness and diversity associated with spatiotemporal data.

2.2.1 Properties

There are two properties of spatiotemporal data that brings in challenges and opportunities in the data mining approaches. Classical data mining algorithms work on the assumption that the data under consideration is *independently generated and identically distributed*. This is not true for spatiotemporal data.

The following are the properties of spatiotemporal data.

1. *Auto-correlation* [14, 15, 16]—From the very early days, works in spatial approaches are prevalent. Tobler's first law of geography states "Everything is related to everything else, but near things are more related than distant things" [14]. This is called the auto-correlation effect. The auto-correlation effect is rational in spatiotemporal data, as the measurements of nearby locations are always dependent on the adjacency factor. For example, the temperature measurements at nearby locations are always dependent and consistent. Assuming independence on spatiotemporal data will yield salt and pepper errors for classical data mining algorithms. As the data is not independently generated, the standard evaluation schemes also may become invalid.

2. *Heterogeneity* [14, 15, 16]—By identically distributed, it is implied that every instance belong to the same population. Spatiotemporal data can exhibit heterogeneity in varying space and time in different granularities. A common case for non-identical distribution is that the satellite measurement of a location on earth at seasonal cycles is differently distributed. Hence the models built for mining spatiotemporal data should learn to adapt to the different distributions possible for the data. Thus, contrary to the classical data mining assumption of

homogeneity of data, even though every instance of spatiotemporal data is drawn from the same population, they are not identically distributed.

2.2.2 Data Types

There are a variety of spatiotemporal data types that is used in the real world for various applications. The data differ in what way space and time are used in the data gathering and representation process, resulting in multiple types of spatiotemporal data mining problem formulations. The taxonomy adopted by [10] is followed in this thesis, by which the kinds of spatiotemporal (ST) data types are: (i) event data, which encompasses of discrete events occurring at distinct point locations and times (ii) trajectory data, where the measurements are trajectories of moving bodies (iii) point reference data, where a continuous spatiotemporal field is being measured at moving spatiotemporal reference points and (iv) raster data, where observations of a spatiotemporal field is being collected at fixed cells in a spatiotemporal grid.

Event Data

The advent of event kind of data can be cited in the early nineties [17] in the literature. Event data includes discrete events that occur at distinct points and times. Such kind of data are common in criminology [18], epidemiology [19], transportation [20], and social network [21]. Examples of event data include incidence of crime, disease outbreak, accident, and even a social event. Spatiotemporal, as well as non-spatiotemporal attributes, can characterize event data. As an example, the type of crime, location, and time at which the time activity occurred can be characterized as a crime event. A series of space-time events is called a spatial point pattern [22]. A depiction of the same is shown

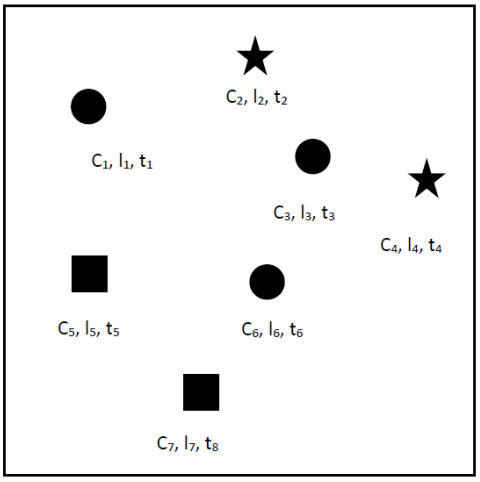

Figure 2.1: Events belonging to three types

in Fig.2.1. The circles, squares, and asterisks denote the three types of crime characterized by (c_i, l_i, t_i) where c_i is the type of crime, l_i, is the location of the crime and t_i is the time at which the crime occurred. A disease outbreak can also be represented using the location and time where the patient was first infected. An event data can also have a time period of appearance, denoting the birth and death of the event. Spatiotemporal events are generally represented by the Euclidean coordinate system, even though for certain spatiotemporal events, shortest distance connecting events are seen on spatial road networks [23].

Trajectory Data

Trajectories represent the path outlined by bodies moving in space over time. Trajectory examples include the route taken by a cab from the origin point to the destination and the migration trail of animals. Sensors are typically attached to the moving bodies that convey the body's position over

time. Thus a moving body can be a person, an animal, a vehicle, a mobile device, or even a phenomenon. Fig.2.2 illustrates the trajectory of three moving bodies A, B and C. Each trajectory is characterized by a sequence of $\{(l_1, t_1), (l_2, t_2), \ldots, (l_n, t_n)\}$ where t_i is the time when the moving object passes the location l_i. An extensive survey of mining trajectory data can be found in [24]. Trajectory data collections are sampled depending on storage and energy limitations. The trajectory data consists of spatial, temporal as well as spatiotemporal attributes. A wide spectrum of applications are driven by trajectory data mining techniques like path discovery [25, 26], location or destination prediction [27, 26, 28], movement behavior analysis [29, 30], group behavior analysis[31] and urban service [32, 33, 34]. Trajectory data such as human trajectory, urban traffic trajectory and location trajectory are becoming ubiquitious in today's world of mobile applications, GPS, Wi-Fi networks, RFID and sensors. This kind of data is being exploited to improve the urban life to a great extent.

Point Reference Data

Point reference data is the measurement of continuous spatiotemporal fields over a set of moving reference points [10]. Point reference data can be represented as a set of tuples $\{(s_1, l_1, t_1), (s_2, l_2, t_2), \ldots, (s_n, l_n, t_n)\}$ where each item denotes the measurement of sensor s_i at location l_i at time t_i. Sensors are placed at different locations referred to as reference points, which changes over time.

Raster Data

Raster data is the measurement of continuous or discrete spatiotemporal fields over fixed locations in space at fixed time points [10]. The difference between

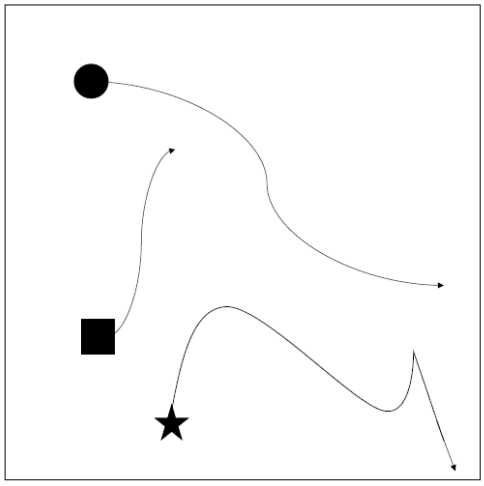

Figure 2.2: Trajectories of three moving bodies

point reference data and raster data is that the locations are fixed in raster data where locations are moving in point reference data. The fixed locations and fixed time can be regularly or irregularly distributed. So for 'm' fixed locations, say, $l_1, l_2, \ldots, l_m$ and 'n' timestamps, say, $t_1, t_2, \ldots, t_n$, the raster data is represented by an entry in the matrix $S^{m \times n}$, where each entry s_{ij} is the measurement at location l_i at time t_j. This matrix, which records the distinct measurement, is also referred to as a spatiotemporal grid. The images of the earth's surface collected by the satellites at fixed revisit times are an example of raster data. Other examples of raster data include data from climate science, epidemiology, and brain imaging. Observations of raster data can be recorded at points as well as regions.

Another feature associated with raster data is the resolution of the spatiotemporal grid, in terms of space and time. For example, satellite measurements of the earth's surface obtained from the LANDSAT sensor are

at 30 m spatial resolution every 16 days, where the MODIS sensor is at 500 m spatial resolution on a daily scale. The computational requirements of the raster data analysis are highly dependent on the resolution of the same. Thus the resolution of the raster data is a challenging factor to extract the required information from the spatiotemporal field being measured.

An important aspect of spatiotemporal data is that the data collected in a particular data type can be transformed into a different data type for relevant reasons. By aggregating the number of events in each cell of a spatiotemporal grid, an event data type can be transformed to a raster data form.

2.2.3 Data Instances

Data instance is the basic unit of data upon which the algorithms operate upon. The standard categories of data instances for the spatiotemporal data types discussed in the previous section are as shown in Fig. 2.3. Spatiotemporal events are represented as point instances, where trajectories can be described as an ordered collection of points, trajectory instance or as a time-series of locations. Point reference data also can be represented as points where each instance is a reference point of the spatiotemporal field with respect to space and time. Spatiotemporal raster data can be represented as time series, spatial maps, or raster as per the need of application.

The choice of the right approach to the construction of spatiotemporal instances depends on the nature of the questions being studied and the family of available approaches for the task.

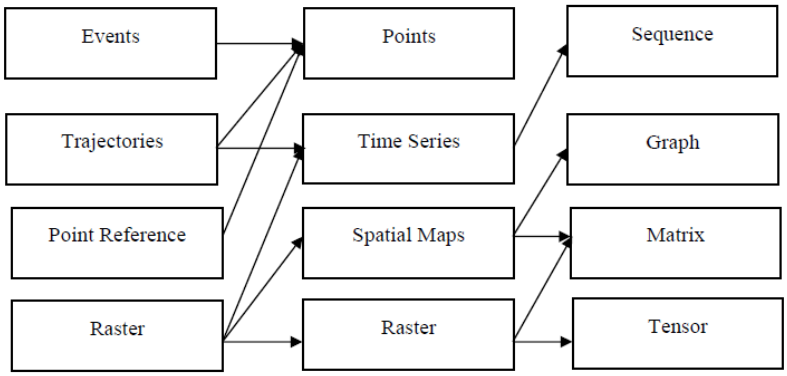

Figure 2.3: Data types, Data Instances and Data Representation of ST Data

2.2.4 Data Representations

For the above-mentioned data instances, the standard data representation techniques are the sequence, graph, matrix, and tensor as depicted in Fig. 2.3.

Trajectories and time series can be represented as sequences. Trajectories can also be represented as matrices, where the row and column are the dimensions of the spatiotemporal grid, and an entry value indicates whether the trajectory traverses the corresponding grid. Matrices can also be represented as graphs. For example, in a spatiotemporal road network, sensors deployed in the expressways are nodes in a graph, and the edges denote the road segments between sensors.

As this research thesis is concentrating on raster data, a detailed study of data representation for the same is attempted in this section. Raster data is generally represented in matrices and tensors. Even though matrix is a more straightforward data representation as compared with tensor, it loses the spatial correlation information among the locations, and hence the matrix

representations are generally not encouraged for spatiotemporal raster data.

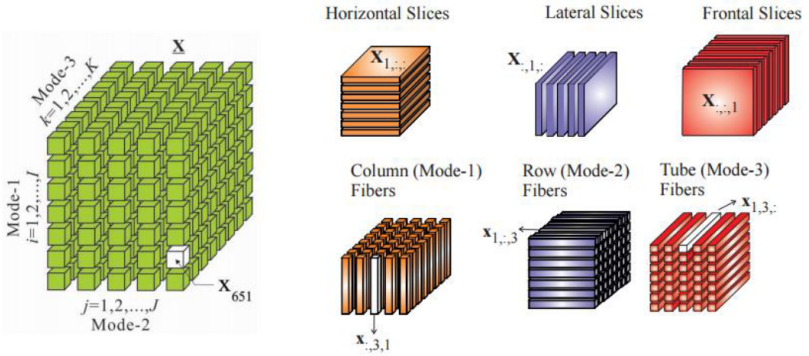

Figure 2.4: Concepts of Tensors, Fibers and Slices
Figure Courtesy - Cichoki et al.[35]

Concepts of Tensors

Tensors are the multidimensional generalization of arrays or matrices that are often used to represent large scale, high dimensional data. The convention adopted in this thesis is to represent tensors in calligraphic font, matrices in capital letters, and vectors in small bold letters. A N-order tensor is represented as

$$\mathcal{X} \in \mathbb{R}^{I_1 \times I_2 \times \cdots \times I_N}.$$

The order of a tensor is the number of its modes, ways, or dimensions, which can be space, time, frequency, classes, and so on. An $N \times 1$ vector $\mathbf{x}$ is considered a tensor of order one, and an $N \times M$ matrix $\mathbf{X}$ a tensor of order two. Subtensors are parts of the original data tensor, created when only a fixed subset of indices is used. Vector-valued subtensors are called fibers, defined

by setting every index but one, and matrix-valued subtensors are called slices, obtained by setting all but two indices [35].

Fig.2.4 depicts the concepts of tensors, fibers, and slices. The slices can be obtained in horizontal, lateral, and frontal forms, whereas the fibers exist in column, row, and tube forms. The figure shows the different views of fibers and slices in a nutshell.

Operations on Tensors

Matricization of Tensors

The manipulation of tensors often requires their reformatting or reshaping; a particular case of reshaping tensors to matrices is termed matrix unfolding or matricization. The matricization of a 3-order tensor is shown in Fig.2.5.

Multiplication of Tensors

Various product rules exist for the tensor, which is summarized in Table 2.1[35].

Factorization of Tensors

Tensor factorization aims to represent the tensor as a product of low order factors. This is also called tensor decomposition in tensor algebra. The most common factorization methods in tensors are Canonical Polyadic Decomposition (CPD) and Tucker decomposition (TKD) [35].

A CPD of an Nth order tensor, say $\mathcal{X} \in \mathbb{R}^{I_1 \times I_2 \times \cdots \times I_N}$ is a linear combination of rank-1 tensors.

$$\mathcal{X} = \sum_{r=1}^{R} b_r^1 \odot b_r^2 \odot \cdots \odot b_r^N. \tag{2.1}$$

The tensor rank R is the smallest value for which the above equation holds.

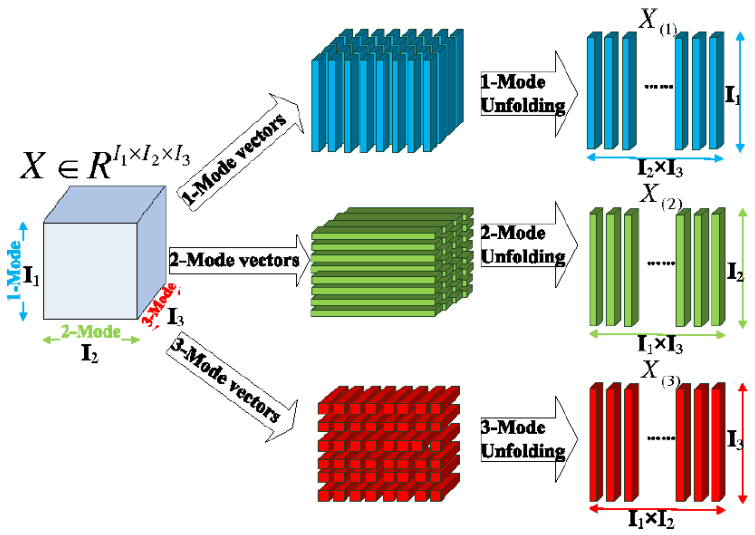

Figure 2.5: Matricization of Tensors
Figure Courtesy - Cichoki et al.[35]

The matrix form of the CPD can be obtained through Khatri-Rao product. Determining the rank of a tensor is an NP-hard problem [35]. Since the computation of CPD is intrinsically multilinear, the solution is obtained through a sequence of linear subproblems as in the alternating least squares (ALS) framework, whereby the least-squares cost function is optimized for one component matrix at a time, while keeping the other component matrices fixed [36]. The concept of CPD for a 3-order tensor is presented in Fig.2.6.

TKD of a Nth order tensor say $\mathcal{X} \in \mathbb{R}^{I_1 \times I_2 \times \cdots \times I_N}$ is a multilinear combination of a core tensor $\mathcal{G} \in \mathbb{R}^{R_1 \times R_2 \times \cdots \times R_N}$ and factor matrices $B^n = [b_1^n b_2^n \ldots b_{R^n}^n]$.

$$\mathcal{X} = \sum_{r1=1}^{1} \sum_{r2=1}^{2} \cdots \sum_{rN=1}^{R_N} b_{r1}^1 \odot b_{r2}^2 \odot \cdots \odot b_{rN}^{R_N}. \tag{2.2}$$

Table 2.1: Definition of Tensor Products

Mode-n product $\mathcal{C} = \mathcal{A} \times_n \mathbf{B}$	$\mathcal{A} \in \mathbb{R}^{l_1 \times l_2 \times \cdots \times l_N}$ and $\mathbf{B} \in \mathbb{R}^{J_n \times l_n}$ yields $\mathcal{C} \in \mathbb{R}^{l_1 \times \cdots \times l_{n-1} \times j_n \times l_{n+1} \times \cdots \times l_N}$ with entries $c_{i_1 \ldots i_{n-1} j_n j_{n+1} \ldots i_N} = \sum_{i_n=1}^{l_n} a_{i_1 \ldots i_{n-1} i_n i_{n+1} \ldots i_N} b_{j_n i_n}$ and matrix representation $\mathbf{C}_{(n)} = \mathbf{B}\mathbf{A}_{(n)}$
Full multilinear product $\mathcal{C} = \|\mathcal{A}; \mathbf{B}^{(1)}, \mathbf{B}^{(2)}, \ldots, \mathbf{B}^{(N)}\|$	$C = \mathcal{A} \times_1 \mathbf{B}^{(1)} \times_2 \mathbf{B}^{(2)} \cdots \times_N \mathbf{B}^{(N)}$
Tensor or Outer Product $\mathcal{C} = \mathcal{A} \circ \mathcal{B}$	$\mathcal{A} \in \mathbb{R}^{I_1 \times I_2 \times \cdots \times I_N}$ and $\mathcal{B} \in \mathbb{R}^{J_1 \times J_2 \times \cdots \times J_M}$ yields $\mathcal{C} \in \mathbb{R}^{I_1 \times I_2 \times \cdots \times I_N \times J_1 \times J_2 \times \cdots \times J_M}$ with entries $c_{i_1 i_2 \ldots i_N j_1 j_2 \ldots j_M} = a_{i_1 i_2 \ldots i_N} b_{j_1 j_2 \ldots j_M}$
Tensor or Outer Product of Vectors $\mathcal{X} = \mathbf{a}^{(1)} \circ \mathbf{a}^{(2)} \circ \cdots \circ \mathbf{a}^{(N)}$	$\mathbf{a}^{(n)} \in \mathbb{R}^{I_n}$ $(n = 1, \ldots, N)$ yields a rank-1 tensor $\mathcal{X} \in \mathbb{R}^{i_1 \times i_2 \times \cdots \times i_N}$ with entries $x_{i_1 i_2 \ldots i_N} = a_{i_1}^{(1)} a_{i_2}^{(2)} \ldots a_{i_N}^{(N)}$
Kronecker Product $\mathbf{C} = \mathbf{A} \otimes \mathbf{B}$	$\mathbf{A} \in \mathbb{R}^{I_1 \times I_2}$ and $\mathbf{B} \in \mathbb{R}^{J_1 \times J_2}$ yields $\mathbf{C} \in \mathbb{R}^{I_1 J_1 \times I_2 J_2}$ with entries $c_{(i_1-1)J_1+j_1,(i_2-1)J_2+j_2} = a_{i_1 i_2} b_{j_1 j_2}$
Khatri-Rao Product $\mathbf{C} = \mathbf{A} \odot \mathbf{B}$	$\mathbf{A} = [\mathbf{a}_1, \ldots, \mathbf{a}_R] \in \mathbb{R}^{I \times R}$ and $\mathbf{B} = [\mathbf{b}_1, \ldots, \mathbf{b}_R] \in \mathbb{R}^{J \times R}$ yields $\mathbf{C} \in \mathbb{R}^{U \times R}$ with columns $\mathbf{c}_r = \mathbf{a}_r \otimes \mathbf{b}_r$

The matrix form of the TKD can be obtained through Kronecker products. The N-tuple $(R_1, R_2, R_3, \ldots, R_N)$ is called the multilinear rank of the tensor. The concept of TKD for a 3-order tensor is shown in Fig.2.7. As a rule of thumb, the literature advises using CPD for latent parameter estimation and TKD for

subspace estimation, compression, and dimensionality reduction [37].

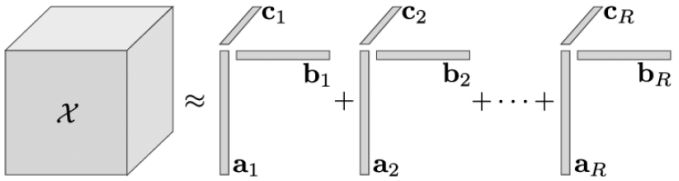

Figure 2.6: Canonical Polyadic Decomposition

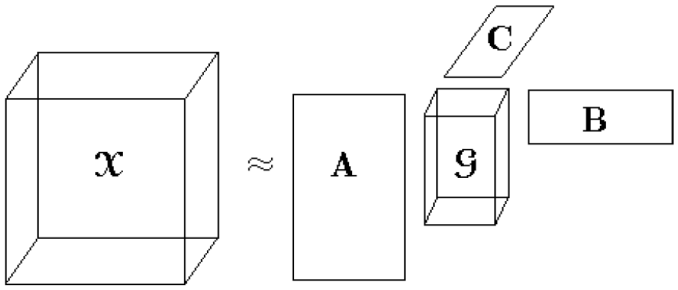

Figure 2.7: Tucker Decomposition

2.3 Spatiotemporal Data Mining Approaches

2.3.1 Clustering

Clustering is the grouping of instances based on the feature values. Clustering can be applied on points, trajectories, time series, spatial maps, and raster for spatiotemporal data. As clustering is based on similarity, techniques to measure similarity in spatiotemporal features are to be looked into. Similarity among points in a spatiotemporal field has to be defined in terms of space as well as time. When measuring similarity among trajectories, commonly

adopted techniques are colocation frequency [38], longest common subsequence [39], Frechet distance [40] and dynamic time warping [41]. Among these methods, Frechet distance and dynamic time warping can also be used to measure similarity in time series representations. Standard proximity measures like Euclidean distance can be used to measure similarity among spatial maps, whereas spatiotemporal raster similarity is computed based on the extracted features.

There are two commonly observed purposes of clustering points as per the literature. The first purpose is to find hotspots. Examples of such hotspots includes finding outbreaks of diseases [42], law-breaking hotspots [43] and shared movements in twitter data [44]. This is also referred to as event detection. The problem of finding hotspots was initially studied in spatial statistics in the late nineties [45]. The second purpose is to find clusters that have similar non-spatial attributes. This objective is studied in different applications in the context of crime data [46], twitter data [47], geo-tagged photos [48] and traffic accidents [49]. ST-DBSCAN [50] and its extensions are the most popularly seen algorithms in the literature to cluster points. The significant facets of trajectory clustering are the choice of distance measure and choice of clustering technique used. A detailed review of the trajectory clustering can be found in [51]. “Moving clusters” is a recent development seen in trajectory clustering where moving bodies meet and exit a cluster as it moves through time in space. Examples are the movement of a convoy of cars and migrating flocks of animals. Algorithms for moving clusters are seen in [52, 53, 54]. Time-series clustering involves finding spatially rational groups of locations with the same temporal behavior. This problem is usually achieved through the common clustering

techniques like k-means [55] and hierarchical clustering [55]. A disadvantage associated with the traditional techniques is that the resultant clusters are not spatially contiguous, which should be rectified by a post-processing step. Clustering spatial maps are to find timestamp groups with similar spatial maps such as time stamps of brain activity having similar patterns of spatial activity [56].

2.3.2 Predictive Learning

Predictive learning is a mapping from the input features to the output variable with the aid of training samples. In the spatiotemporal domain, both input and output variables are spatiotemporal instances, thus paving the way for varieties of problem formulations. A common problem is predicting an output variable at every spatial location using the time-series as input variables. This is the context of classification and regression problems. Latent space models for traffic prediction using time-series is a typical application of a predictive learning approach [57]. Prediction of the future location of a moving object based on past data of visited locations is yet another example [58]. Another common predictive learning problem in the spatiotemporal domain is to predict the response at a specific location and time using observations collected at other locations (usually neighborhoods) and timestamps. Such instances can be seen while estimating ecology [59], and mapping earth sciences data from remotely observed scenes [60]. Numerous works are seen in the literature that uses temporal information and spatial information separately to perform predictions with respect to temporal points and spatial locations.

The research in predictive learning has now migrated to deep learning models. The traffic accident prediction problem is studied using Convolutional

Long Short Term Memory neural network model in [61]. In this architecture, the point data is merged to form a spatiotemporal field and is represented as a tensor. A road level traffic prediction using stacked encoder [62, 63] and deep belief networks [64] is also proposed.

2.3.3 Frequent Pattern Mining

There exist several kinds of frequent patterns that can be formulated in the context of spatiotemporal data, of which the common ones are colocation patterns, co-occurrence patterns and sequential patterns.

Colocation patterns are subsets of data that occur in close spatial proximity of each other. Colocation pattern is termed as co-occurrence pattern when the proximity is in terms of space as well as temporal context. Colocation pattern was first termed in spatial statistics by Huang [65]. A summary of colocation pattern mining in the current state of-the-art is presented in Chapter 4. A first approach to discover co-occurrence patterns using Apriori principle is seen in [66]. Sequential pattern mining is the occurrence of spatiotemporal events of a specific kind that generates a sequence of spatiotemporal events of other types, as seen in [67]. For example, the occurrence of a car accident can trigger traffic jams in the spatiotemporal neighborhood. A slicing-STS-miner is proposed in [68] which discovers an ordered list of event types, which discovers significant sequential patterns. Sequential patterns can also be mined in trajectories, which constitute the spatial locations visited by moving objects. Extension for association rule mining in spatiotemporal context referred to as STAR [69] is proposed to find regions visited by moving objects. Sequential pattern mining can also be sought in spatiotemporal raster, wherein a pattern of events is discovered in the grid. A commonly studied topic is the study of

community structure and interactions in the social network [70, 71].

2.3.4 Anomaly Detection

Anomalies are instances that are dissimilar from the majority of the instances. Detecting anomalies are a by-product of clustering. The anomalies due to their dissimilarity will not belong at any cluster and are termed as *outliers*. Examples of anomalies from the perspective of spatiotemporal context are an anomalous trajectory taken by a vehicle, anomalous ecological behavior in either spatial or temporal context. A detailed survey of anomaly detection in time series data is seen in [72] and spatial data in [73, 74]. The presence of spatial and temporal aspects together will result in novel ways of describing anomalies.

Distance-based methods to discover anomalous trajectories are discussed in [75], where trajectories that are in distant spatial regions compared to others are considered as anomalies. Detecting traffic outliers as edge anomalies are proposed in [76] where the spatiotemporal trajectories are modeled as a graph. A trajectory can also be categorized as anomalous if it deviates from the local neighbors, thus exhibiting the outlier characteristics. Anomalies seen in raster data are usually group anomalies such as regions or group of locations that show abnormal behavior during a short period of timestamp when rare events happen. The approach seen in the literature for group anomalies is the stitching of spatial and temporal anomalies to find spatiotemporal anomalous values [77]. A similar method to find ocean eddies by using local space thresholding technique followed by a stitching process in temporal attributes is proposed in [78]. Abnormal activities in crowded scenes are difficult to detect due to the challenge associated with defining normal activities. Borrowing the activity recognition literature, attempts have been made to detect anomalies by using

dynamic mixture models [79]. Another category of group anomaly is the mining of burst activities for specific terms like an earthquake, flood in twitter data [80, 81].

2.3.5 Change Detection

Change detection is the process of identifying timestamp at which a system deviates significantly from past behavior. Change detection in the spatiotemporal domain is highly useful in the study of earth science data and neuroimaging data. Changes are mined contextually in both space and time in spatiotemporal raster data. There exists a number of novel formulations for the contextual concept. For example, the context of time can be thought of as time series observed at spatial locations in close proximity or time series similar to a given time series for a period of time. A decrease in vegetation can be detected using a space-window enumeration and pruning approach as discussed in [82]. A taxonomy of different changes from the perspective of spatiotemporal data is briefed in [83].

The earth science data in the form of images are analyzed for land cover or land use. Land cover, as the observed physical cover, and land use, as the function it serves, are, in most cases, interrelated. Change detection methodologies for spatiotemporal data in the form of remote sensing images are generally grouped into two categories, (a) pixel-based approaches and (b) object-based approaches.

A pixel is considered to be an atomic unit of the image, and the spectral reflectance values associated with a pixel can be used to detect changes. Statistical operators are generally used to analyze the pixel values. Common techniques in pixel-based approaches are image differencing [84], image

ratioing [85] and image regression [86]. Another common approach is vegetation index differencing [87], where vegetation indices of two temporal images are found separately, and the technique of either differencing or ratioing is applied to find the changes that have happened in the vegetation. In the change vector analysis method [88], the pixel values of different spectral bands are treated as vectors, and a change vector is found by calculating the difference between the pixel values at different dates.

In object-based change detection methods, the unit of analysis in these methods is an object. The concept is similar to the way a human do analysis, who identifies the objects from an image, rather than individual pixels and their associated values. By considering the image as a collection of objects, the properties of objects like shape, size, texture, and spatial arrangement of objects in a neighborhood helps to gain the semantics of an image more effectively. A direct comparison of objects in two images can be sought for as seen in [89, 90]. Different classification algorithms also can classify the bi-temporal images to different objects. A change matrix of from-to is outlined to describe the changes in objects. The performance of this method is strongly related to the classification accuracy of the algorithms. In multi-temporal object-based change detection [91, 92], image segmentation, and classification are applied to stacked multi-temporal images, and the spatially corresponding changes between the images can be detected. An extensive survey of the change detection methods is seen in [93].

A brief summary of data types, instances and representations from the perspective of applications for the various data mining tasks in the spatiotemporal field is provided in Table 2.2.

Table 2.2: Summary of Spatiotemporal Applications, Approaches, and Representation

Application Domain	**Data Mining Approach**	**Data Types**	**Data Representation**	**Related Research**
Epidemiology	Hotspot Detection	Events	Points	[6],[19],[20], [22],[42]
	Spatial Pattern Analysis		Sequence	
Earth Science	Spatiotemporal Queries	Events, Time Series, Point Reference, Spatial Maps, Raster	Events, Time Series	[11], [17], [18], [41], [58], [59], [76], [77], [83-86], [91], [115], [133], [141], [142], [144]
	Temporal analysis		Events, Time Series, Spatial Maps	
	Causal Relationship Mining		Time Series, Sequence	
	Estimation of Geographical Data		Events, Time Series, Sequence	
	Outlier Detection		Points, Events	
	Change Pattern Detection		Time Series, Spatial Maps, Matrix, Raster	
	Event Prediction		Time Series, Sequence, Graph	
	Colocation Pattern Mining		Time Series, Raster, Matrix	
Transportation	Location Prediction	Trajectory, Spatial Maps	Points, Time Series	[5], [23], [33], [34, [40], [49], [56], [60-63], [75]
	Route Prediction		Time Series	
	Group Behavior Analysis		Trajectory Instance	
	Mobility Pattern		Time Series, Trajectory Instance	
	Path Discovery		Time Series	
	Urban Service		Time Series, Trajectory Instance	
Criminology	Hotspot detection	Events	Points	[9], [43], [46]
	Similar Clusters			
Mobility	Mobility Pattern	Trajectory	Time Series	[25-28], [30-32], [48], [57], [74]
	Next Place Prediction		Sequence, Time Series	
	Route Recommendation		Spatial Maps	
	Pedestrian Estimation		Time Series	
	Path Prediction		Time Series	
	Anomaly Detection		Time Series, Sequence	
Neuroscience	Anomaly Detection	Events	Sequence	[7], [13], [55]
	Brain Dynamics Detection	Raster	Tensor	
Social Media	Abnormal Event Detection	Events	Points, Sequence	[21], [38], [44], [47], [69], [70], [79], [80]
	Social Relationship Pattern		Points, Graph	
	Localized Event Detection		Points	
	Community Detection		Matrix	
	Identification of Social Burst		Events, Time Series	

2.4 Summary of the Chapter

The variety of data types, data instances and techniques for representing spatiotemporal data are described in detail in this chapter. A comprehensive study of tensor representation methods and its relevant operations are also done, as the thesis is based on the concept of tensor algebra. A survey of spatiotemporal data mining problems like clustering, predictive learning, frequent pattern mining, anomaly detection and change detection approaches are detailed in this chapter. The following pointers are the highlights of the study.

- The challenges and opportunities in the field of spatiotemporal data mining is due to the generic properties of spatiotemporal data, namely, auto-correlation and heterogeneity.
- Novel and natural formulations of data representation are necessary to perform the data mining task effectively.
- It is understood that the work in the young field of spatiotemporal data mining is generally application-driven.
- The representation of multi-faceted data by tensor methods helps to perform and exploratory analysis of spatiotemporal data, which helps to discover significant patterns.
- Blending of ideas across disparate application domains is a promising area in the field of spatiotemporal data mining.

The thesis attempts to bring in effective data representation techniques for spatiotemporal data and discover significant patterns from spatiotemporal data.

Chapter 3

Intra-spectral and Inter-spectral Features

3.1 Introduction **36**
3.2 Related Research **37**
3.3 Proposed Features **38**
3.4 Results and Discussions **41**
3.4.1 Dataset 41
3.4.2 Experiments 42
3.5 Summary of the Chapter **47**

This chapter intends to learn the data representations for spatiotemporal raster data. For this purpose, remote sensing images are chosen as the spatiotemporal dataset in this study. Experiments on different data representation techniques are done on the remote sensing images, and the data mining task of classification is performed. In this study, a novel set of features from the perspective of remote sensing images is proposed, namely, intra-spectral and inter-spectral features. The features are analyzed in detail

with other feature extraction techniques from the perspective of remote sensing image classification.

3.1 Introduction

The pixels of remote sensing image contains a set of values, whose count is proportional to the number of bands of the satellite in which the reflectance is captured. The classification of remote sensing images involves the task of categorizing all pixels in an image of terrain into land cover/land use classes. The basis of the numerical values of each pixel aids in the categorization of the image. Generally, all land cover/land use classification utilizes pixel by pixel spectral reflectance values for the same. In a low or medium spatial resolution satellite images, single-pixel houses more than one class, thus leading to errors in the classified output. In high or very high-resolution satellite images, the variability between pixels will be high, and each pixel houses only one class. To detect each type of land cover/land use classes, appropriate combinations of bands have to be sought, which is not known in advance. Low or medium resolution satellite has three to four bands, where the high and very high-resolution satellites have hundreds of bands. Thus it is evident that to perform classification, appropriate combinations of bands have to be iterated through. This will result in more number of computations with increased time complexity.

The spatiotemporal raster data is studied for different data representation techniques in this work. For the remote sensing images, instead of finding band combinations of the pixels for each land cover/land use class, the variance of the pixels in the same spectral channel and different spectral channel (named

as *intra-spectral* and *inter-spectral* features) are chosen as the discriminant for performing classification. The features are being fed into different classifiers and are analyzed in detail. Appropriate conclusions are drawn from the experiments by comparing the classification accuracy of the classifiers with the traditional features.

The chapter is organized as follows. The next section 3.2 brings out the related research in the field of classification of remote sensing images. The proposed features are detailed in Section 3.3. Experimental setup and discussions are explained in Section 3.4. The chapter is concluded in Section 3.5.

3.2 Related Research

The literature points to the fact that the task of classification is highly improved by appropriate feature selection in the particular domain of classification [94, 95]. Classification in low, medium, and high-resolution remote sensing images is generally attempted using the standard features of raw pixel intensities. Textures of the images are also a major feature which is used for classification [96]. Image channels are convolved into Gabor filters, and the response obtained from the features are used as input to the classifier [97]. The performance of the classifier varies depending on the type of the texture, and hence each filter has to be fine-tuned for the feature relevant to the class. The intensities within a predefined neighborhood around a pixel can also be gathered to perform classification with larger certainty [98]. Other approaches in the literature depend upon the concept of reduction of space dimensionality through conventional methods like LDA [99], PCA [100], partial least squares [101] or

genetic algorithms [102] for the huge set of pixel features before training the classifier. In very high-resolution images, the end member feature extraction is studied separately, and methods are outlined for the same [103, 104].

Machine learning techniques depends on the classifier models to perform the task of classification. An exclusive study for images from the perspective of classification is done in [105]. From the study, it is seen that (a) there are certain classifiers like Neural Networks and k-NN, wherein the features have to be fed into them and (b) another set of classifiers like random forests and boosting classifiers, wherein the informative features are being picked by the classifier during the training phase. An advantage in the second scenario is that the classifier picks the features that are most discriminative, such that the selected features work best in combination with a particular classifier and related classes. The literature advises that the joint problem of feature selection and classification will be more interesting to solve than to consider both of them separately. Examples of such work are seen in [106, 107].

3.3 Proposed Features

Sensors of a satellite capture spectral reflectance in multiple spectral bands. Each band is recorded in a single channel; thus, there are several intensities per pixel. Usually, all pixel values (spectral values corresponding to each channel) are chosen as features for classification. This is because it is not known in advance, which combination of spectral bands will help in separating the land cover or land use classes optimally. If all the spectral values of a pixel are considered, then the feature dimension is equivalent to the number of channels. Instead of building a huge feature space, two new features, namely,

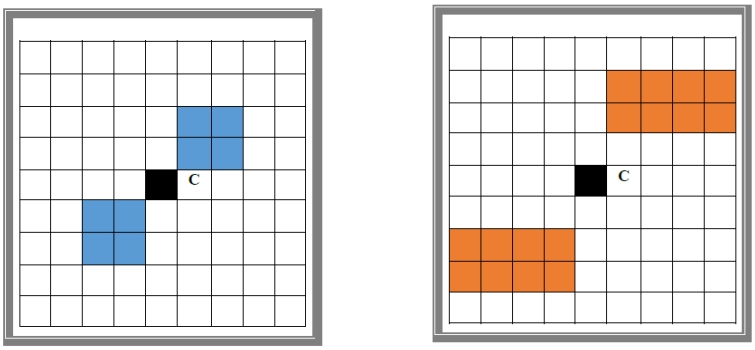

Figure 3.1: Echoing of (a) Square patch and (b) Rectangular patch in the Sliding window

intra-spectral features (IASF) and inter-spectral features (IESF), are proposed in this study.

A window of appropriate size is chosen inside an image patch as depicted in Fig.3.1. The central pixel of the window is marked as solid dark and is represented by C. Square patches, and rectangular patches are chosen inside the window and are echoed with respect to the central pixel C. The figure depicts square patches and rectangular patches and the echoed correspondences.

The patches are randomly generated, and they help to capture the texture ranges in the image. Patches of the same sizes (both square and rectangular) are grouped under the category of "alike" patches and that of different sizes (both square and rectangular) are grouped under the category of "unalike" patches. The difference between the mean intensities of both the square and rectangular patches are calculated. The intra-spectral features and inter-spectral features of the image are defined as follows.

- *Intra-spectral features (IASF)*—The difference between the mean values

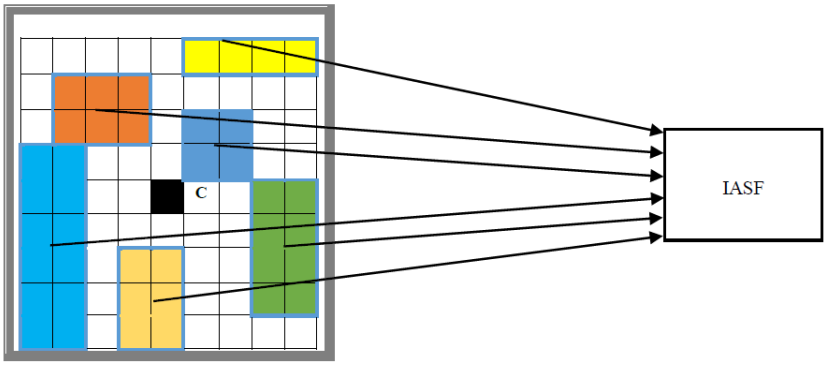

Figure 3.2: Intra-spectral Features

of "unalike" patches in the same spectral channel.

- *Inter-spectral features (IESF)*—The difference between the mean values of "alike" patches in the different spectral channels.

Fig.3.2 represents the intra-spectral features. The "unalike" patches are marked in different colors. The difference between the mean values of "unalike" patches is summed up. The operation is performed in the same spectral channel.

Fig.3.3 represents the inter-spectral features. From the name itself, it is clear that the feature is extracted from different spectral channels. The "alike" patches in all spectral channels are marked in colors. The difference between the mean values of "alike" patches in the different spectral channels constitutes the inter-spectral features.

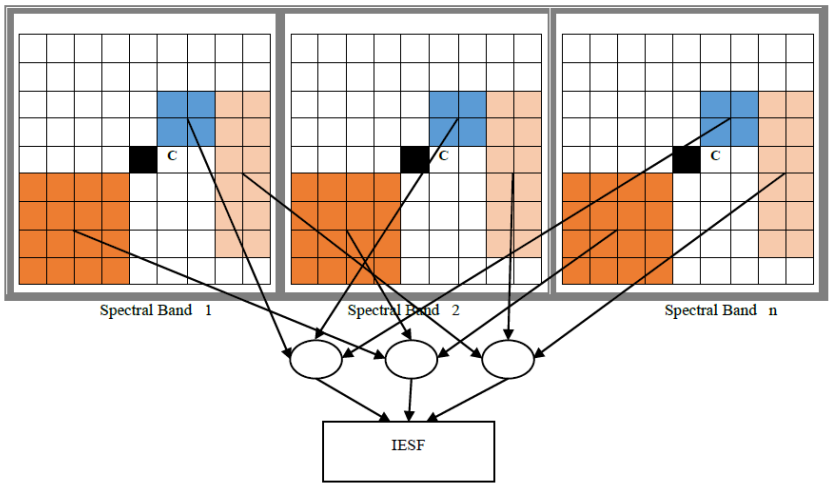

Figure 3.3: Inter-spectral Features

3.4 Results and Discussions

The experiments are performed on different datasets to compare the different features and to assess the performance of different classifiers for the different features.

3.4.1 Dataset

The experiments are run on datasets from WorldView-2 satellite images acquired from [108]. Samples are shown in Fig.3.4. The specifications of WorldView-2 satellite is described in Appendix A. The images have dimensions 615×615 and is of resolution 0.5 m. The images chosen are suburban parts of famous cities covered in the dataset. The four different images in the dataset are divided into five strips, wherein four strips are used for training, and the fifth strip is used for testing (as motivated from [109]). The iterations are repeated by

Figure 3.4: World View-2 Images

interchanging the training and testing sets. The final result values are obtained through averaging.

3.4.2 Experiments

The feature sets used in the experiments are (a) IASF and IESF (b) Raw pixel values (c) Reduced Pixel Values through PCA (Raw Pixel Values + PCA) (d) Reduced Pixel Values through LDA (Raw Pixel Values + LDA) and (e) Mean Features of the Echoed Pixel Values (Echoed Mean Features—EMF). Classifiers used in this evaluative experiments are of two types. The first category of classifiers does not perform feature selection, whereas the second category performs feature selection during the training phase. The classifiers used in

the experiments are (a) Bayesian (b) Neural Networks (NN) (c) Decision Trees (DT) (d) Support Vector Machines (SVM) (e) Support Tensor Machines (STM) and (f) AdaBoost.

The four classes identified from the images are labeled as buildings, roads, greenery and water. The overall classification accuracy results of the classifiers achieved for each classifier is as shown in Table 3.1. The different features are tested for the classifiers. The accuracy is presented with respect to the four classes—buildings, roads, greenery, and water. The bold-faced values are the best accuracy values for that particular feature in the concerned class label. The spectral channel for extracting values of IASF are chosen based on the classification label. The combined features of IASF and IESF is the feature vector, which is a discriminant for the purpose of classification.

For the proposed features, IASF and IESF, better classification results are seen when compared with the raw pixel values. However, certain classifiers like Bayesian and Neural Networks are not performing at par. Decision Trees and AdaBoost classifiers show good classification accuracy results for certain classes. On a generic overview, for the proposed features, the STM shows good and appreciable values for all classes. One possible explanation for these results is that the discriminative capability of the proposed features are best captured by the STM and also by AdaBoost to an extent.

Among the classifiers analyzed, the boosting classifier shows consistent performance for all features except the raw pixel values. On an analysis with respect to the class label, to model buildings and roads in high-resolution images, the decision trees are the best one, when using raw pixel values. All other classifiers suffer from inconsistent performance with raw pixel values.

When applying PCA and LDA to raw pixel values, the accuracy level fluctuates between the different class labels, and hence the conclusion drawn is that they are dependent on the input data points. It is noted that the boosting classifier is run for 300 iterations.

The raster data is modeled as a matrix as well as a tensor, and is fed to the corresponding classifier. The matrix representation is also broken down into vectors, for the sake of input to SVM. The tensor representation of the data is directly fed into STM. As STM gives better result than SVM, it is evident that the matrix representation of raster data, does not yield good results. The tensor representation of the data in STM and the performance of the same leads to the conclusion that the tensor data representations captures the spatiotemporal information more accurately than the matrix representation.

Before drawing the final conclusion, it is also necessary to analyze the results with respect to the feature extraction, training, and testing time of each classifier with respect to the features. Table 3.2 represent the execution time for feature extraction, training time, and testing time for each classifier. The evaluations have been performed on the AMD Opteron 16 core 12 GB RAM processor. The time is specified in minutes for all cases. A comparative case study of classifiers that performed well on the classification accuracy is chosen for further analysis. They include DT, STM, and AdaBoost classifiers. Also, the features are downsized to three types, namely, IASF + IESF, Raw Pixel Values, and EMF. The reason for avoiding reduced feature space methods is because the dimensionality coefficient is set by experiments, and this coefficient highly influences the time-related in all other areas. Hence they are not chosen for experiments with respect to time. For the proposed features, feature extraction,

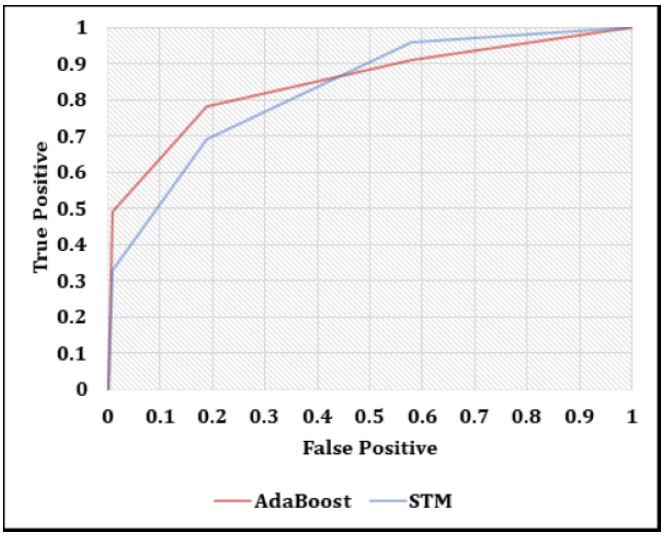

Figure 3.5: ROC Curve for AdaBoost and STM using IASF + IESF

training, and testing time are much higher when compared with other features. This is attributed to the fact that the features are made by echoing in the same channels as well as different channels, rather than simply vectorizing the whole range of band values.

The AdaBoost and STM classifier is further analyzed with respect to their ROC, as shown in Fig.3.5. From the ROC, it is evident that the AdaBoost classifier has an accuracy average of 84%, whereas the STM averages on 78%. But the AdaBoost classifier takes a significant amount of CPU time in performing the boosting iterations, and also, the accuracy depends on the number of iterations performed. The ROC is plotted for all the images, and the true positives and false positives are averaged for all classes in the image.

To fix the optimal patch size, while processing IASF and IESF, an iterative method is adopted, and the patch size is varied from $N/10$ to $N - 1$ for an

Table 3.1: Accuracy of classifiers for different features

Features	Classifier	Accuracy (%)			
		Building	Roads	Greenery	Water
IASF+ IESF	Bayesian	67.1	67.1	69.9	67.8
	NN	70.1	71.3	66.8	69.9
	DT	71.6	79.9	71.6	**81.1**
	SVM	75.6	78.9	77.9	80.2
	STM	80.1	83.2	**86.8**	80.3
	AdaBoost	**82.1**	**83.4**	80.2	79.2
RAW Pixel Values	Bayesian	65.3	61.1	62.7	59.9
	NN	67.3	69.9	72.1	71.1
	DT	77.5	77.9	71.6	73.5
	SVM	70.0	71.2	77.2	70.2
	STM	76.2	77.8	78.9	74.2
	AdaBoost	70.2	71.8	67.3	71.8
Raw Pixel Values + PCA	Bayesian	67.5	62.5	70.2	61.3
	NN	61.1	68.4	67.1	67.5
	DT	79.9	76.7	80.1	72.1
	SVM	69.9	70.2	71.1	72.3
	STM	77.8	72.1	77.6	78.9
	AdaBoost	71.5	78.5	69.1	78.8
Raw Pixel Values + LDA	Bayesian	55.6	66.8	61.2	67.1
	NN	60.7	67.1	60.1	59.8
	DT	60.2	57.8	57.8	63.7
	SVM	71.0	73.2	71.4	71.9
	STM	77.8	73.1	76.1	78.9
	AdaBoost	79.9	80.1	75.3	76.1
EMF	Bayesian	66.7	66.2	66.5	69.1
	NN	65.2	61.9	61.5	66.8
	DT	78.9	77.5	71.5	71.0
	SVM	67.1	58.9	74.1	76.1
	STM	61.1	67.5	66.3	66.2
	AdaBoost	74.1	78.3	76.1	70.1

Table 3.2: Execution Time in minutes for Feature Extraction, Training and Testing

Feature Extraction	**DT**	**STM**	**AdaBoost**
IASF + IESF	112	87	56
Raw Pixel Values	3	3	121
EMF	12	10	48
Training			
IASF + IESF	227	124	56
Raw Pixel Values	12	12	121
EMF	44	12	48
Testing			
IASF + IESF	18	7	9
Raw Pixel Values	6	6	10
EMF	21	25	14

image of size $N \times N$. Experiments are run for different classifiers and the corresponding classification accuracy is observed closely. It is seen that the patch size of ranges from 15×15 to 25×25 gives better results than sizes greater or lesser than this. The results are plotted in Fig.3.6. For the experiments reported in this chapter, the patch size is fixed as 24×24, which shows a stable value in the experiments.

3.5 Summary of the Chapter

This chapter summarizes the proposed novel feature which is a combination of the intra-spectral and inter-spectral features of a remote sensing image. The proposed features perform appreciably well with classifiers like Decision Trees, Support Tensor Machines and AdaBoost. However, as the features are computed from different spectral channels as well as from the same spectral channel, the process of feature extraction consumes time, when compared with

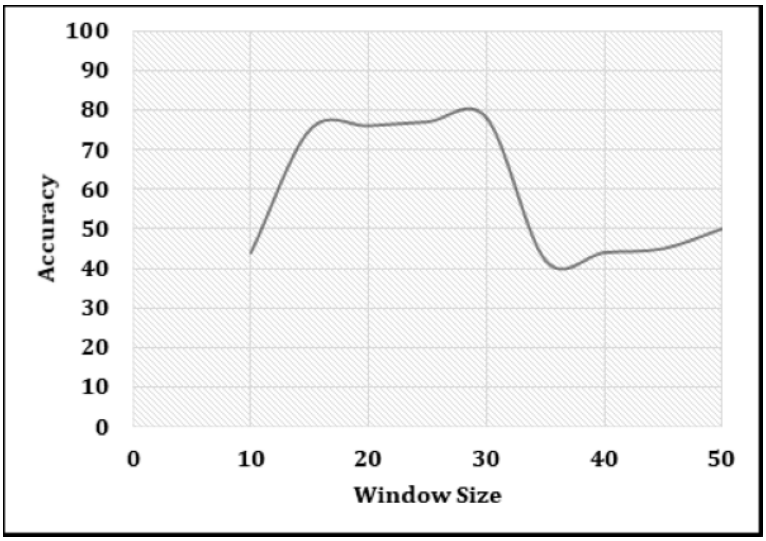

Figure 3.6: Window Size and Accuracy

the raw pixel values. But, as the classification accuracy gives better results, the above disadvantage is compromised with. The results of the classification show appreciable values with Support Tensor Machine for all classes and Adaboost for certain classes. Hence, it is concluded that the Support Tensor Machine captures the discriminative ability of the proposed features most effectively.

An insight acquired through the research is that the adequate representation of spatiotemporal data for the efficacy of the mining task is crucial. It is seen that the representation of the proposed features by a tensor produces better results for the mining task of classification. It is therefore concluded that tensor is an appropriate scheme to represent spatiotemporal raster data and is used in subsequent studies. The tensor representation of spatiotemporal data and its effectiveness in colocation pattern mining and change detection is attempted in the forthcoming chapters.

Chapter 4

Spatial Colocation Pattern Mining

4.1 Introduction 50
4.2 Related Research 52
4.3 Tensor Model for Pattern Discovery in Image-Objects 53
4.3.1 Tensorization 54
4.3.2 Spatial Pattern Discovery from Tensorized Image-Objects . 55
4.4 Spatial Colocation Pattern Mining Framework 57
4.4.1 Pixel Mapping to Image-Objects (PMIO) 58
4.4.2 Spatial Colocation Pattern Mining using Tensor Factorization (SCLP-TF) 60
4.5 Results and Discussions 64
4.5.1 Dataset 64
4.5.2 Experiments 64
4.5.3 Evaluation 66
4.6 Summary of the Chapter 70

In this chapter, a spatial colocation mining framework is proposed that mines spatial colocation of image-objects present in spatiotemporal raster data using a tensor factorization approach. The framework takes in spatial raster image data, tensorize it and perform the mining task, thus eliminating the need

to convert it into a transaction. An interestingness measure called, "spatial dominance" is also proposed in this work. This measure is an indicator of the prevalence of the mined colocation pattern. Algorithms are designed in this framework, first to map the classified pixels as members of image-objects, which is a pre-stage before mining and second to find spatial colocation patterns. Experiments are performed to establish the strength of the proposed spatial colocation mining algorithm.

4.1 Introduction

Colocation pattern mining is the process of finding patterns that are located together in close proximity. Mining of colocation patterns can be done in spatial, temporal, and spatiotemporal aspects. Colocation pattern mining yields important insights in application domains like environment monitoring [4], earth science [60], mobile services [27], and urban facility analysis [5]. The task of colocation pattern mining is challenging because of the following facts (a) the features of the data under study is embedded in continuous space in contrast to the traditional transaction type discretized structure and (b) numerous spatial relationships exist between the features of the data thus resulting in considerable computation time for finding the significant number of colocation instances.

Traditionally, spatial colocations are mined in transaction databases, where each space instance is modeled as a row in a table. Spatial colocation mining finds spatial colocation instances and generalize the same to a pattern, based on interestingness measures. This will result in enormous computation time as the instances are to be discovered, modeled appropriately, and further downsized to obtain patterns. The complexity of the work structure mentioned increases

as there are no transaction databases for image data. Building a transaction database for image data is a manual interventional task. Hence there is a crucial need to find spatial colocations from image data without the aid of a transaction database.

The spatial colocation mining algorithm proposed in this chapter is based on the concept of tensors, which are basically multi-way arrays. The tensor data structure captures all kinds of spatial relationships that exist between objects or entities. The objects or entities in this research are from images, which are termed as image-objects. Hence there is a necessity of a pre-stage of finding image-objects from pixel-wise classified images, which is also taken care of in this work. To the best of our knowledge, this is the first work that proposes to apply spatial colocation in images. The advantages of modeling image-objects as tensors are (i) management of huge amount of data with tensors is easy (scalable images/image-objects) (ii) tensors are easily reducible to lower dimensions resulting in easy understanding of latent information and (iii) extraction from tensor data to lower dimensions results in more components of information than ordinary matrix-based methods.

The chapter is organized as follows. Section 4.2 briefs about the related research in colocation pattern mining of spatial data. The theoretical study of the tensor model for pattern discovery in image-objects is described in Section 4.3. The spatial colocation pattern mining framework and the proposed algorithms are explained in Section 4.4. The experiments, results, and discussions are detailed in Section 4.5. The chapter is concluded in Section 4.6.

4.2 Related Research

Spatial colocation patterns represent the subsets of spatial events whose instances are often located in close geographic proximity. The first reference of colocation pattern is seen in spatial statistics by Huang [65]. An attempt to perform spatial colocation mining is initially observed in [110]. This work captures a subset of spatial features for a particular class, which is different from the colocation mining concept in today's world. An effective approach is presented in [111] that depicts a space partitioning method for identifying neighborhood regions that contain instances of colocations. However, the algorithm may miss colocations across the different neighborhoods, due to distinct partitions. A join-based colocation mining algorithm is presented in [112] which works similar to Apriori [113]. This is a computationally expensive process with an increase in the number of colocation instances. An approach to perform a partial join to increase computational efficiency is seen in [114]. In this work, the spatial data is modeled as a clique neighborhood, and the cut in the neighborhood determines the colocation instances mined. The joinless approach [115] reduces the computational time by introducing the instance look-up scheme instead of the regular join operation. The algorithm does not miss any colocation patterns, even though the computational time is dependent on the size of the data.

A framework for spatial colocation pattern mining based on association analysis and maximal clique representation of the spatial data is presented in [116]. However, in this case, the spatial data has to be modeled as transaction type data to perform mining of the spatial colocation instances. Representative Colocation Pattern (RCP) mining is introduced in [117] to

reduce the exponential number of patterns that arise due to an increase in data size. Instead of the distance measure, a new prevalence measure is introduced in this work to find the covering relationship among spatial colocation instances. In [118] maximal colocations are identified through a maximal clique based approach wherein a Sparse undirected Graph is used for the purpose. Each instance clique of a maximal colocation is further stored in a Condensed Tree to reduce the storage size. This algorithm is hereafter referred to Sparse Graph Condensed Tree algorithm (SGCT). But the algorithm does redundant computations when the instances generated have a huge number of object types.

4.3 Tensor Model for Pattern Discovery in Image-Objects

Image-objects are entities in an image, which are actually groups of pixels of similar digital values. Image-objects possess size and shape in addition to the pixel value and location, that is, an image-object holds spatial as well as non-spatial attributes. Non-spatial attributes are the characteristic features holding nominal values like label or name of image-objects. Spatial attributes are the spatial location (longitude and latitude), spatial extent (area, perimeter, size), spatial shape (point, extended, polygon), and even spatial elevation. As the non-spatial attributes and their relationships are explicit, the focus is on discovering the implicit spatial attributes and their relationships. The spatial relationships or patterns that exist among image-objects can be sought in set space, topological space, metric space, or distance space. Hence it is felt that the pattern discovery of image-objects in all spaces will yield knowledge beneficial for decision-making systems. A tensor model for pattern discovery of image-objects is proposed in this work. Tensor modeling enables a

paradigm shift from two-way to multi-way components or analysis of the spatial image-objects.

4.3.1 Tensorization

The multifaceted/multidimensional spatiotemporal data has to be stacked as a tensor. The 'N' spatial relationships between the image-objects can be modeled as tensor to start with. Let the tensor be represented as $\mathcal{S}$. The tensor is to be stacked with the spatial relationship between all image-objects. Assuming there are K image-objects in the datasets $(I_1, I_2, I_3, \ldots, I_S)$ and the number of spatial relationships can be $(S_1, S_2, S_3, \ldots, S_N)$. Thus the image-objects can now be looked upon as a tensor as follows.

$$\mathcal{S} \in \mathbb{R}^{K \times K \times S_1 \times S_2 \times \cdots \times S_N} \tag{4.1}$$

Depending on the spatial relationship in set space, topological space, metric space, or distance space chosen for study, the set $\{S_1, S_2, S_3, \ldots, S_N\}$ can be decided.

For each image-object, say $X \in (I_1, I_2, I_3, \ldots, I_S)$, generate a set of matrices $K \times K$, where K is the number of image-objects. The next step is to stack these matrices to form a third order tensor $\mathcal{S} \in \mathbb{R}^{K \times K \times N}$. For a chosen set of spatial parameters , say, ρ_n from $\{S_1, S_2, S_3, \ldots, S_N\}$, the nth matrix for $(k_1, k_2, ..., k_K)$ image objects can be constructed as

$$s(k_1, k_2, \rho) \text{ in } (k_1, k_2, \ldots k_K) \times (k_1, k_2, \ldots k_K) \text{ with parameter } \rho_n$$

Definition 4.1 —*Tensorization*—The process of converting or stacking all spatial relationships in the defined space existing between the image-objects into a tensor.

4.3.2 Spatial Pattern Discovery from Tensorized Image-Objects

The modeled tensor contains information about the patterns of spatial relationship that exists between the image-objects. The question posed here is how to uncover the pattern that exists inside the tensor. The spatial patterns that exist between the image-objects have to be discovered by extracting the lower dimensional factors of the tensor. This can be achieved by canonical decomposition of the tensor, which is introduced in Chapter 2.

Consider a 3-order tensor $\mathcal{S} \in \mathbb{R}^{X \times Y \times Z}$. The tensor in factorized form can be expressed as the sum of component rank-1 tensors as follows, where the rank-1 tensors are vectors, say, a, b, c.

$$\mathcal{S} = \sum_{r=1}^{R_s} a_r \circ b_r \circ c_r. \tag{4.2}$$

The symbol $\circ$ represent the outer product of the vectors and R_S is the number of components in this model and the smallest value of R_S is the rank of the tensor $\mathcal{S}$. The tensor rank cannot be calculated by any known algorithm, as it is a NP-hard problem. A typical use of 3-order tensor is to model the interaction between three image-objects, say, X, Y, and Z. An entry s_{ijk} of the tensor denotes the interaction pattern of (x_i, y_j, z_k). In accordance with the factorization model described as above, each entry in the tensor is the product of three latent vectors.

$$s_{ijk} = \sum_{r=1}^{R_s} x_{ir} \circ y_{jr} \circ z_{kr}. \tag{4.3}$$

Thus the tensor contains latent feature represented for the image-objects under consideration. The interaction pattern of the image-objects can be recovered once the decomposition is done successfully.

Continuing with Eq (4.2), to generalize, the set of vectors $\mathbf{a}\{1, 2, \ldots, R_S\}$, $\mathbf{b}\{1, 2, \ldots, R_S\}$ and $\mathbf{c}\{1, 2, \ldots, R_S\}$, can be written as a matrix, where each of the R_S vectors is a column of the matrix. Thus the factorization of a 3-order tensor can thus be represented in terms of three matrices, say, $\mathbf{A}, \mathbf{B}, \mathbf{C}$. To conclude, an effective factorization is to minimize the difference between $\mathcal{S}$ and $[\mathbf{A}, \mathbf{B}, \mathbf{C}]$ as

$$\min_{A,B,C} \|\mathcal{S} - [\mathbf{A}, \mathbf{B}, \mathbf{C}]\|_{F^2} \tag{4.4}$$

where $\mathbf{A}, \mathbf{B}, \mathbf{C}$ have dimensions $X \times R$, $Y \times R$, and $Z \times R$ respectively and $R < R_S$.

The way to solve this problem is to find R rank-1 tensors that best approximate the tensor. The decision of the value of R helps to find the patterns that exist between image-objects. A lower value of R yields only the strongest underlying patterns, whereas a higher value of R will produce weakest patterns, and is also prone to the risk of over-fitting. Thus choosing R is an optimization problem, and the resulting R number of components yield the spatial patterns that exist between image-objects.

Definition 4.2 —*Spatial Pattern Discovery from Tensorized Image-Objects*—The process of finding explicit patterns in the latent space that exists between image-objects through the decomposition of tensorized data.

Advantages of using Tensor based Model

(i) The high dimensionality associated with the spatial relationships is to find different compact spatial patterns without modifying the algorithm in its entirety.

(ii) The tensor model can be used for finding the spatial pattern in any space that exists between the image-objects as long as the relationship patterns can be appropriately represented. Hence the model can find patterns that capture multiple interactions in addition to standard pairwise interactions.

4.4 Spatial Colocation Pattern Mining Framework

The spatial pattern discovery using the tensor-based model is attempted in the metric space. There are two kinds of relationships in the metric space, namely, distance and topological. Mining the distance relationship that exists between image-objects helps to discover spatial colocation patterns. In this framework, the generalized tensor model is adopted for finding spatial colocation patterns. The workflow of the framework is presented in Fig. 4.1.

The proposed framework has two components (i) a neighborhood growing technique to find image-objects from a pixel-wise classified image and (ii) discovering spatial colocation patterns by factorizing the tensorized image-objects.

The first component performs the mapping of pixels to appropriate image-objects through a neighborhood growing technique and is named as "Pixel Mapping to Image-Objects" (PMIO) phase in the framework. The second component consists of two phases (a) tensorization of image-objects and (b) tensor factorization to mine spatial colocation patterns and is named as SCLP-TF.

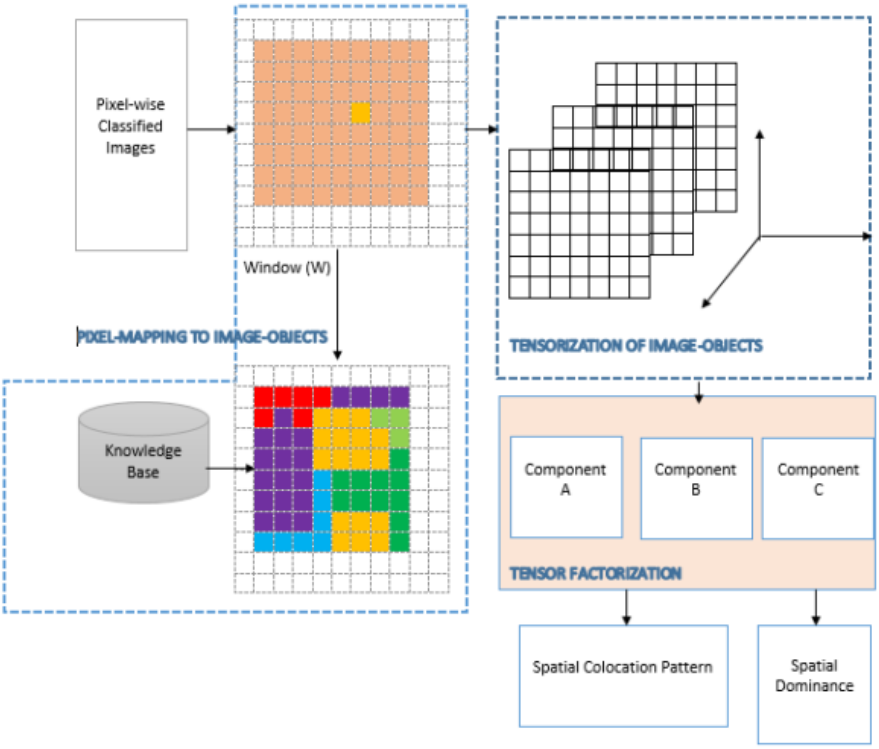

Figure 4.1: Spatial Colocation Mining Framework

4.4.1 Pixel Mapping to Image-Objects (PMIO)

The first phase, abbreviated as PMIO, is the phase in which a neighborhood growing technique is applied on a window of classified pixels. The objective of this phase is to extract image-objects from the classified image. The heuristic approach proposed, selects a window of random size, say W. The window size is generally set to a power of 2, for better computational results. From the centroid pixel of the window, the neighborhood is examined in $\log_2 W$ group of pixels, which is referred to as sub-window. On examining the neighborhood,

find the most occurring class label and assign it to the entire sub-window. The growing technique terminates when the threshold limits in terms of size (from the knowledge base input) are reached. The entire set of image-objects in the image can be identified when this algorithm is applied throughout the image. The algorithm also finds out the position of image-objects from the centroid pixel.

The selection of the size of the window as well as the sub-window is the deciding criteria for the extraction of image-objects. An appropriate window-size helps to find the image-objects accurately, whereas an under-fitting window will not identify all image-objects, and an over-fitting window will result in more computational complexity.

Algorithm 4.1: Pixel Mapping to Image-Objects (PMIO)

Result: Labels of Image-Objects and corresponding Positions

1 Input Classified Image, Window-Size W, Threshold size of Image-Objects α ;
2 Intialize subwindow size as log_2 W;
3 **while** *size of subwindow* $\geq \alpha$ **do**
4 Find class label of each pixel, say,C_j;
5 For each class label find count (C_j);
6 label (C_j) $\leftarrow$ max(C_j);
7 Return C_j as class label of I_k and centroid as P_{I_k};
8 Repeat steps 3 to 8 for the whole image;

4.4.2 Spatial Colocation Pattern Mining using Tensor Factorization (SCLP-TF)

After obtaining image-objects and the corresponding position, the next objective is to mine spatial colocation patterns. The spatial colocation patterns are mined using the tensor factorization method explained in the previous section.

Tensorization of Image-Objects

The image-objects $(I_1, I_2, \ldots, I_K)$ and their corresponding positions P_{I_1}, $P_{I_1}, \ldots, P_{I_k}$ in images under this study have to be stacked as a tensor, and the process is referred to as tensorization. As the intention is to find spatial colocation patterns, the spatial relationship has to be sought in metric space, and Euclidean distance is fixed as the relationship type. The tensor stack has to model the distance relation between all image-objects. The tensor is built with labels of image-objects in 1^{st} and 2^{nd} dimension (say, N image-objects), 3^{rd} dimension is tensorized using the Euclidean distance between image-objects (say, S). Let the tensor be represented as $\mathbf{S}$.

Tensor Factorization to find SCLP

The latent spatial patterns present in the tensorized data have to be discovered by using the principle of tensor factorization. Tensor factorization yields components of the tensorized image-objects and their distance relationships. The tensor $\mathcal{S}$ obtained after stacking is of 3^{rd} order kind. The canonical decomposition is applied on $\mathcal{S}$ for factorization using Alternating Least Squares method as explained in Chapter 2. The general solution is to find different number of components until the factorization fits into a defined error ratio.

The tensor $\mathcal{S}$ is of the order $N \times N \times S$. The tensor $\mathcal{S}$, has to be

factorized to obtain the decomposed components (matrices) say $\mathbf{A}$, $\mathbf{B}$ and $\mathbf{C}$ of the dimensions $N \times R$, $N \times R$ and $S \times R$ respectively, where R is the rank of the tensor. To start with the factorization, initialize R as $R_{\min}$ and randomly choose any two components say A and B. Find C using the formula given in the Eqn 4.5. The symbol $\odot$ indicates Khatri-Rao product and ‡ is the Moore-Penrose pseudo inverse.

$$C = S_3(B \odot A)((B^T B) \times (A^T A))^{\ddagger} \tag{4.5}$$

Repeatedly change the entries in $\mathbf{A}, \mathbf{B}$ and $\mathbf{C}$ and iterate this process over a definite number of times, where the deciding factor is the difference between the entries in the original tensor and the recovered tensor from the components $\mathbf{A}, \mathbf{B}$ and $\mathbf{C}$. The optimal selection of rank is done by finding the fitting of the original tensor and the decomposed components. The process terminates when R reaches $R_{\max}$ or the difference between the original tensor ($\mathcal{S}$) and recovered tensor ($\widehat{\mathcal{S}}$) meets the error-ratio, ϵ. Thus the decomposed R components for $\mathbf{A}, \mathbf{B}$ and $\mathbf{C}$ is obtained. The matrices $\mathbf{A}$ and $\mathbf{B}$ are same, as the two dimensions of the tensors are labels of image-objects. Each element in the recovered tensor is calculated as the inner product of $\mathbf{a}_i, \mathbf{b}_j, \mathbf{c}_k$ and the value s_{ijk} is assigned the association between $(\mathbf{a}_i, \mathbf{b}_j, \mathbf{c}_k)$, which is expressed as follows.

$$s_{ijk} = \mathbf{f}(\mathbf{a}_i, \mathbf{b}_j, \mathbf{c}_k) = \sum_{r=1}^{R} a_{ir} \cdot b_{jr} \cdot c_{kr}. \tag{4.6}$$

The decomposed components (a_{ir}, b_{jr}, c_{kr}) shows the interaction with respect to image-objects and the distance relation. The R components of $\mathbf{A}$, shows the interaction among image-objects (or frequent image-objects) with respect to the spatial pattern under consideration. The prominent/frequent

Algorithm 4.2: Spatial Colocation mining using Tenson Factorization (SCLP-TF)

Result: Decomposed components A, B, C, Spatial Colocation Pattern a_{ir} and Spatial Dominance c_{kr}

Input Minimal rank R_{min}, Maximum Rank R_{max}, Image Objects I_1,.., I_K, Positions P_{I_1},..., P_{I_K};
Input Error Ratio ϵ, Thresholds - Colocation t_{CL}, Dominance t_D;
Tensorize I_1,.., I_K and P_{I_1},..., P_{I_K} to form $\mathcal{S}$;
Intialize A and B randomly, R as R_{min};
repeat
    C = $S_3\ (B \odot A)\ ((B^T B) \times (A^T A))^{\ddagger}$;
    B = $S_2\ (C \odot A)\ ((C^T C) \times (A^T A))^{\ddagger}$;
    A = $S_1\ (C \odot B)\ ((C^T C) \times (B^T B))^{\ddagger}$;
    Find approximate tensor $\widehat{\mathcal{S}}$ = [[A,B,C]] , $diff_{A,B,C}$ = s_{ijk} - $\hat{s}_{ijk}$;
until $diff_{A,B,C}$ *ceases to improve*;

image-objects are chosen from $\mathbf{A}$ as

$$\prod_{r=1}^{R} a_{ir} \geq t_{CL}. \tag{4.7}$$

The R components of $\mathbf{C}$, shows the degree of spatial dominance for each image-object pattern identified from $\mathbf{A}$.

Definition 4.3 —*Spatial Dominance*—It is an interestingness measure in spatial domain that determines the degree of domination of a particular spatial colocation pattern in the set of images and is an indicator of how strong the pattern is in the given set of images.

$$\prod_{r=1}^{R} a_{ir} \geq t_{CL} \text{ and } c_{kr} \geq t_D \tag{4.8}$$

The prominent image-objects chosen are termed as a spatial colocation

pattern if and only if the corresponding spatial dominance in $\{c_{kr}\}$ is greater than the threshold dominance value t_D.

Correctness of the Algorithm

The decomposed components from the tensorized data, namely $\mathbf{A}$, $\mathbf{B}$ and $\mathbf{C}$ contain latent structure of the data under study and are equal components. The component $\mathbf{A}$ is of the dimension $N \times R$, where N is the number of image-objects, and R is the rank of the tensor. It has to be understood that the R vectors/columns of $\mathbf{A}$ contain a weighted assignment of the image-objects and their spatial relationship. On examining the R components, the weighted values show variation from a minimum to a maximum value, indicating the weak or strong association between image-objects. The threshold value called colocation threshold (t_{CL}) has to be chosen so that the strong associations of image-objects are to be extracted as patterns from the R columns of $\mathbf{A}$.

The decomposed component $\mathbf{C}$ is of the dimension $S \times R$, where S is the spatial relationship (distance) modeled, and R is the rank of the tensor. The R components contain a weighted component of the spatial relationship that exists between image-objects of all images under study. Hence this component gives a clear indication of the spatial measure under consideration. This is termed as 'spatial dominance' in the study. This interestingness measure gives an indication of the relevance of the spatial colocation pattern obtained from A. Associating the spatial dominance with the pattern from A; we obtain a set of image-objects termed as spatial colocation pattern with a prevalence measure called spatial dominance.

4.5 Results and Discussions

4.5.1 Dataset

Sparse and dense datasets are being used in this study to find spatial colocation patterns. $Data_1$ [119] consists of 10103 images and is a sparse kind of dataset. $Data_2$ [120] consists of 2873 images and is a dense kind of dataset. These pixel-wise classified images are first run through PMIO (stage 1) and image-objects, and their positions are identified. After the identification of image-objects, the SCLP-TF (stage 2) is applied to find the spatial patterns.

4.5.2 Experiments

The first stage in the framework is to perform the mapping of classified pixels to image-objects. As the output of stage 1, the labels of image-objects and their corresponding positions in the images are obtained. Sample examples of classified image-objects from $Data_1$ and $Data_2$ are shown in the Fig.4.2. The threshold sizes for the datasets are fixed through manual intervention. After the stage 1, 59 and 107 image-objects were extracted from $Data_1$ and $Data_2$ respectively. The image-objects are labeled semantically, and their positions in the images are also obtained as the output in stage 1. On doing an evaluation of the image-objects extracted with respect to the ground truth data, $Data_1$ consists of 68 image-objects, and $Data_2$ consists of 146 image-objects. Thus there are some missing image-objects when the PMIO method is applied, amounting to 0.09% in $Data_1$ and 0.39% in $Data_2$. The higher error rate in $Data_2$ is accounted for the following two reasons (a) $Data_2$ is a highly dense data set and consists of overlapping objects (b) $Data_2$ consists of different types of image-objects which vary much in size (pointing to the fact that the single threshold value is the cause

(a) $Data_1$ (b) $Data_2$

Figure 4.2: Image-Objects from the Dataset after PMIO

of 39 objects missed in the mapping).

In stage 2, the image-objects in all images, and the spatial relationship between them is tensorized. The tensor thus holds the association between image-objects and the distance between them. When the distance between the image-objects is computed, the resolution of the image helps to find the same. The distance value is tensorized only after normalization with respect to the resolution of the image.

After tensorization, the tensor is decomposed by applying ALS method, into which the minimum and maximum rank of the tensor has to be inputted. The range is chosen from 2 to 24. For each of the dataset, the convergence of the rank happens at different points. For $Data_1$, the rank of the approximate tensor is 7 and for $Data_2$, the rank is 11. At these rank values, the decomposed components resulting from factorization are projected to find spatial colocation patterns as per Algorithm 4.2.

Table 4.1: Sample Spatial Colocation Patterns Mined

Sl No.	Dataset	Sample Spatial Colocation Patterns with Spatial Dominance
1	$Data_1$	{ tvmonitor, cabinet, sofa [0.89] }
		{ computer, cup, person [0.78] }
		{ bicycle, person, road, sidetrack [0.56] }
2	$Data_2$	{ deskpart, doorside, screen [0.83] }
		{ desk, chairpart, chairwhole, bookshelf [0.77] }
		{ mousepad, deskwhole, keypad, mouse [0.77] }
		{ chairpart, table, stand, personsitting, shelf [0.68] }
		{ telephone, personstanding, poster [0.56] }

4.5.3 Evaluation

The objective of the proposed framework is to find spatial colocation patterns. The sample patterns mined from the datasets are summarized in the Table 4.1. The threshold value for spatial dominance is set at 0.5. Following the antimonotone property, the subsets of spatial colocation patterns are also colocated.

The number of spatial colocation patterns mined by the proposed framework and the relevant literature in [117] and [118] are compared for understanding the significance. The number of image-objects involved in each spatial colocation pattern is chosen as the performance parameter. The comparison is made in terms of the number of image-objects involved in mined patterns. It is observed that patterns containing more number of image-objects are being mined by the proposed algorithm. It is also understood that longer patterns are less understandable and hence, the threshold value to choose from the decomposed components is fixed to obtain a maximum of eight image-objects in the pattern. Fig. 4.3 shows the number of patterns (indicating the count of image-objects)

for Data_1 and Data_2.

The execution time for the algorithm is also compared with [117] and [118] for finding computational efficiency. The number of images being input to the data is taken as a function to find the execution time. The influence on computation time on the size of the input dataset for different algorithms is compared for Data_1 and Data_2. The computation time for SCLP-TF increases as the size of the dataset increases, just like other algorithms. The exponential increase in the computational time stabilizes after a particular feature/image size, attributed to the reason that the colocation patterns are largely extracted in the initial phase. The performance of RCP [117] is better as compared to the proposed algorithm, SCLP-TF because RCP mines only representative colocation patterns, and not all patterns in the image dataset. SGCT has longer computation time as it builds a sparse graph condensed tree for the dataset and traverses it to find the patterns, whereas SCLP-TF directly operates on the tensorized data and the factorized components to obtain the colocation patterns without a pre-processing step. Fig.4.4 plots the scenario described in this context for both the datasets.

To summarize the discussions on the experiments, the following points are noted.

- The tensor-based model to find spatial colocation patterns results in scalable computation time as compared with other algorithms and exhibits less sensitivity in dense data environments. The dense data set used in the experiments have helped to evaluate a scenario similar to large data sets, as it contains more number of image-objects and associated relationships.

- The colocation patterns yielded from the proposed models contain patterns

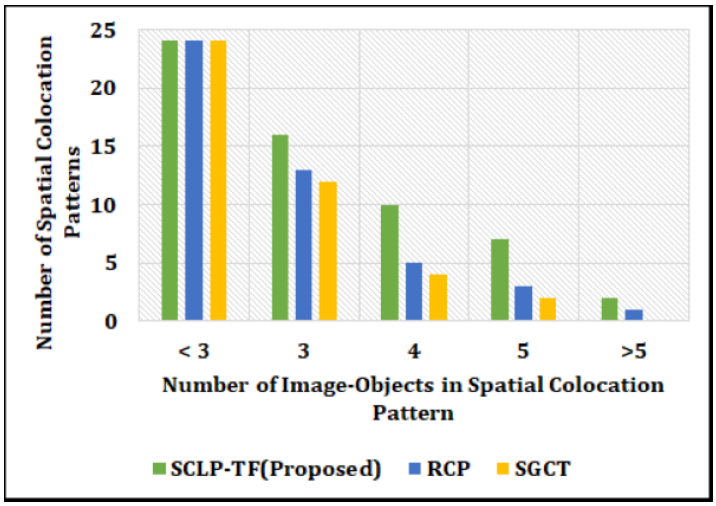

(a) $Data_1$

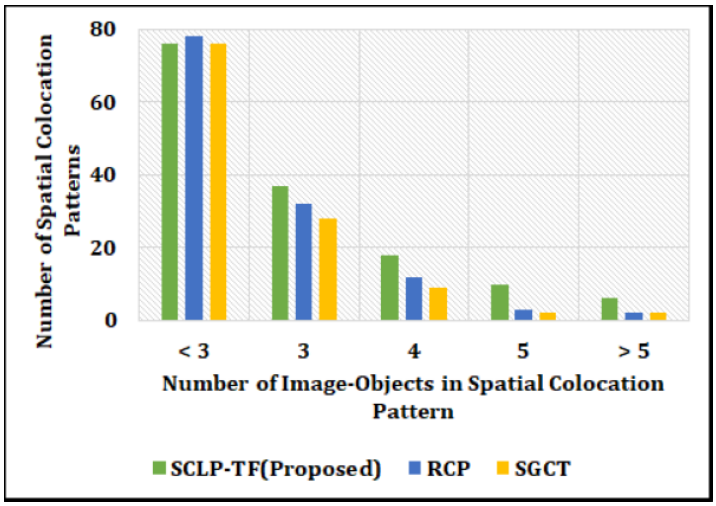

(b) $Data_2$

Figure 4.3: Number of SCLP mined vs Number of Image-Objects

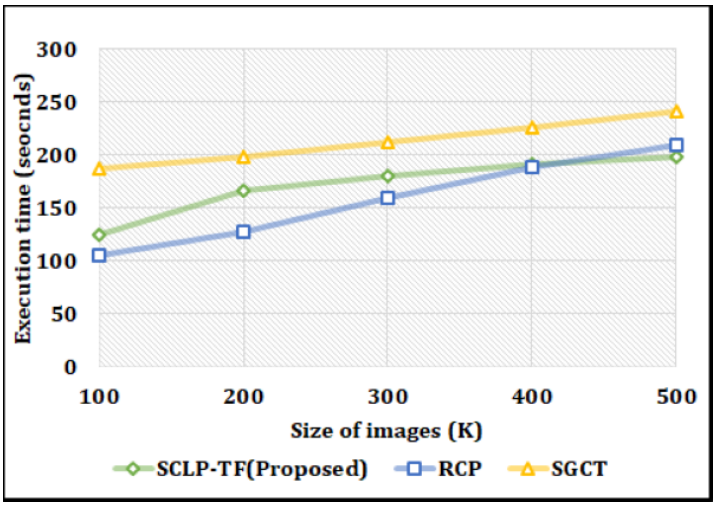

(a) $Data_1$

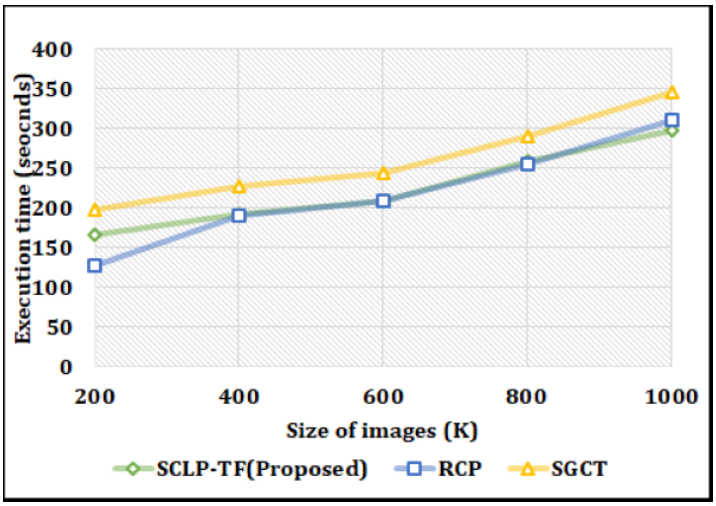

(b) $Data_2$

Figure 4.4: Computation Time Vs Size of Images

with more significance in terms of containment of the number of image-objects.

- The tensor modeling supports the image data without the need of conversion to transaction type data.

4.6 Summary of the Chapter

In this chapter, a spatial colocation pattern mining framework is proposed. In the proposed framework, a pixel mapping of the classified image to image-objects and their corresponding locations is done in the initial phase. The image-objects and their positions are then tensorized to stack the objects and their spatial relationship in a 3-order tensor. The tensorized data is decomposed to obtain the association between the image-objects in terms of the spatial colocation relationship existing between them. The significant colocated patterns are identified with the aid of the spatial dominance factor from the decomposed component of the tensor. On analysis of the spatial colocation patterns, it is observed that patterns containing more than three image-objects are obtained from the proposed framework, and the computation time associated with the framework also is at par with the existing relevant literature. Thus the proposed work attains the objective to mine spatial colocation patterns consisting of image-objects. By tuning the threshold size of the image-objects, the colocation patterns mined can contain image-objects of varying size.

In this work, the tensor model is used to mine spatial colocation in distance space. The tensor model can be enhanced to define other spatial relationships in topological space, metric space, or set space to find patterns accordingly. Successful spatial colocation mining using the method of tensor factorization

paved the path to extend the idea to the spatiotemporal colocation model described in the next chapter. So in the forthcoming chapters, the tensor factorization methodology is extended to obtain spatiotemporal colocation patterns, where the temporal relationship between image-objects is the decisive factor in addition to the spatial relationship.

Chapter 5

Spatiotemporal Colocation Pattern Mining

5.1 Introduction 74
5.2 Related Research 75
5.3 Spatiotemporal Colocation Pattern Mining Framework 76
5.3.1 Spatiotemporal Colocation Pattern Mining using Boolean Tensor Factorization (STCLP-BTF) 77
5.3.2 Spatiotemporal Colocation Pattern Mining using Incremental Boolean Tensor Factorization (STCLP-ITF) . . 80
5.4 Results and Discussions 84
5.4.1 Datasets 84
5.4.2 Experiments 84
5.4.3 Evaluation 87
5.5 Summary of the Chapter 93

This chapter proposes a design to mine spatiotemporal colocation patterns using the tensor factorization approach. Spatiotemporal colocation patterns are discovered using the Boolean tensor factorization method. As the time series data grow immensely, an incremental approach of tensor factorization

is also brought into the enhanced design. The results of mining are discussed in length, and the proposed algorithm is evaluated for decisive parameters. The incremental approach consumes optimal storage space, even when the number of time slots increases.

5.1 Introduction

Spatiotemporal Colocation Pattern mining is the process of finding patterns that are located together in space and time. Spatiotemporal colocation pattern mining problem can be applied in all kinds of spatiotemporal data types. For example, if the data type is event, the colocated events with a hurricane is a heavy flood, strong winds, and evacuation of low lying land areas. Spatiotemporal patterns are important in many application domains like crime analysis, change detection, public safety, and disease outbreak detection. Spatiotemporal pattern discovery is a challenging problem for two key reasons: (1) quantifying the measure of interestingness of ST patterns has complex constraints that include computational tractability and (2) the large cardinality of candidate patterns, which is exponential in the number of event types, that makes the problem complex.

In this work, spatiotemporal colocation patterns are sought in raster data. The raster data is modeled in terms of Boolean features, and the concept of Boolean Tensor Factorization [121] is applied to discover the spatiotemporal patterns.The Boolean features are adopted in this work because the pattern being mined is the presence or absence of a particular spatial colocation on a temporal tag. As the spatiotemporal data grows in size, an incremental approach to Boolean Tensor Factorization is applied to save space and time in computational

aspects. The algorithm based on an incremental approach is analyzed in detail to evaluate the computational efficiency.

The chapter is organized as follows. The related research pertaining to spatiotemporal pattern mining is summarized in Section 5.2. The Spatiotemporal Colocation pattern mining framework and the proposed algorithms are detailed in Section 5.3. The experiment setup, results, and discussions are meticulously presented in Section 5.4. The chapter is concluded in Section 5.5.

5.2 Related Research

Celik et al. introduced the mixed-drove spatiotemporal co-occurrence patterns (MDCOPs) in [122]. The work used the distance-based event-centric neighborhood approach to generate spatiotemporal neighborhoods when mining MDCOPs. In MDCOP mining, the time frames are collapsed, wherein the temporal framework is divided into disjoint time frames. For each time frame (1) the event instances are considered to be in the temporal neighborhood, and (2) the prevalent spatial colocations, which occur during the same time frame, are found. Then, MDCOPs, which can be interpreted as temporally persistent spatial colocation patterns, are determined by checking their temporal persistence (time prevalence). In [122], the time prevalence is measured as the ratio of time frames where a colocation pattern is present to the total number of time frames. In Celik's succeeding work [123], the discovery of partial spatiotemporal co-occurrence patterns (PACOPs) is inspected. PACOPs are very similar to MDCOPs. These two works differ in finding the time prevalence of co-occurrence patterns. When finding PACOPs, the algorithm considers the

partially present (i.e., less frequently occurring) object types, and uses temporal participation index when determining the time prevalence. MDCOP mining uses a support-like time prevalence measure, which is based on the frequency, while PACOP mining uses temporal participation index, which is based on the relative participation (frequency). Pillai et al. introduced spatiotemporal co-occurrence patterns (STCOP) and spatiotemporal co-occurrence rules (STCOR) from datasets with evolving regions [66, 124, 125]. Recently, spatiotemporal event sequence (STES) mining algorithms also make use of spatiotemporal co-occurrence relationships among the evolving regions [126]. Event instances are considered to form a spatiotemporal co-occurrence if there exists a spatiotemporal overlap among these instances.

5.3 Spatiotemporal Colocation Pattern Mining Framework

In this framework, a tensor model is adopted for finding spatiotemporal colocation patterns. The workflow of the framework is analogous to the previous chapter.

As in the previous chapter, the proposed framework operates in a two-stage scenario, wherein (i) a neighborhood growing technique to find image-objects from the pixel-wise classified image and (ii) discovering spatiotemporal colocation patterns by tensorizing image-objects. The first stage performs the "Pixel Mapping to Image-Objects" (PMIO) phase in the framework, which was detailed in the previous chapter. The second stage consists of two phases (a) tensorization of image-objects and (b) tensor factorization to mine spatiotemporal colocation patterns and is named as STCLP-BTF.

5.3.1 Spatiotemporal Colocation Pattern Mining using Boolean Tensor Factorization (STCLP-BTF)

After obtaining image-objects and their corresponding positions, the next objective is to mine spatiotemporal colocation patterns. The process is described in the following subsections.

Tensorization of Image-Objects

As the objective is to find spatiotemporal colocation patterns, the spatial and temporal relationship has to be modeled as a tensor. The spatial relationship modeled is the distance relationship in terms of Euclidean measure. The temporal relationship is a temporal tag for the time series data available. To perform tensorization of image-objects, a distance threshold value (d_{th}) has to be provided, depending on the domain of the images under consideration. The tensor is built with labels of image-objects in 1^{st} and 2^{nd} dimension (say, N image-objects), and the 3^{rd} dimension for the particular temporal tag. The entry in the tensor is marked as a binary value depending on the distance between the two objects, say O_i and O_j on that particular temporal tag. If the distance value is greater than d_{th}, the presence of spatial colocation is marked as 1, otherwise as 0. Let the tensor be represented as $\mathcal{T}$.

Tensor factorization to find STCLP

The latent spatiotemporal colocation patterns present in the tensorized data is discovered by using the principle of tensor factorization. Tensor factorization yields components of the tensorized image-objects and their spatiotemporal relationships. The tensor $\mathcal{T}$ obtained after stacking is of 3^{rd} order kind. The canonical decomposition is applied on $\mathcal{T}$ for factorization using Alternating

Least Squares method. The general solution to perform factorization is to find the different number of components, until the factorization fits into a defined error ratio.

The tensor $\mathcal{T}$ is of the order $N \times N \times T$. The tensor $\mathcal{T}$, has to be factorized to obtain the decomposed components (matrices) say $\mathbf{A}, \mathbf{B}$ and $\mathbf{C}$ of the dimensions $N \times R$, $N \times R$ and $T \times R$ respectively, where R is the rank of the tensor. To start with the factorization, initialize R as $R_{\min}$ and randomly choose any two components say A and B. Find C using the formula given in the Eqn. The symbol $\odot$ indicates Khatri-Rao product and ‡ is the Moore-Penrose pseudo inverse.

$$\mathbf{C} = \mathbf{S_3}(\mathbf{B} \odot \mathbf{A})((\mathbf{B^T B}) \times (\mathbf{A^T A}))^{\ddagger} \tag{5.1}$$

Repeatedly change the entries in $\mathbf{A}, \mathbf{B}$ and $\mathbf{C}$ and iterate this process over a definite number of times, where the deciding factor is the difference between the entries in the original tensor and the recovered tensor from the components $\mathbf{A}, \mathbf{B}$ and $\mathbf{C}$. The optimal selection of rank is done by finding the fitting of the original tensor and the decomposed components. The process terminates when R reaches $R_{\max}$ or the difference between the original tensor ($\mathcal{T}$) and recovered tensor ($\widehat{\mathcal{T}}$) meets the error-ratio, ϵ. Thus the decomposed R components for $\mathbf{A}, \mathbf{B}$ and $\mathbf{C}$ is obtained. The matrices $\mathbf{A}$ and $\mathbf{B}$ are same, as the two dimensions of the tensors are labels of image-objects. Each element in the recovered tensor is calculated as the inner product of $\mathbf{a}_i$, $\mathbf{b}_j$, $\mathbf{c}_k$ and the value t_{ijk} is assigned the association between $(\mathbf{at}_i, \mathbf{bt}_j, \mathbf{ct}_k)$, which is expressed as follows.

$$t_{ijk} = \mathbf{f}(\mathbf{at_i}, \mathbf{bt_j}, \mathbf{ct_k}) = \sum_{r=1}^{R} at_{ir}.bt_{jr}.ct_{kr} \tag{5.2}$$

The decomposed components $(at_{ir}, bt_{jr}, ct_{kr})$ shows the interaction with respect to image-objects and the distance relation. The R components of $\mathbf{A}$, shows the interaction among image-objects (or frequent image-objects) with respect to the spatiotemporal pattern. The prominent/frequent image-objects are chosen from A as

$$\prod_{r=1}^{R} at_{ir} \geq t_{\text{CL}} \tag{5.3}$$

Algorithm 5.1: STCLP-BTF

Result: Decomposed components A, B, C, ST Colocation Pattern a_{ir} and ST Dominance c_{kr}

Input Minimal rank R_{min}, Maximum Rank R_{max}, Image Objects I_1,.., I_K, Positions P_{I_1},..., P_{I_K};
Input Error Ratio ϵ, Thresholds - Distance d_{th}, Colocation t_{CL}, ST Dominance st_D;
Tensorize I_1,.., I_K and P_{I_1},..., P_{I_K} to form $\mathcal{T}$;
Initialize A and B randomly, R as R_{min};
repeat
    C = $T_3\ (B \odot A)\ ((B^T B) \times (A^T A))^{\ddagger}$;
    B = $T_2\ (C \odot A)\ ((C^T C) \times (A^T A))^{\ddagger}$;
    A = $T_1\ (C \odot B)\ ((C^T C) \times (B^T B))^{\ddagger}$;
    Find approximate tensor $\widehat{\mathcal{T}}$ = [[A,B,C]] , $diff_{A,B,C}$ = t_{ijk} - $\hat{t}_{ijk}$;
until $diff_{A,B,C}$ *ceases to improve*;
Repeat steps 4-9 until R= R_{max} or $\mathcal{T}$ - $\widehat{\mathcal{T}} \leq \epsilon$;
Return A, B, C ;
for r = 1 to R, $\prod_{r=1}^{R} at_{ir} \geq t_{CL}$;
for each a_{ir} find corresponding spatiotemporal dominance c_{kr} ;
Choose image-objects at_{ir} whose $ct_{kr} \geq st_D$;

The R components of $\mathbf{C}$, shows the degree of spatiotemporal dominance for each image-object pattern identified from $\mathbf{A}$.

Definition 5.1 —*Spatiotemporal Dominance*—It is an interestingness measure in spatiotemporal domain that determines the degree of domination of a particular spatiotemporal colocation pattern in the set of images and is an indicator of how strong the pattern is in the given set of images.

$$\prod_{r=1}^{R} at_{ir} \geq t_{\text{CL}} \text{ and } ct_{kr} \geq st_{D}. \tag{5.4}$$

The prominent image-objects chosen are termed as a spatiotemporal colocation pattern if and only if the corresponding spatial dominance in $\{ct_{kr}\}$ is greater than the threshold dominance value st_{D}.

Remarks. As the temporal resolution increases, the 3^{rd} dimension of the tensor grows in size, and the storage space is in terms of 'T' modes for 'T' time slots. Usually, in a time-series image data, each second can contribute data, henceforth the rise in 'T' is considerable in terms of computation time. Thus for the proposed Boolean Tensor factorization approach, the storage space for temporal tensors increases.

Hence an incremental approach for Boolean Tensor factorization is proposed, which saves space and time.

5.3.2 Spatiotemporal Colocation Pattern Mining using Incremental Boolean Tensor Factorization (STCLP-ITF)

A. Tucker Decomposition

The previous section adopted canonical polyadic decomposition to factorize tensors. In this section, Tucker decomposition is applied to perform tensor factorization [35], which was introduced in Chapter 2. Unlike canonical decomposition, the Tucker model allows for there to be a different number of factors, say, R_1, R_2, R_3 along with each mode of a third-order tensor. It can be

stated that canonical decomposition is a special case of Tucker decomposition where $R_1 = R_2 = R_3$.

The Boolean Tucker decomposition of the binary tensor $\mathcal{X}$ and three integers R_1, R_2, R_3 is given as the product of binary core tensor, $\mathcal{G}$ of size R_1, R_2, R_3 and binary factor matrices $A \in \mathbb{R}^{N \times R_1}$, $B \in \mathbb{R}^{N \times R_2}$, $C \in \mathbb{R}^{T \times R_3}$.

$$\mathcal{X} = \vee_{r_1=1}^{R_1} \vee_{r_2=1}^{R_2} \vee_{r=1}^{R_3} \mathcal{G}_{r_1,r_2,r_3} \cdot ABC. \tag{5.5}$$

The factorization is optimized when

$$\min \left| \mathcal{X} - \vee_{r_1=1}^{R_1} \vee_{r_2=1}^{R_2} \vee_{r=1}^{R_3} \mathcal{G}_{r_1,r_2,r_3} \cdot ABC \right|. \tag{5.6}$$

Heuristic methods are used to find the core tensor and factor matrices. The task is more involved than any other decomposition, due to the presence of core tensor, for whose each value can affect the binary factors. A change in a single element in $\mathcal{G}$ can completely change the product matrices. The algorithm is guaranteed to converge as the error reduces in each iteration. The core tensor and factor matrices help to yield the underlying patterns more effectively, as the interpretation is made in low-order components. The Boolean factorization will yield a core tensor $\mathcal{G}$ and binary factor matrices $\mathbf{A} \in \mathbb{R}^{N \times R_1}$, $\mathbf{B} \in \mathbb{R}^{N \times R_2}$, $\mathbf{C} \in \mathbb{R}^{T \times R_3}$.

Each non-zero entry in the matrix $A \in \mathbb{R}^{N \times R_1}$, say at_{ir_1}, will indicate the presence of the i^{th} object. For the non-zero entry in the matrix $C \in \mathbb{R}^{T \times R_3}$, say ct_{kr_3} points to the presence of the time slot.

The reason for preferring Tucker decomposition is that the incremental approach is already performing an approximation of the tensorized data by taking covariance between different time slots, and we wish not to perform another approximation in terms of R_1, R_2, and R_3.

B. Algorithm

The incremental approach introduced to Boolean Tensor Factorization contributes to this work. The intuition for incremental approach is based on the following two points, (a) when dealing with time stamp models, the recent data is more important than historical data and hence the storage space can be reduced by storing only the recent one and (b) the change patterns of different timestamps is best detected by the covariance of the factor matrices during the iteration.

To perform incremental Boolean Tensor factorization, the initial steps include initialization of binary factor matrices $\mathbf{A} \in \mathbb{R}^{N \times R_1}$, $\mathbf{B} \in \mathbb{R}^{N \times R_2}$, $\mathbf{C} \in \mathbb{R}^{T \times R_3}$ randomly and three integers R_1, R_2, R_3 which are the components for factorization. The initial core-tensor is all set to zeroes. For all images, $t = t_3, t_4, \ldots, t_T$, the factor matrices are updated as per the Boolean Tucker factorization using ALS method. After the factor matrices are updated, the covariance of each of them is calculated. The covariance matrix is updated in an incremental mode, as given as follows for each matrix.

$$CA = CA_{\text{(old)}} \cdot F(T) + CA_{\text{(new)}} \tag{5.7}$$

The new covariance matrix is incrementally added to the old one. The selection of the old covariance matrix is made as a function of time, $F(T)$. The function can regulate the selection of the old covariance matrices, which can be opted to be stored after each incremental addition of a new time slot. The function can also be modified to take particular covariance matrices at selected time slots for finding seasonal changes that have happened in the covariance matrix. Once the covariance matrices are updated, the updation of the core tensor happens. The iteration continues until the approximation error of factorization is within

Algorithm 5.2: STCLP-ITF

Result: Decomposed components CA, CB, CC, ST Colocation Pattern a_{ir} and ST Dominance c_{kr}

Input Image Objects I_1,.., I_K , Positions P_{I_1},..., P_{I_K}, Error Ratio ϵ, Thresholds - Distance d_{th},ST Colocation t_{CL}, ST Dominance st_D;
Tensorize I_1 and I_2 and P_{I_1} and P_{I_2} to form $\mathcal{T}$;
Initialize A (N $\times$ R_1), B (N $\times$ R_2), C(N $\times$ R_3) randomly, $\mathcal{G}$=0 ;
For t = t_3, t_4,...t_T
update_A(T_1, A, $\mathcal{G}$(1), $(C \otimes A)^T$);
CA_{new} = cov(A) ;
CA = CA_{old} . F(T) + CA_{new};
update_B(T_2, B, $\mathcal{G}$(2), $(A \otimes C)^T$) ;
CB_{new} = cov(B) ;
CB = CB_{old} . F(T) + CB_{new};
update_C(T_3, C, $\mathcal{G}$(3), $(B \otimes A)^T$) ;
CC_{new} = cov(C) ;
CC = CC_{old} . F(T) + CC_{new};
update_$\mathcal{G}$ (T, $\mathcal{G}$, CA, CB, CC);
Find approximate tensor $\widehat{\mathcal{T}}$ = [[A,B,C]] , $diff_{A,B,C}$ = t_{ijk} - $\hat{t}_{ijk}$;
Calculate error as $\mathcal{T}$ - $\vee_{r_1=1}^{R_1} \vee_{r_2=1}^{R_2} \vee_{r_3=1}^{R_3} \mathcal{G}_{r_1,r_2,r_3} .CA .CB .CC$;
Repeat steps 4-16 until error $\leq \epsilon$;
Return CA, CB, CC ;
for r = 1 to R_1, $\prod_{r=1}^{R_1} ca_{ir} \geq t_{CL}$;
for r = 1 to R_2, $\prod_{r=1}^{R_2} cb_{ir} \geq t_{CL}$;
for each $ca_{ir} \cup cb_{ir}$ find spatiotemporal dominance cc_{kr} ;
Choose image-objects a_{ir} whose $cc_{kr} \geq st_D$;

the minimum error threshold value. The computational cost associated with the proposed approach is dependent on the rank of the tensor.

The advantage of the incremental Boolean Tensor Factorization lies in the fact that the space consumption is only dependent on the core tensor whose dimension is $R_1 \times R_2 \times R_3$, which will be very less than storing 'T' mode tensors for all the T time slots. The computational cost associated with this incremental approach only lies in finding the variance matrix of the binary factors.

The remaining steps are analogous to Algorithm 5.1.

5.4 Results and Discussions

5.4.1 Datasets

The spatiotemporal data set used in this experiment consists of

(i) Synthetic images acquired in 100 time frames consisting of 735 classes (hereafter referred as Spatiotemporal_Dataset_1 [127])

(ii) Geospatial images acquired in 120 time frames (hereafter referred as Spatiotemporal_Dataset_2 [128]). The number of objects/classes associated with the geospatial images are a) Agricultural b) Urban c) Forest d) Road e) Bare ground (f) Beaches (g) Rivers and (h) Sea-water.

5.4.2 Experiments

Experiments are performed for Algorithm 5.1 and Algorithm 5.2. The tensorization of image-objects results in a Boolean tensor. For Algorithm 5.1,which uses the canonical decomposition method, the R values are 12 and 18 for the first and second dataset, respectively.

The Algorithm 5.2 depicted the incremental mode of Boolean Tensor factorization. As Algorithm 5.2 is based on Tucker decomposition, the size of the core tensor is a decisive factor. The approximation of the original tensor is achieved through fine-tuning the reconstruction error for different ranks of core tensor. Fig. 5.1 presents the experimentation result for iterating on different values of core-tensor size to bring down the reconstruction error within the threshold value. The core tensor size of (4, 8, 8) is within the permissible value of the error threshold for Spatiotemporal_Dataset_1. The core tensor size values of (4, 4, 4) and (4, 4, 8) are within the permissible values of error threshold for Spatiotemporal_Dataset_2. From the experiments, the conclusion drawn is that the core tensor size permissible within the error threshold value is highly dependent on the dataset. The intention of choosing the synthetic dataset is to prove that the incremental Boolean Tensor Factorization works theoretically correct.

Another important measure for the spatiotemporal colocation pattern mining using STCLP-BTF is the distance threshold value (d_{th}) which is fed to the algorithm. To know the effect of the distance threshold, the value is varied in different ranges for the datasets. The observations are made in Fig.5.2. The distance threshold values for the sparse dataset is varied from 10 to 60 units. It is seen that the execution time increases when the threshold value is increased. This is attributed to the fact that as the distance threshold increases, the number of spatiotemporal colocation patterns mined increases.

The spatiotemporal colocation patterns mined from the datasets are presented in Table 5.1. Spatiotemporal Domination is indicated in the results, which is a measure of the prevalence of the spatial colocation during the time

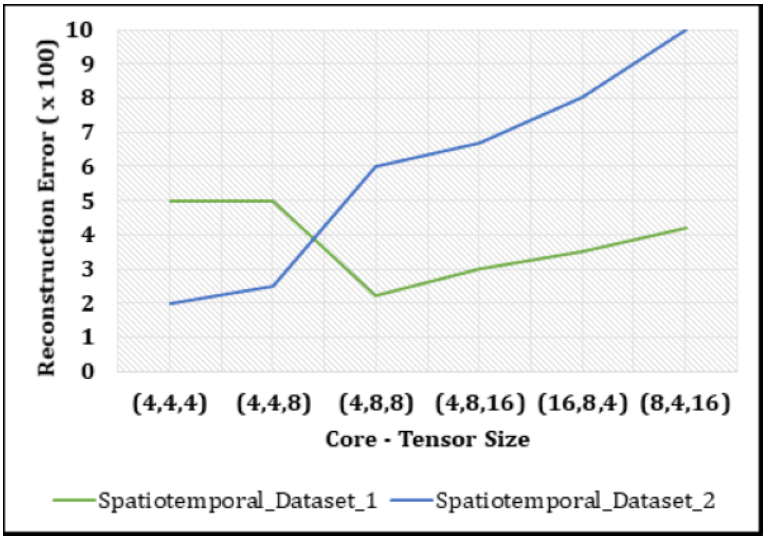

Figure 5.1: Optimization of Core Tensor Size

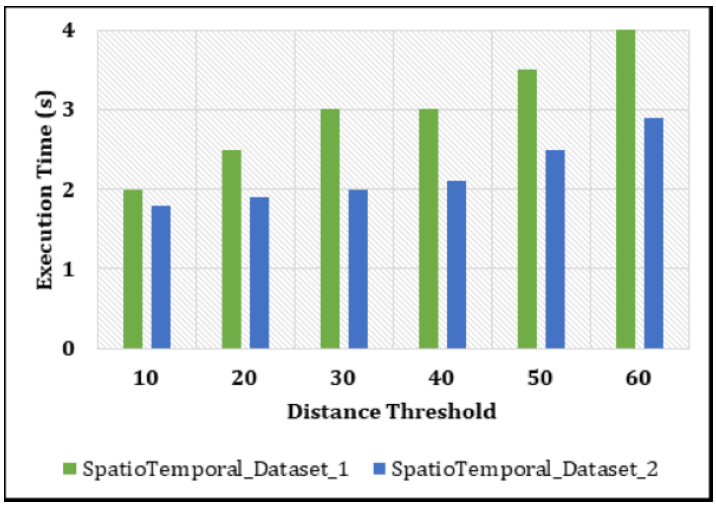

Figure 5.2: Execution Time as a function of neighbourhood distance threshold for STCLP-BTF

Table 5.1: Sample Spatiotemporal Colocation Patterns Mined using STCLP-BTF

Sl. No.	**Dataset**	**Spatiotemporal Colocation Pattern with Domination Strength**	**Distance Threshold**
1	SpatioTemporal_Dataset_1	$\{1, 3, \underline{296}[0.86]\}$ $\{711, 392, \underline{412}[0.63]\}$ $\{415, 412, 529, \underline{741}[0.63]\}$ $\{3, 296, 510, \underline{686}[0.41]\}$	100
2	SpatioTemporal_Dataset_2	{ baregrounds,beaches [0.51] } { baregrounds,waterbodies [0.49] } { river, roads, baregrounds [0.61] } { river, roads, buildings [0.42] }	50

frame in which the patterns are sought.

The change patterns are generally modeled for geospatial image datasets. Modeling of change patterns is henceforth performed only in Spatiotemporal_Dataset_2, as we feel that change models can be clearly understood when there is a limited number of objects.

The proportion of class changes over the period of the time frame is given by Fig. 5.3. In this graph, each bar presents the relative weighted amount of each class from the core tensor values as each time frame is increased. To see the overall gain and loss that has happened for the entire time period, Fig. 5.4 provides the proper insight. The red-colored portion indicates the percentage of loss that has happened to the particular class, and the green colored portion indicates the percentage of gain.

5.4.3 Evaluation

The algorithms proposed in this chapter, (a) STCLP-BTF and (b) Incremental BTF (STCLP-ITF) are compared with the relevant work in the literature to

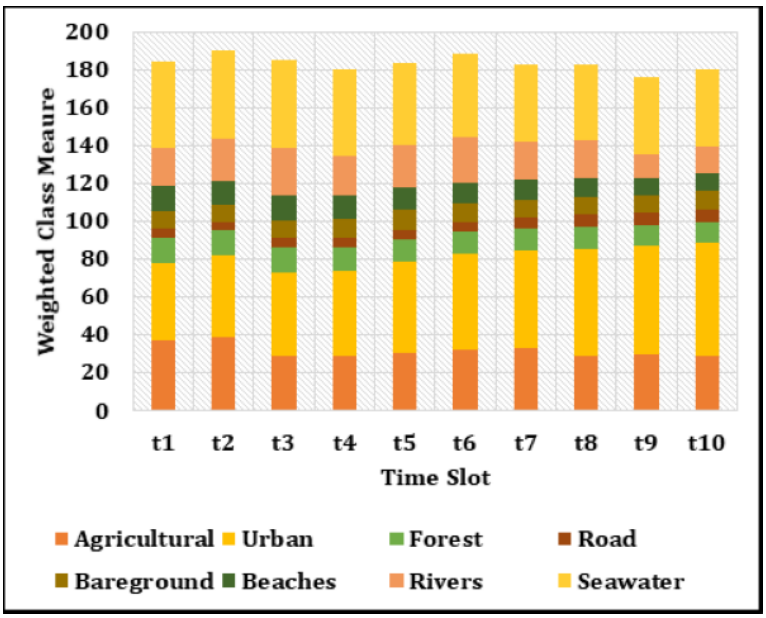

Figure 5.3: Proportion of class changes over the period of time frame

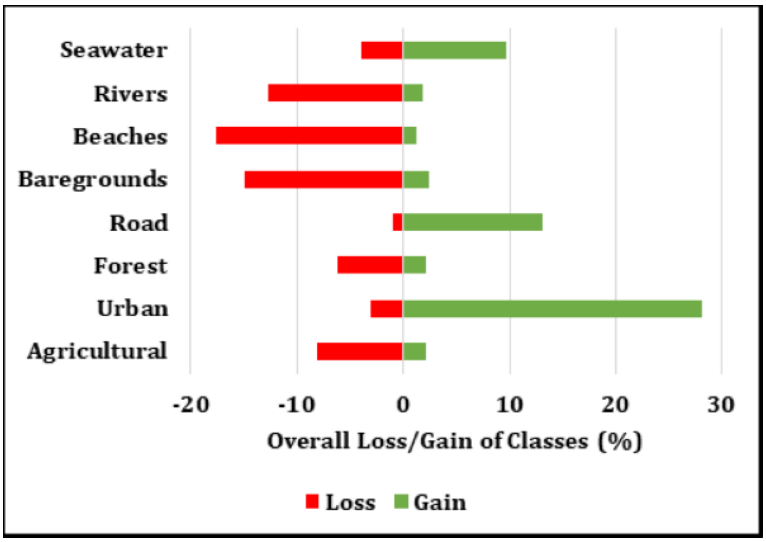

Figure 5.4: Overall loss/gain of classes over the period of time frame

understand the efficiency in terms of different factors.

The comparison of STCLP-BTF algorithm with MDCOP [122] is presented in Fig. 5.5. The figure presents the execution time as a function of the number of time slots. As the number of time slots increases, the execution time also increases for both the algorithms, as a result of the increase in the number of spatiotemporal colocation instances. The ratio of increase of execution time is smaller for STCLP-BTF in comparison with MDCOP, as the latter is based on the candidate approach, which results in an increased number of database scans with an increase in the number of spatiotemporal colocation instances. The distance threshold for the above experiments was set at 100 units. The patterns mined for the same datasets for MDCOP is presented in Table 5.2. It is seen that certain patterns are missing in this result when compared with Table 5.1.

Table 5.2: Sample Spatiotemporal Colocation Patterns Mined using MDCOP

Sl. No.	**Dataset**	**Spatiotemporal Colocation Pattern with Domination Strength**	**Distance Threshold**
1	SpatioTemporal_Dataset_1	$\{1, 3, \underline{296}\}$ $\{711, \underline{412}\}$ $\{415, \underline{741}\}$	100
2	SpatioTemporal_Dataset_2	{ baregrounds,<u>beaches</u> } { baregrounds,<u>waterbodies</u> } { river, <u>buildings</u> }	50

The second experiment for spatiotemporal dataset evaluates the effect of the number of classes/objects on STCLP-BTF and MDCOP. The distance threshold is set to 100 units. It is seen that for both the algorithms, as the number of objects increases, the execution time also increases. A sudden change in both the algorithms is observed between slots 18 and 22; it can be concluded that

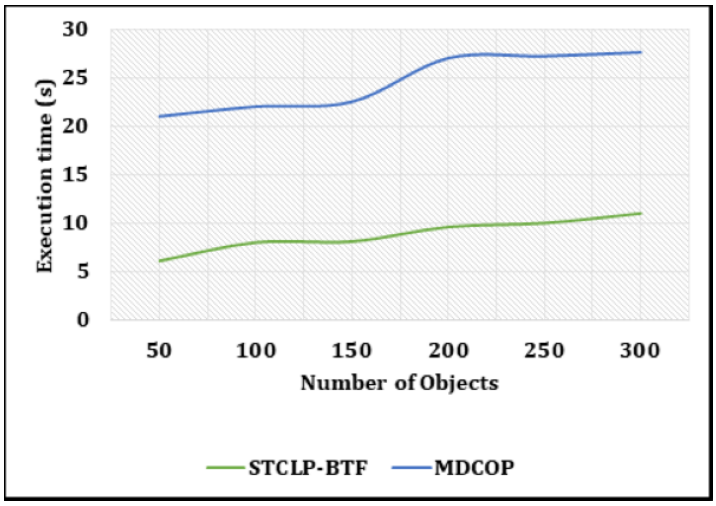

(a) Spatiotemporal_Dataset_1

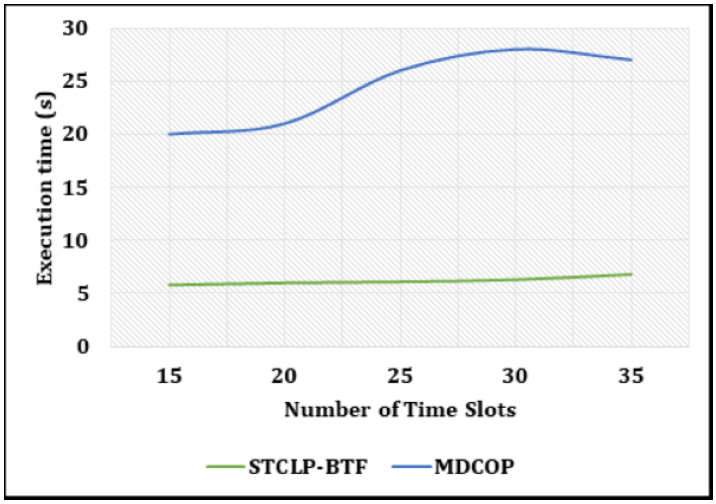

(b) Spatiotemporal_Dataset_2

Figure 5.5: Comparison on the effect of time slots on execution time

the newly added objects between 18 and 22 have more neighboring relations than other recently added objects after and before that particular slot. As the

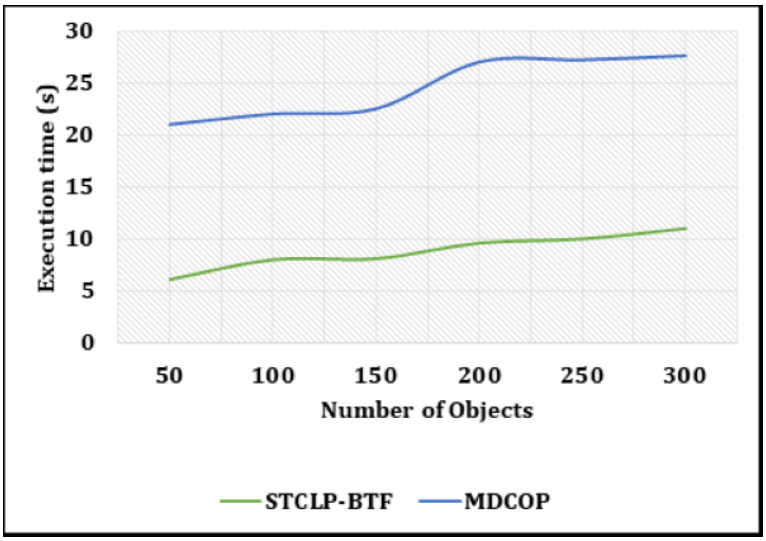

Figure 5.6: Comparison of the effect of number of objects on execution time

plots of graphs in Fig. 5.6 does not show a trend, the conclusion drawn is that the cost of the algorithm is dependent on the neighboring relations of the newly added objects to the existing objects. Experiments are performed only on SpatioTemporal_Dataset_1 as it is abundant in the number of object classes.

To perform an experimental evaluation of BTF and its incremental version, the Tucker factorization technique is applied to BTF also. The incremental BTF is compared with the traditional BTF to deduce the efficiency in terms of (a) Core Tensor size (b) Factor Matrix Density and (c) Convergence Time.

Both the datasets are evaluated for the core tensor size for (a) BTF and (b) Incremental BTF approaches. The results are presented in Fig. 5.7. It is seen that the reconstruction error is less for both the datasets in the same rank of core-tensor for the incremental approach. It can be deduced that the incremental approach converges faster as compared to the traditional method.

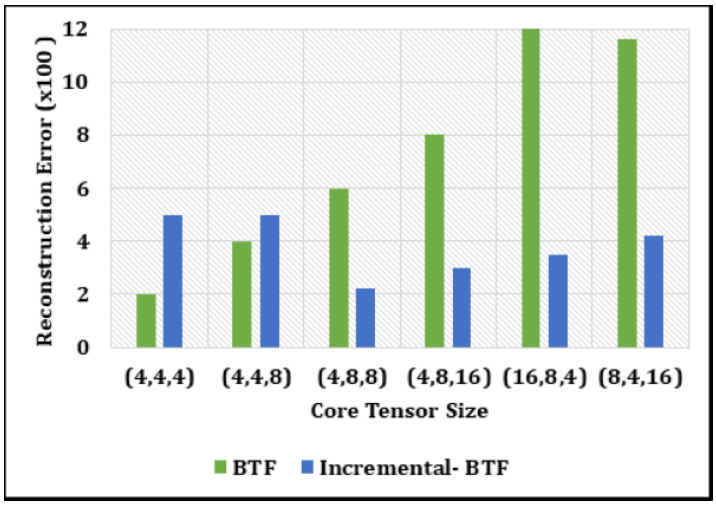

(a) Spatiotemporal_Dataset_1

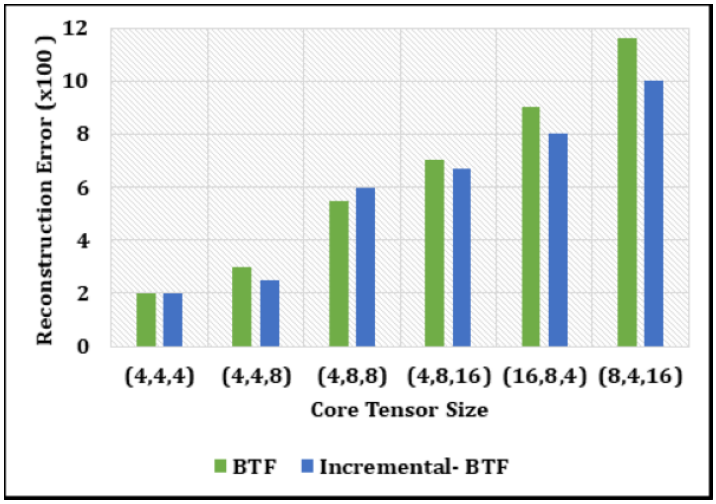

(b) Spatiotemporal_Dataset_2

Figure 5.7: Reconstruction Error for different Core Tensor Size

The convergence point of the datasets is also analyzed with respect to the factor matrix density. Fig. 5.8 presents the plot of reconstruction error versus

factor matrix density. Both methods perform synonymously in this analysis for the datasets. The denser the data, the higher the reconstruction error, as expected. Data with dense values will make the performance of algorithms more complex.

All the above said analysis points to the fact that the total convergence time for the incremental approach will be less as compared to the traditional method.

Fig. 5.9 shows the experimental results wherein the convergence time for the Boolean Tensor Factorization for the traditional and incremental approach is analyzed for both the datasets. It is seen that the incremental approach converges faster when compared to the traditional approach. It is also noted that there is a steep rise in the change from the first time slot to the second time slot in incremental approach, which owes to the computational cost of finding the variance of the factor matrices and associated diagonalization problem. However, after the second time slot, the convergence time does not increase drastically in the incremental approach.

5.5 Summary of the Chapter

The chapter proposed spatiotemporal colocation pattern mining algorithms, STCLP-BTF and STCLP-ITF, for raster data. The algorithms rely on tensor factorization approaches to find the colocation instances. STCLP-BTF uses traditional Boolean tensor factorization, whereas STCLP-ITF uses an incremental BTF. The incremental approach deviates from the traditional BTF approach and adopts a variance approach in finding the core-tensor and factor matrices. It is observed that the execution time for incremental approach is less as compared with the traditional approach.The core tensor yielded after

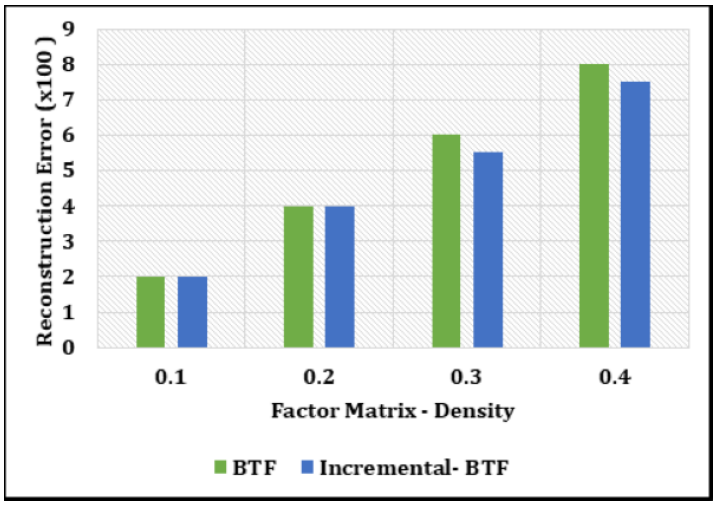

(a) Spatiotemporal_Dataset_1

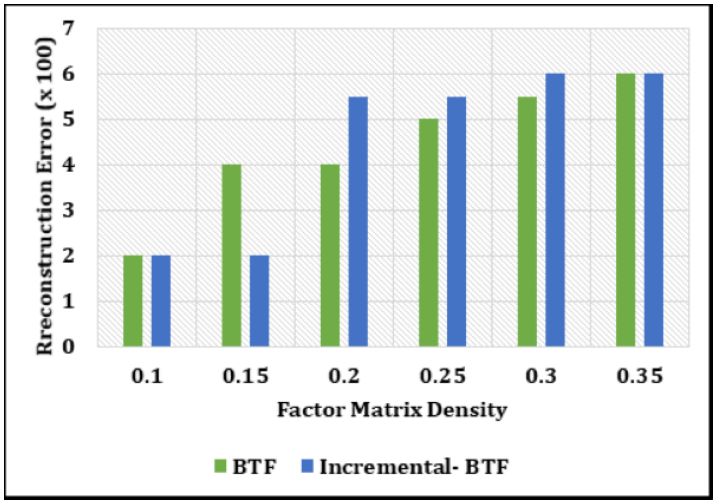

(b) Spatiotemporal_Dataset_2

Figure 5.8: Reconstruction Error for different Factor Matrix Densities

factorization will show the overall changes which have happened to the objects in the area under consideration. There is also a notable save in the space for

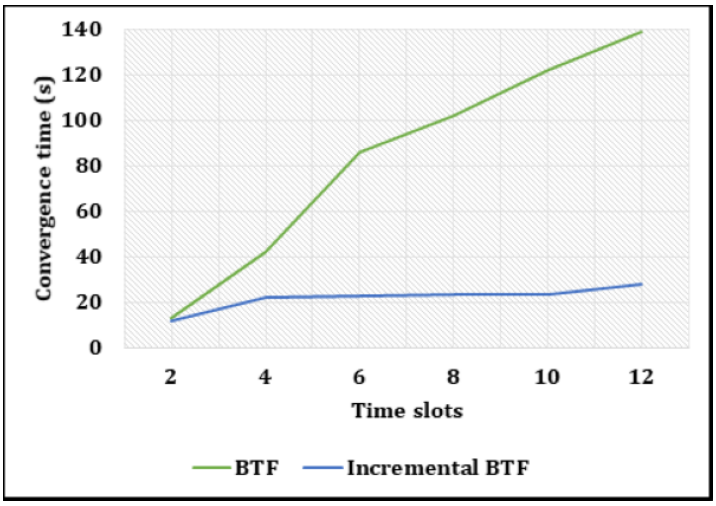

(a) Spatiotemporal_Dataset_1

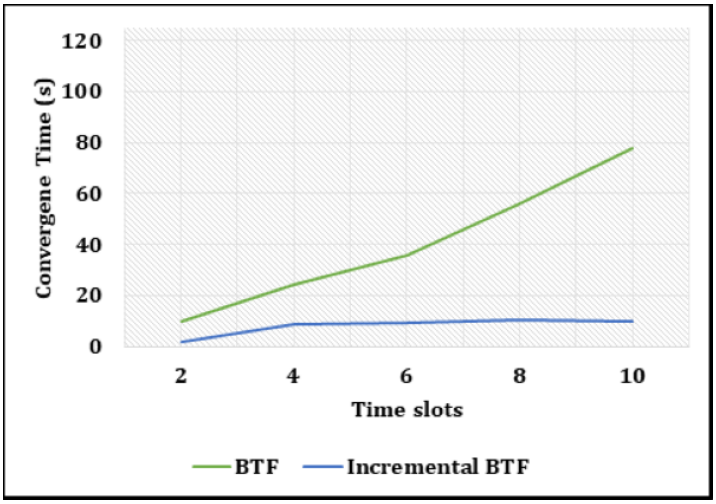

(b) Spatiotemporal_Dataset_2

Figure 5.9: Comparison of Convergence Time

incremental approach as $\mathcal{T}$ tensors associated with the time slots are not being stored.

From the studies, it is understood that the problem of change detection in spatiotemporal mining of landscapes can be attempted using the above-said approach, which is explained in the forthcoming chapter.

Chapter 6

Change Detection in Urban Landscapes

6.1 Introduction 98
6.2 Evaluative Study of Landscape Metrics 100
6.2.1 Background on Landscape Metrics 100
6.2.2 Dataset 102
6.2.3 Assessment of Landscape Metrics 104
6.3 Related Research 112
6.4 Design of the Proposed System 112
6.4.1 Tensorization of Image Regions 114
6.4.2 Identification of ROI, TOI and MOI 115
6.4.3 Hierarchical Spatiotemporal-Metric (STM) Miner 115
6.5 Results and Discussions 119
6.5.1 Datasets 119
6.5.2 MOIs associated with Growth Indices 121
6.5.3 Evaluation 124
6.6 Summary of the Chapter 129

The work proposed in this chapter is a Spatiotemporal-Metric Miner, which uses the spatial, temporal, and landscape metric data to discover the changes

that have occurred in a region. The model works on a hierarchical basis, wherein the regions of interest are chosen in a landscape and are aggregated to find the change that has happened over the entire region. The growth of a region is quantified by two novel parameters, namely, Inter-Class Growth Index and Intra-Class Growth Index. Experiments are performed on the landscape regions of Indian cities, and a ranking of cities is presented based on the growth indices.

6.1 Introduction

Characterization of changes that happened in a region has been a domain of study for quite a span of time. The understanding of how the region has changed/evolved in a particular time frame is essential to town planners in various aspects. The growth of a region is driven by many contributing factors, which is not in the scope of the study. This chapter characterizes the change detection of a geographic area through the landscape metrics [129]. Landscape metrics help in determining landscape characteristics, which are structural as well as functional. The structural metrics are related to the landscape configuration in terms of the situation of mosaics in space, and evenness of the land. The functional metrics are related to the landscape functioning in terms of land use and its change pattern evolving the land. Due to the vast number of landscape metrics available in the literature, there always exists confusion as of which are the prominent one, or what are the different metrics which help to quantify the smart growth of a region or which metrics helps to identify the change pattern occurred in a landscape. In this chapter, a study to identify a set of landscape metrics that helps to detect changes in a landscape, is attempted.

Followed by this, the prominent landscape metrics thus identified are utilized to develop a Spatiotemporal-Metric Miner (STM-Miner).

The STM -Miner proposed mines the change patterns of the classified land area over a particular temporal domain, to obtain further knowledge about the change regarding class labels and associated features that have occurred in a geographic region. In this work, mining of change patterns takes the task further forward by characterizing the change detected using different metrics. Usually, the change which has happened in a landscape area, after detection is only characterized by the associated class label and the area spanned. From this, the knowledge mined is insufficient. The work proposed considers not only *area* as the metrics of evaluation but also other metrics that measure the shape complexity associated with the area, diversity of the growth related to a region, evenness of the change detected in a landscape and so on. The change characterization in this work is built on a hierarchical model. To characterize a landscape area in terms of change pattern occurred, the whole land area is not mined. Instead of this, certain selected regions within the landscape are chosen and are mined. These regions are then aggregated in a hierarchical fashion to characterize the growth of the entire landscape.

The chapter is organized as follows. An evaluative study of landscape metrics is performed, and the decisive landscape metrics which help to detect changes are described in Section 6.2. Section 6.3 briefs about the related research which detects changes in urban landscapes. The design and architecture of the STM-Miner is proposed in Section 6.4. The experiments and results of the study are outlined in Section 6.5. The chapter is concluded in Section 6.6.

6.2 Evaluative Study of Landscape Metrics

This section introduces the different landscape metrics. A brief description of the same is also provided. The subsection performs an evaluative comparison of different landscape metrics to find the prominent or relevant ones to find changes associated with a region.

6.2.1 Background on Landscape Metrics

Landscape metrics [7] or indices help to describe the structure and pattern of a landscape. There are numerous metrics available at different levels, like patch, class, and landscape. From the literature, a set of relevant landscape metrics are identified, which are tabulated in Appendix B. The terms in the landscape metrics are also explained in Appendix B. A summary of all the metrics chosen for study are as follows.

(i) Area and Edge Metrics—Landscape Area denotes the total area of the land under consideration. Usually, the landscape area is expressed in hectares. The landscape is characterized by different classes or themes. These classes/themes characterize a landscape uniquely. Hence the measure *Class Area* is important as it provides an insight into the constitution of a landscape in terms of area. There can be numerous patches (cells) that may belong to the same class. A summation of these patches over a class is taken to find the class area of a particular class, say C. This metric is also expressed in hectares. *Mean Patch Size* is a function of class area and the number of patches. Individually, *Mean Patch Size* will not provide any information regarding how many patches are present for each class. Variation of *Mean Patch Size*, which evolves, will point to the growth/deterioration of a particular class in the landscape.

(ii) Shape Metrics—The *Mean Perimeter-Area Ratio* is a function of perimeter and area. *Contiguity Index* helps to measure the spatial connectedness, thus measuring compactness or elongation of a class in a patch. *Area Weighted Mean Fractal Dimension* is also a function of perimeter and area. It is computed over each patch and is averaged on each class in the landscape. It is calculated by regressing the logarithm of the perimeter on the logarithm of *Class Area*. The metric helps to assess the shape complexity associated with a patch of a particular class/landscape. Thus, this measure gives a value to the patch depending on the area of the patch, whereas *Mean Shape Index* is a measure that behaves independently of the size of the patch. An analogous measure to this is *Contrast Weighted Edge Density*, which standardizes edge to a per unit area and helps to compare between different regions of a landscape.

(iii) Aggregation Metrics—Aggregation metrics deals with the aggregation or clunking of different patch types. *Patch Density* is the number of patches on a per unit area that helps in comparing landscapes of varying sizes. The aggregation metrics of a landscape can also be assessed through *Contagion Index* and *Interspersion and Juxtaposition Index* (IJI) . The *Contagion Index* is based on the sum of different patch types expressed as the product of two probabilities such as (i) probability that a cell chosen randomly belongs to patch type i, and (ii) the conditional probability that given a cell is of patch type i, and one of its neighboring cells belong to patch type j. In short, the product of these probabilities equals the probability that two randomly chosen adjacent cells belong to different patch types i and j. The *contagion index* is thus based on cell adjacencies. *Interspersion and Juxtaposition index* is based on patch adjacencies. The adjacency of each patch is evaluated with

respect to all other patch types. IJI measures the extent to which the different patches types are equally adjacent to each other. *Splitting Index* is a measure of change of patch distribution. The value increases as the number of patches in the landscape increases and achieves maximum value when the landscape is maximally subdivided. *Splitting index* is an indicative measure of the number of patches in a landscape, when the landscape is divided into patches of equal size.

(iv) Diversity Metrics—Diversity metrics measure the richness and evenness of the different patch types in a landscape. These two factors are the compositional and structural indicators of a landscape. *Shannon's Diversity Index* (SDI) is a diversity metric based on information theory. There is no limit value for SDI, as the value grows higher, the interpretation is that the landscape is diversified in nature. This index represents the amount of information per patch of the landscape. *Shannon's Evenness Index* (SEI) is also a diversity metric obtained from dividing SDI by the maximum SDI for that number of patch types. The value ranges between 0 and 1. When the value approaches zero, the distribution of area among the different patch types becomes uneven.

(v) Contrast Metrics—Contrast Weighted Edge Density (CWED) standardizes edge to a per unit area that helps in computing landscape of different sizes. Thus landscape with the same value of CWED will have the same magnitude for edges from a functional view.

6.2.2 Dataset

The study area is Kochi region of Latitude 9°58'N and Longitude 76°17' E. Fig.6.1 depicts the regional division of Kochi into 11 regions. The western part of the Kochi region is covered by the Arabian Sea. The locations and boundaries

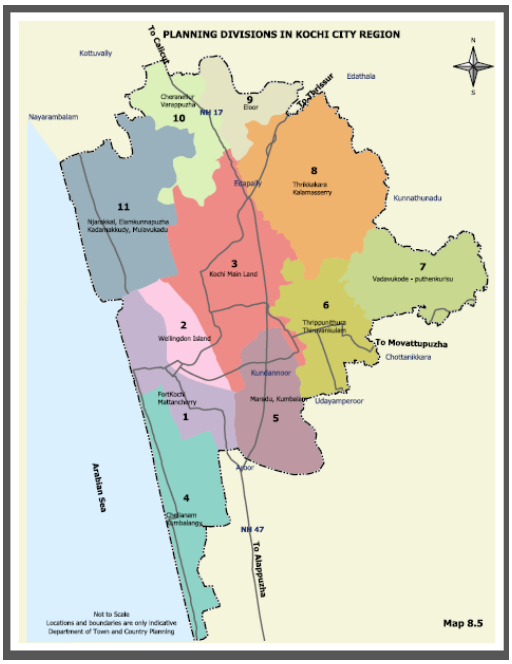

Figure 6.1: Regional Division of Kochi
Map Courtesy - *Department of Town and Country Planning, Kochi Corporation*

are only indicative. The water bodies in between the regions are not shown on this map.

Satellite images of LANDSAT 7 [130] and LANDSAT 8 [131] is used for the study. The specifications of LANDSAT 7 and LANDSAT 8 is given in Appendix A. The images were collected for two temporal tags of the year, say, 2006 and 2016. This study is highly restricted by the quality of the data obtained for analysis. The seasonal difference, illumination of the sun, radiometric distortions, and cloud coverage of the land are the challenging factors that restrict the quality of the image under consideration. The image is georeferenced and geometrically corrected before detecting the land use pattern. The spectral

data obtained from the satellite is classified into thematic information containing different classes. The land use classes for the image under study are Builtup, Water Bodies, Vegetation, and Barren Land. The classes are decided as so, due to the linear separation possible with the spectral information of the satellite. Land use patterns for the temporally tagged images of 2006 and 2016 are derived. The land use pattern obtained is verified with respect to the available ground truth information.

6.2.3 Assessment of Landscape Metrics

The study attempts to identify the landscape metrics, which help to quantify the change pattern in a geographic area over a temporal domain. The computation of the landscape metrics is done with the aid of the FRAGSTATS [132]. FRAGSTATS is a spatial pattern analysis tool that helps in quantifying the landscape structure. FRAGSTATS can quantify any landscape in terms of the landscape metrics defined in the literature. The quantification is possible in patch, class, and landscape level. Depending upon the analysis required, the appropriate metrics are chosen, as class and landscape metrics are more relevant for medium resolution images than the patch level metrics which are chosen for high-resolution images.

The landscape metrics listed in Appendix B is computed and analyzed in detail, to aid in finding out the parameters that help to characterize the change pattern of the study area. The study area is analyzed in terms of zones 1 (region 3), 2 (region 5), 3 (region 6) and 4 (region 8) in the central, northern, north-eastern and southern regions. The land use utilization in terms of each of the class, is the first measure of any change detection process. The land use classes used in the study are built-up, water bodies, vegetation, and barren

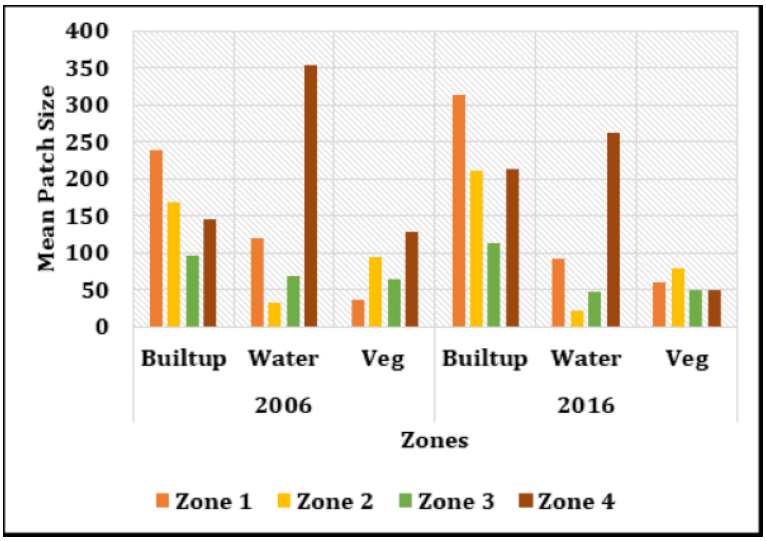

Figure 6.2: Mean Patch Size in Different Zones

land. The two timestamps under consideration are 2006 and 2016. Conventional methods depend only on the land-use area for change detection. In this work, the measurement of the area is done in terms of *Mean Patch Size*, which will help to know how the division of landscape into patches has happened. *Mean Patch Size* for the time domain is given in Fig. 6.2. *Mean Patch Size* is found in terms of the number of patches of the same type. The figure depicts the growth/retardation of each land-use class in terms of *Mean Patch Size*. However, to find the dominant class in a zone, the *Patch Inde*x is measured as a percentage of *Class Area* of each land-use class with respect to the total *Landscape Area*.

It is observed that the built-up land has increased tremendously in zone 1 by 2016, whereas zone 4 equaled with zone 2 in built-up land by 2016. True to the above findings, heavy vegetation lost is seen in zone 4. An interesting fact which is observed in the figure is that in spite of the tremendous growth of built-up land

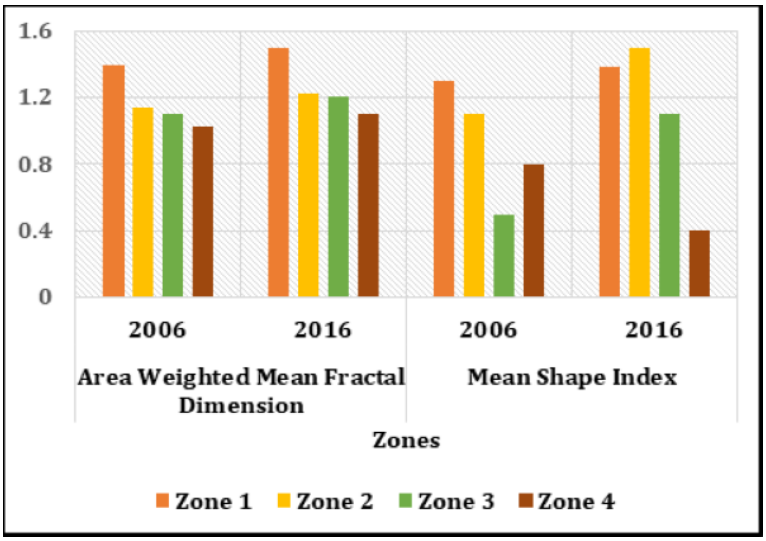

Figure 6.3: Comparison of Mean Shape Index and Area Weighted Mean Fractal Dimension

in zone 1, there is an increase in the vegetation, by a small percentage. Thus it is concluded that *Mean Patch Size* is a relevant area metric as worthy as *Class Area* and *Landscape Area*.

Shape complexity of the land use class in the landscape is an important indication of how far a landscape/class has undergone changes in the time domain. The shape metrics taken into consideration are *Mean Perimeter-Area Ratio, Mean Shape Index, Area Weighted Mean Fractal Dimension*, and *Contiguity Index*. The literature throws light into the fact that the perimeter-area ratio value varies with the size of the patch under consideration and does not provide an overall shape complexity of each land-use class. Hence this metric is not taken into consideration for analysis. *Mean Shape Index* overcomes this problem by adjusting the value for a square standard, and it is the simplest

measure of shape complexity. As observed from Fig. 6.3, *Mean Shape Index* is not aiding to find the shape complexity across different zones. The value of *Mean Shape Index* behaves indifferently and cannot be assessed properly. *Area Weighted Mean Fractal Dimension* is a more reasonable measure in the sense that it gives understandable values over a range of patch sizes.

From the figure, it is observed that the growth in terms of shape complexity is happening in all the zones almost equally. The two plots of *Area Weighted Mean Fractal Dimension* in 2006 and 2016 almost runs parallel, thus throwing light to the fact that the shape complexity evolved during this time remains almost constant. For the analysis of the shape, any compactness or elongation of the particular class is given by the *Contiguity Index*. Fig. 6.4 presents the *Contiguity Index* of each zone under consideration. It is seen that a drastic change in *Contiguity Index* is observed in zone 1 when compared with other zones, pointing to the conclusion that the rate of growth was high in zone 1 with respect to shape metric.

Aggregation metrics of the landscape indicate the dispersion and interspersion of a landscape. Both dispersion and interspersion is an indicator of landscape texture. Interspersion indicates the degree of intermixing of the different spatial classes, or more concisely, it is a measure of the degree of adjacency. Dispersion is the opposite sense of interspersion in indicating how often a spatial class is adjacent to the same spatial class. *Contagion Index* subsumes the measure of interspersion and dispersion.

Interspersion and Juxtaposition Index (IJI) is a measure that indicates only interspersion. The index measures the extent to which the patch types are equally adjacent to each other. Lower values of IJI indicate how the patches are

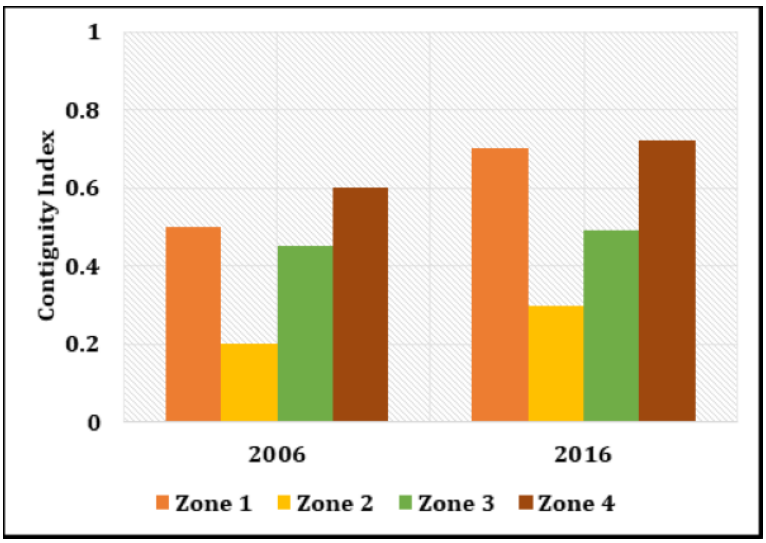

Figure 6.4: Comparison of Contiguity Index of different zones

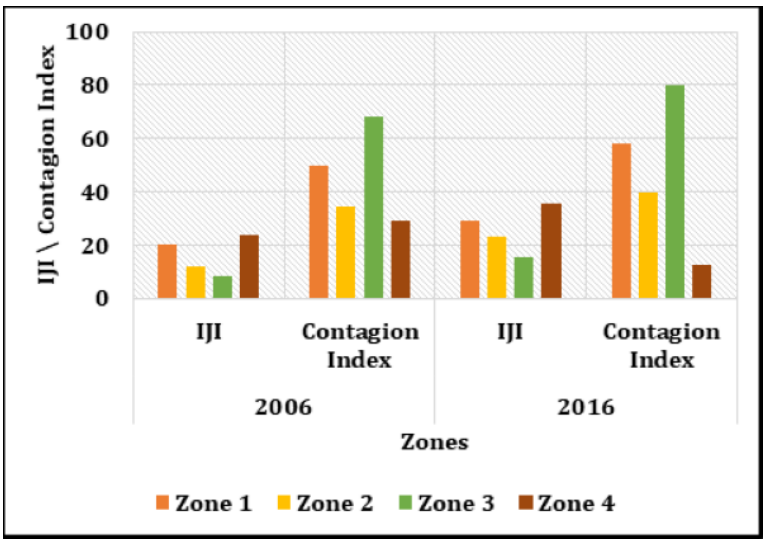

Figure 6.5: Comparison of IJI and Contagion Index

poorly interspersed. Fig. 6.5 is the IJI and contagion metrics for the different zones of the study area. The analysis of contagion measure is not indicating a justified rise or fall in any zones of the landscape. The contagion measure has to be studied by holding either of the interspersion or dispersion constant. IJI index is not affected by the number of patches, in contrary to the contagion index. Moreover, the *Contagion Index* is affected by the resolution of the image. In the figure, the lower values of IJI are seen in zone 2 and 3, which points to the reality that those zones are poorly interspersed. A relatively higher value of IJI is seen in zone 4, which tells that the class types in zone 4 are equally adjacent to each other.

Another aggregation metric called *Splitting Index* gives an indication of the growth in the number of patches of the landscape area. The analysis is given in Fig. 6.6. It is seen that zone 1 is overwhelmed with numerous patches when comparing the years 2006 and 2016.

Diversity measures of the landscape indicate the richness and evenness of a landscape. Richness indicates how diversified are the classes present in the landscape, whereas evenness indicates how uniform is the classes distributed in the landscape. *Shannon's Diversity Index* (SDI) is the most prominent diversity indicator in the metrics that measure of a landscape. The SDI values of the zones are plotted in Fig. 6.7. The absolute value of SDI does not indicate anything meaningful. But a relative comparison of SDI among the same landscape area at different timestamps is a good indicator of how diversely the landscape has changed over the time domain. From the SDI values under consideration, the most diversified growth has happened in zone 4, towards the southern region of the landscape. The growth is an aggregated one when the SDI values are lower

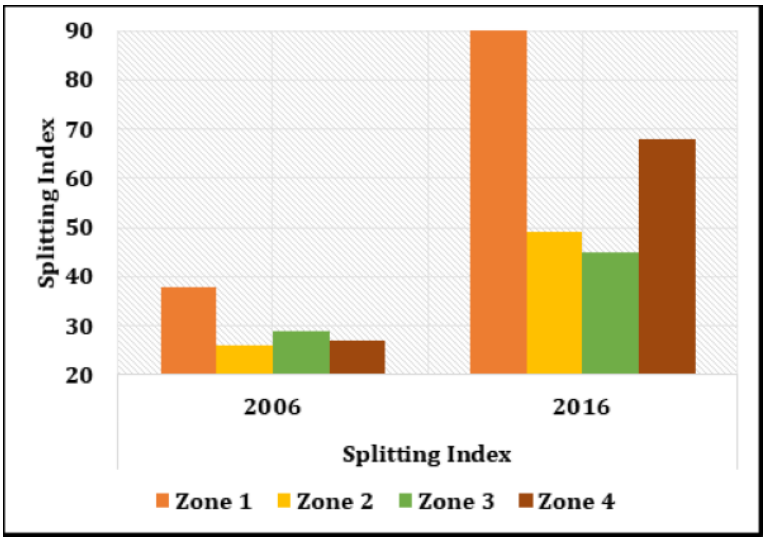

Figure 6.6: Splitting Index of different zones

and is a dispersed one when the SDI values are higher. The figure depicts that the growth happened in zone 4 is a dispersed one, whereas in other zones, the growth is aggregated type. It points to the fact that diversified and dispersed growth of the landscape has happened to the southern part of the mainland. SDI has an associated disadvantage as the index value is highly influenced by rare patch types in a landscape area. Thus to compromise for this disadvantage, *Shannon's Evenness Index* (SEI), which measures the contribution of landscape area to each patch, also has to be taken into consideration. Both SDI and SEI has to be read hand in hand for understanding a landscape composition.

The observations made from the analysis of the study region (Kochi) points to the following facts.

- The vast growth of Kochi city has occurred in zone 1, in terms of built-up area. An increase in vegetation area is also observed in the zone 1, which

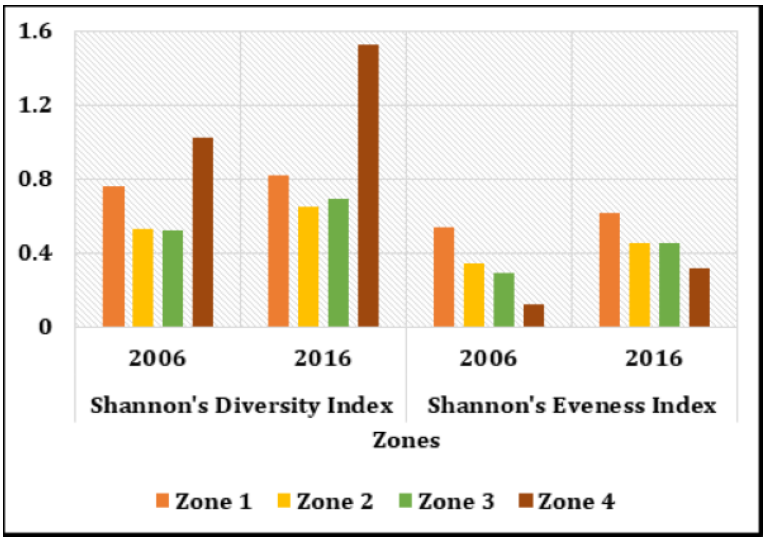

Figure 6.7: SDI and SEI of different zones

points to the smart development happening in the mainland, in spite of the built-up increase.

- The structure of the growth pattern is almost uniform in all the selected zones under analysis.
- The southern region of Kochi, which was very poorly developed in 2006, is now exhibiting a diversified growth in 2016.
- The growth of the southern region is in such a manner that it exhibits smooth texture growth in terms of adjacency.

The landscape metrics which are found to be relevant from these experiments are carried forward for the purpose of designing STM-Miner and is presented in Table 6.1.

6.3 Related Research

Assessing a landscape structure is of immense importance for the different applications of landscape monitoring and planning. The literature points to this aspect in the very early stages. An attempt to generalize the past, present, and future of the landscape is seen in [133], wherein the landscape metrics are utilized for the purpose. The broad set of landscape metrics are analyzed in this work, and an indicative measure of each landscape metrics is spelled out for each characteristic of the same, with convincing reasons. There are examples where landscape metrics have been utilized for learning geo-diversity [134, 135] and biodiversity [136, 137]. The usage of landscape metrics for evaluating urban fragmentation is seen in [138]. Continuous autocorrelation indices presented in [138], along with chosen landscape metrics, helps to characterize the spatial patterns of land-use. A new statistical measure called Urban Public Green Space [139] has been evolved from the landscape metrics to study the urban space concerning networking connectivity in the space. The study of landscape metrics on remotely sensed satellite images of different resolutions was attempted to identify the attributes that rule the values of metrics [140]. Spatiotemporal analysis of Indian cities is always an interesting area for the researchers as evident in [141, 142, 143, 144, 145] in all-time spans.

6.4 Design of the Proposed System

Change pattern analysis is a significant research problem which helps the governance system to monitor the change and plan the future developments of the land under their control more smartly and effectively. A landscape can be

analyzed under different scope, depending upon the interest of the governance system. In this work, the change pattern analysis of a landscape in a hierarchical manner is proposed. The system works as described below. Images of different regions are acquired at different timestamps. The region considered can be varying from a small region to a town, city, state, or landscape. The hierarchical nature is brought into the system based on the concept that small regions are aggregated to form towns or cities, and cities are aggregated to form states, and states are aggregated to form landscapes. Similarly, the change pattern in each layer under consideration is aggregated in a hierarchical model to observe the overall change pattern in the next layer. The model presented in Fig. 6.8 explains the entire flow of the system.

The input to the design proposed is the classified remote sensing imagery at different time slots/time frames. The next step in the design is *tensorization*, that models the classified image into a tensor as detailed in Chapter 4. An appropriate tensor order has to be chosen for the classified image and its associated features. From the tensorized representation of the imagery, appropriate regions of interest (ROIs) are identified for landscape under study and are aligned/sorted in terms of certain time slots called as the time of interest (TOI). The next step is the novel approach proposed in this thesis, wherein the labeled regions and associated features are hierarchically build to understand the change pattern in different higher-level regions. The steps involved in the hierarchical spatiotemporal-metric miner are detailed in the following sections. The STM-Miner computes growth indices for different ROIs. The growth indices of different ROIs are aggregated to form the indices for the corresponding cities.

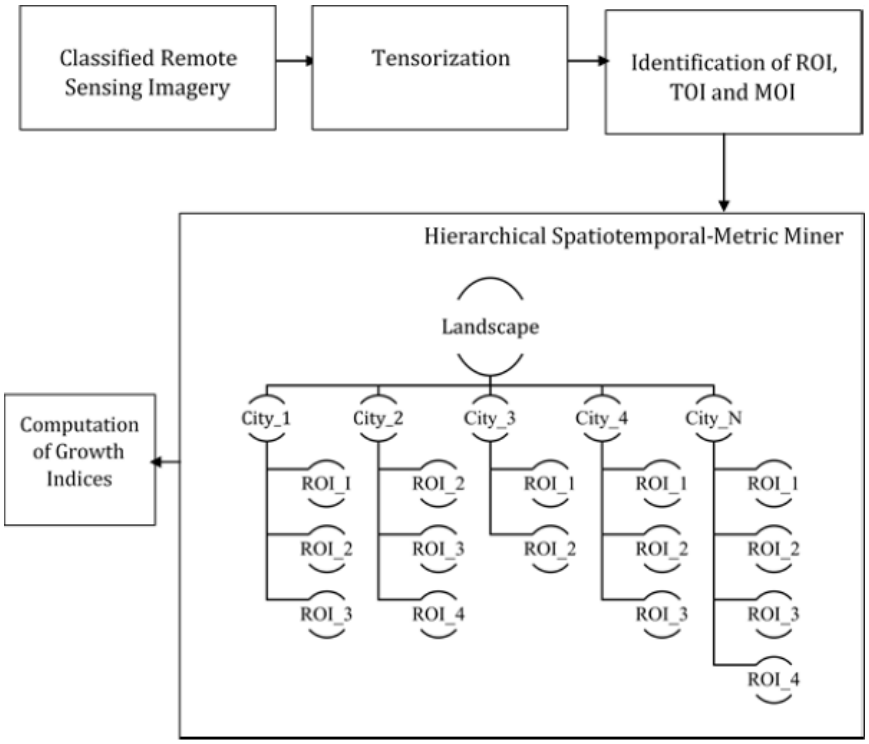

Figure 6.8: Design of Spatiotemporal-Metric Miner

6.4.1 Tensorization of Image Regions

The section explains the method to represent the image region using tensors. The image dataset is considered in 'T' consecutive intervals, where each image accounts for each time frame. The image instant is modeled as matrix M which has 'C' rows of class labels and 'F' columns of featured landscape metrics. There are 'T' matrices for the different time slots, which are combined to form a 3-order tensor as $\mathcal{X} \in \mathbb{R}^{C \times F \times T}$. This can be considered as a tensor stream, which is a sequence of 3-order tensor, and the value of T increases with time. At every instant $t_1, t_2, t_3, \ldots t_T$, a new tensor is added to the sequence. The images

under consideration, grow in quantity as the TOI increases. The landscape metric features for an ROI are chosen from the earlier study. The metrics are generally at different levels like patch, class, and landscape. Depending on whether the ROI is a patch, class, or landscape category, the appropriate metric can be chosen and added to the metric list. This is referred to as the Metric of Interest (MOI).

6.4.2 Identification of ROI, TOI and MOI

ROIs from an image has to be selected by considering the domain under study. As the study concentrates on remote sensing images, certain regions of each city/state are chosen with the aid of domain expert from Geographical Sciences. The time frame of the study is chosen at different intervals, say, three years, five years, seven years, and ten years. The reasoning of selecting such a TOI solely depends on the availability of the sensor data. The MOIs used in this study are the landscape metrics or indices, which help to describe the structure and pattern of a landscape. The landscape/class metrics can be utilized in quantifying the change pattern in a geographic area over a temporal domain. The MOIs are summarized as in Table 6.1 from Section 6.2. The table lists the MOIs considered in this study and their dependency on each other. The remarks will help to understand the significance of each MOI.

6.4.3 Hierarchical Spatiotemporal-Metric (STM) Miner

The section briefs about the STM miner proposed in this chapter. The steps of STM-Miner is detailed in Algorithm 6.1.

Table 6.1: MOI and their dependencies

Metrics of Interest (MOI)	**Remarks**	**Dependency of MOI**
Class Area	Increase/decrease in the total labeled area indicates a change in the class	–
Mean Patch Size	Average area distribution under each class label	Class Area
Area-Weighted Mean Fractall Dimension	Helps to observe the shape complexity of the class area w.r.t. TOI	Class Area
Contiguity Index	Measures compactness or elongation of a class w.r.t. TOI	–
Contrast Weighted Edge Density	Standardizes edge to a per unit area	Class Area
Patch Density	Indicates how the division of landscape into patches have happened w.r.t. TOI	Class Area
Splitting Index	Measure of change in patch distribution w.r.t. TOI	Patch Density
Interspersion and Juxtaposition Index (IJI)	Measure of degree of adjacency between different spatial classes	Edge Density
Shannon's Diversity Index (SDI)	Indicates the diversified growth that has happened to the new class w.r.t. TOI	–
Shannon's Evenness Index (SEI)	Helps in isolating evenness component to control the value of SDI	Shannon's Diversity Index

Interpretation of Tensor Factors

The image dataset represented as tensor after factorization yields matrices, X, Y, Z, consisting of R columns. Each matrix corresponds to a component. It is assumed that the factorization adopted in this design is a non-negative kind. Each entry of X, say x_{ir} will represent a class instance with a weight value directly proportional to the area of the class under consideration. The Y component will represent the landscape feature and is of the order '$F \times R$'. Each entry say y_{jr}, will represent a landscape metric value whose weight value is directly proportional to the actual value of the landscape metric of a particular ROI.

Algorithm 6.1: STM-Miner

Result: Intra-class Growth Index α, Inter-class Growth Index β

Input Image Dataset I, Labelled Classes C, Landscape Feature F, TOI - 1,2,..,T ;
For every $I_i \in I$, form A_{ij} = *metric_value_of_region*(C_j) ;
Tensorize all A_{ij} to form $\mathcal{X} \in \mathbb{R}^{C \times F \times T}$;
Randomly intialize R ;
Calculate Core-Consistency Value of R, if value CC(R) $\leq$ 0.5, go to next step ;
Find $\widehat{\mathcal{X}} = \sum_{r=1}^{R} X \circ Y \circ Z$;
$Y \leftarrow Y_{rref}$;
For i = 1 to C, j = 1 to T
ROI_{α} (C_T) = $\sum(intra\_MOI(\text{y}))$;
ROI_{β} (C_T) = $\sum(inter\_MOI(\text{y}))$;
For ROI = 1 to N
$\alpha = \sum ROI_{\alpha}$ and $\beta = \sum ROI_{\beta}$

The next component $Z \in \mathbb{R}^{T \times R}$ represents the time frame under study concerning 'T' time intervals. Each entry of Z, say, z_{kr}, will represent the association among the images within the particular TOI. After the tensor

factorization of the of images, the first component can be projected with respect to ROI, the second component with respect to MOI, and the third component with respect to TOI, thus yielding the MOI for a particular ROI at a certain TOI. The MOIs can be appropriately combined to yield the following indices as defined for two modes (i) intra-class and (ii) inter-class

Definition 6.1 *Intra-Class Growth Index (α)* is defined as the weighted composition of the metrics that measure the growth/detainment of a region of interest when there is no change in the class label of the region.
The growth index is calculated as given by

$$\begin{aligned}\alpha &= w_1 n_1 + \cdots + w_m n_n - w_{m+1} n_1 n_j - w_{m+2} n_2 n_p - \cdots - w_n n_k n_p \\ &= \sum_i w_i n_i - \sum_{i,j,k} w_i . n_j . n_k . \end{aligned} \tag{6.1}$$

w_i—set of weights
n_i—set of metrics of interest
n_j, n_k—set of metrics of interest which are interdependent.

Definition 6.2 *Inter-Class Growth Index (β)* is defined as the weighted composition of the metrics that measure the growth/detainment of a region of interest when there is a change in the class label of the region.
The growth index is calculated as given by

$$\begin{aligned}\beta &= v_1 m_1 + \cdots + v_m m_k - v_{m+1} m_1 m_j - v_{m+2} m_2 m_p - \cdots - v_n m_k m_p \\ &= \sum_i v_i m_i - \sum_{i,j,k} v_i . m_j . m_k \end{aligned} \tag{6.2}$$

v_i—set of weights
m_i—set of metrics of interest
(m_j, m_k)—set of metrics of interest which are interdependent.

Note Interdependent triplet metrics can also be incorporated into the above equations (6.1) and (6.2).
The equations can be applied on a global level also. The indices computed in a lower level can be accumulated to the higher level to characterize the change detection on a collection of ROIs.

6.5 Results and Discussions

The section describes the datasets chosen for the study in detail. The subsection also discusses the MOIs and their influence in the proposed indices. The STM-Miner is evaluated to obtain the experimental results on the dataset and their growth indices.

6.5.1 Datasets

The experiments are run on real-time datasets, which are multispectral images obtained from the sensors of LANDSAT 7 [130] and LANDSAT 8 [131]. Both these sensors are used, as the TOI demands it. The study is performed in the Indian Cities. The Indian cities are categorized as given in Table 6.2 by the Government of India [146]. There are three classes of cities, namely X, Y, and Z. Type X consists of the major metropolitan cities in India, which are eight in number. Type Y cities are ninety-four in number and are the major ones in the country which are in the developing phase. The datasets are fixed by sampling from Table 6.2. From the cities sampled, the cities are not analyzed for change pattern as a whole. Instead of it, three or four ROIs are chosen inside each city, and the initial change pattern analysis is performed on them. To understand the growth of the whole city, the hierarchical model is implemented to understand

the growth of the cities. The sampled cities and their ROIs are presented in Appendix C. For 'X' category cities, four ROIs are chosen, whereas, for 'Y' category cities, three ROIs are chosen.

Table 6.2: Categorization of Indian Cities

Category	City	Count
X	Ahmedabad, Bangalore, Chennai, Delhi, Hyderabad, Kolkata, Mumbai, Pune	8
Y	Agra, Ajmer, Aligarh, Allahabad, Amravati, Amritsar, Asansol, Aurangabad, Bareilly, Belgaum, Bhavnagar, Bhiwandi, Bhopal, Bhubaneswar, Bikaner, Bokaro Steel City, Chandigarh, Coimbatore, Cuttack, Dehradun, Dhanbad, Durg-Bhilai Nagar, Durgapur, Erode, Faridabad, Firozabad, Ghaziabad, Gorakhpur, Gulbarga, Guntur, Gurgaon, Guwahati, Gwalior, Hubli-Dharwad, Indore, Jabalpur, Jaipur, Jalandhar, Jammu, Jamnagar, Jamshedpur, Jhansi, Jodhpur, Kannur, Kanpur, Kakinada, Kochi, Kottayam, Kolhapur, Kollam, Kota, Kozhikode, Lucknow, Ludhiana, Madurai, Malappuram, Malegaon, Mangalore, Meerut, Moradabad, Mysore, Nagpur, Nashik, Nellore, Noida, Patna, Pondicherry, Raipur, Rajkot, Rajahmundry, Ranchi, Rourkela, Salem, Sangli, Siliguri, Solapur, Srinagar, Surat, Thiruvananthapuram, Thrissur, Tiruchirappalli, Tiruppur, Tirupati, Ujjain, Vadodara, Varanasi, Vasai-Virar City, Vijayawada, Visakhapatnam, Warangal	94
Z	All other cities	

6.5.2 MOIs associated with Growth Indices

Two parameters, namely, intra-class growth index and inter-class growth index, is introduced in this thesis. Both these indices are the weighted sum of the different metrics of evaluation of a landscape. The challenging part of this procedure is to decide on the metrics that account for the growth indices from the whole set of hundreds of metrics available. The decisive metrics were chosen from the initial study described in Section 6.2. The metrics so obtained has now to be categorized into those aiding the computation of both the growth indices.

Intra-class Growth Index quantifies the change pattern of a landscape which has not changed in its class label over a particular TOI. A change in the *Class Area* can be an important metric that might show an increase/decrease in the total landscape area of the specific class, obviously over the TOI. If there is an increase/decrease in the total labeled area, it is clear that the shape of the area has changed. A change in *Class Area* points to the change in patch distribution also. Hence the *Mean Patch Size* is also chosen as an MOI. It is observed from Section 6.2 that, among the shape metrics, *Area-weighted Mean Fractal Dimension* is a decisive shape metric in assessing the change in the landscape. As the intra-class growth index measures area without a change in label, any compactness/elongation of the class under consideration are evaluated by *Contiguity Index*.

The inter-class growth index quantifies the change pattern of a landscape which has changed in its class label over a particular TOI. To measure how far the interclass variance has occurred, the metric called *Patch Density* is preferable to the *Class Area* metric. *Patch Density* will help to realize how the division of landscape into patches has happened. The *Patch Density* is found by considering

the number of patches of the same type. It depicts the growth or retardation of each land-use class with respect to the patches. The *Patch Density* of each class may vary with TOI. Hence this will be an important metric that will account for the interclass variance. As *Patch Density* is a simple measure, the *Splitting Index* is also considered as an MOI, to find the number of patches, when a landscape is divided into patches of equal size. *Interspersion and Juxtaposition Index* (IJI) is a measure that indicates only interspersion. It is better to quantify only one factor between interspersion and dispersion. SDI is the most prominent diversity indicator in the metrics that measure a landscape. The absolute value of SDI does not indicate anything meaningful. But a relative comparison of SDI among the same landscape area at different timestamps is a good indicator of how diversely the landscape has changed over the TOI. To counter the disadvantages of SDI, SEI index is also taken into consideration.

As the experiments involve the comparison of landscapes of different areas, the MOI, *contrast weighted edge density* is incorporated into both the indices. It standardizes the edge to a per unit area, which facilitates the comparison among different landscape areas. The MOIs for assessing the proposed growth indices is summarized in Table 6.3.

The correlation between the MOIs in Table 6.3 is verified through the correlation matrix as depicted in Fig. 6.9 and Fig. 6.10. Fig. 6.9 presents the correlation matrix for the intra-class growth index, and from the positive correlations, it is evident that the MOIs chosen are appropriate. Similarly, Fig. 6.10 presents the correlation matrix for the interclass growth index and their positive correlations. Hence it is validated that the MOIs chosen are relevant and appropriate for the domain under consideration.

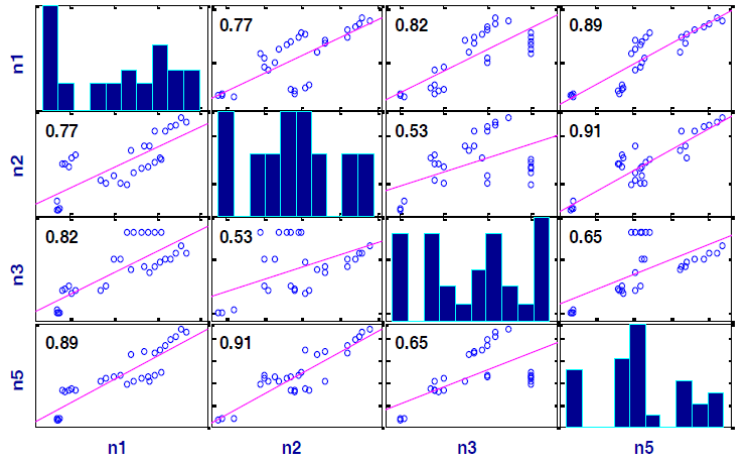

Figure 6.9: Correlation Matrix of MOIs for Intra-Class Growth Index

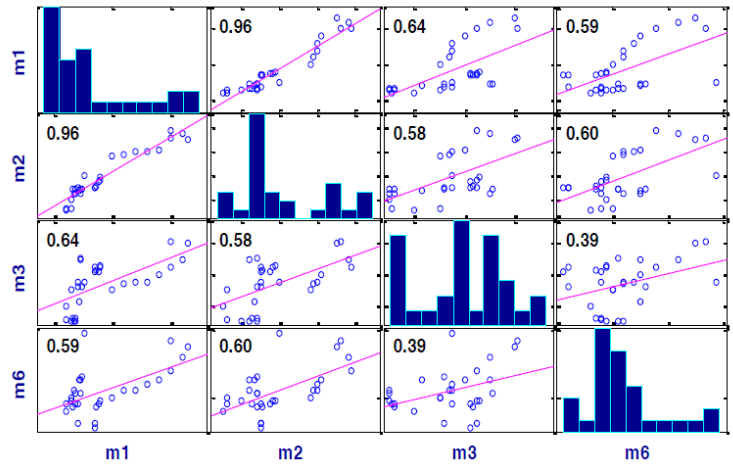

Figure 6.10: Correlation Matrix of MOIs for Inter-Class Growth Index

Table 6.3: MOIs influencing Intra-class Growth Index and Inter-Class Growth Index

Coefficients	Metrics of Interest (MOI)
Intra-Class Growth Index	Class Area (n_1)
	Mean Patch Size (n_2)
	Area-Weighted Mean Fractal Dimension (n_3)
	Contiguity Index (n_4)
	Contrast Weighted Edge desnity(n_5)
Inter-Class Growth Index	Patch density(m_1)
	Splitting Index(m_2)
	Interspersion and Juxtaposition Index(m_3)
	Shannons Diversity Index(m_4)
	Shannons Evenness Index(m_5)
	Contrast Weighted Edge desnity(m_6)

6.5.3 Evaluation

The spatiotemporal-metric miner model depends on tensor factorization. The approximation of the original tensor is achieved through fine-tuning the R components for the specified datasets.

The study is performed on all Type X cities and sampled Type Y cities. The TOI chosen for the study is from the year 2011 to 2016. Definite ROIs are identified inside the sampled cities, and is available in Appendix C. The hierarchical STM- Miner is applied to the ROIs, which result in mining the growth indices for a city. Both the intra-class growth index (α) and inter-class growth index (β) of all the Type X cities for TOI of 5 years are analyzed and are presented in Fig. 6.11. It is seen that the growth index is considerably high for inter-class variance, and the cities Hyderabad and Ahmedabad are the ones that have grown substantially for the TOI under consideration. All other Type X cities have exhibited growth on a shallow scale.

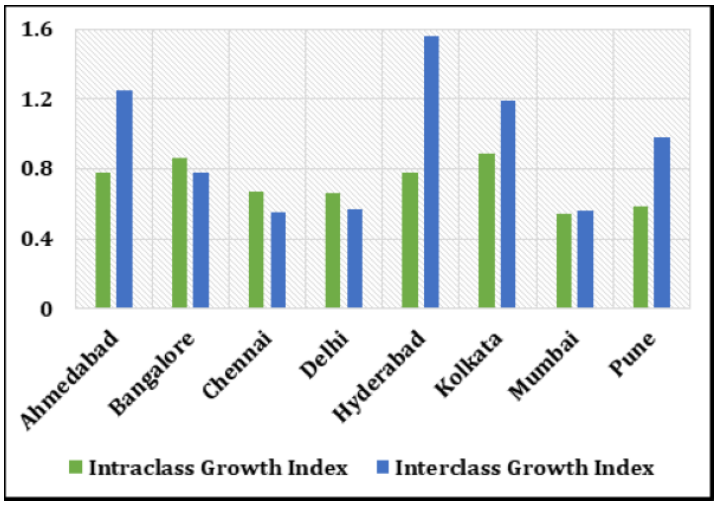

Figure 6.11: Growth Indices for Type X cities

The exciting part of the study is to understand the growth of Type Y cities, as they belong to the *ever-growing* category of cities. Through the experiments, it is attempted to analyze Type Y cities, and find the important cities in the Type Y category depending on their growth index.

The TOI fixed here is ten years, from 2006 to 2016. Table 6.6 presents the growth indices of Type Y cities. The data is presented in descending order; the highest score indicates the city with the most significant growth pattern. It is clear from the tabular data that the same city does not have the highest score for both growth indices. The inter-class growth index points to the fact that the city has changed only on a surface level, with the class-labels remaining the same. The intra-class growth index points to the information that the city has transformed drastically, with new class-labels.

High intra-class growth means that the city has undergone exceptional changes. As far as the analysis of Type Y cities is concerned, Jaipur is the

Table 6.4: Growth Indices - Type Y cities for TOI - 10 years

Type Y Cities	**Inter-Class GI**	**Type Y Cities**	**Intra-Class GI**
Jaipur	2.68	Surat	0.78
Surat	1.77	Kanpur	0.71
Kanpur	1.65	Indore	0.68
Indore	1.62	Jaipur	0.61
Kochi	1.42	Varanasi	0.59
Varanasi	1.15	Agra	0.52
Agra	1.09	Lucknow	0.49
Lucknow	1.07	Kochi	0.49
Patna	0.87	Patna	0.48
Bhopal	0.87	Bhopal	0.48

city with the highest inter-class growth index of 2.68. In the intra-class growth index, Surat and Kanpur are almost at par and ranks high on the table. The growth of these cities are attributed to the socio-economic factors and are not investigated, as they are beyond the scope of this work.

The top-5 highest-ranked cities are further analyzed for the detailed study. The growth pattern of the city at different TOIs are depicted as follows. The figures 6.12 and 6.13 depicts the growth indices at different TOIs. An illustration of such kind helps to understand in which frame of TOI the city has changed regarding growth indices. The study projected the inter-class growth index for ten years of TOI concerning the descending score. For the same top-5 cities, the different TOIs, produced a different ranking for the cities, as evident from the graphs. The figure points to the fact that the growth pattern of the cities is different when seen at different TOIs. Thus, the mechanism of STM- Miner can be applied to different TOIs to understand the growth pattern of a landscape.

The new indices proposed are highly effective, when a comparative analysis

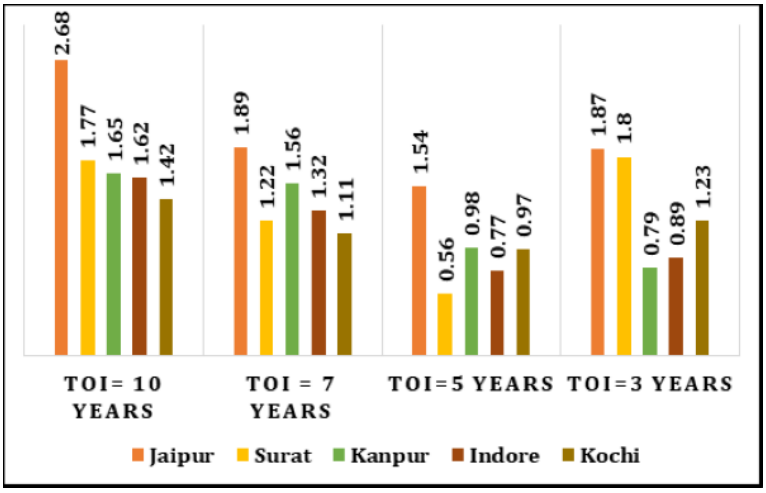

Figure 6.12: Inter-Class Growth Index for top-5 ranked Type Y cities at different TOI

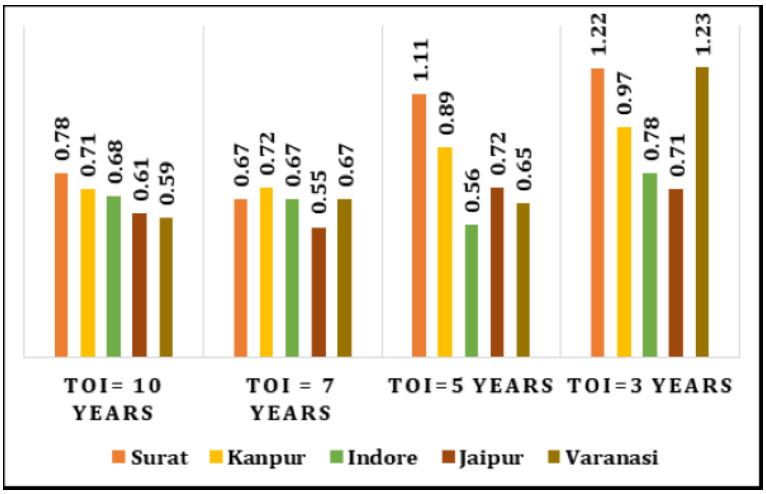

Figure 6.13: Intra-Class Growth Index for top-5 ranked Type Y cities at different TOI

with Gini index [147] of the multi-spectral images at the different TOI is done. In general terms, the Gini Index is a measure of inequality in the distribution of data, or it quantifies the non-uniformity of the data under consideration. In the experiments performed, the average Gini Index value of an ROI over a particular TOI is analyzed herewith. It is observed that the average Gini index value for the different type-Y cities varies non-uniformly and does not result in a pattern, from which effective conclusions regarding change patterns cannot be drawn. The result is depicted in Fig. 6.14. The average Gini index value is not supportive to find the change of land use/land cover that has occurred in ROI.

A comparative analysis of the Inter-Class Growth Index, Intra-Class Growth Index, and Gini Index value is presented in Fig. 6.15 for ten years and seven years of TOI. From the figures, it is seen that the Gini index value for different TOI does not yield any specific information regarding changes that have happened in the landscape. The change in the Gini index value does not show a specific pattern, whereas the two growth indices proposed shows consistent values for changes at different TOIs.

A detailed analysis of only the Type-Y cities is shown in the figure. On a detailed analysis of the growth indices, it is seen that the indices value is different at different TOIs. A region that was exhibiting good growth at a particular TOI retards with respect to another TOI. Hence, such kind of information is also obtained from this study. The higher value of growth index obviously points to the amount of change pattern that has occurred in a particular time frame. To enhance the result obtained, an analysis of TOI of five and three years is also presented in Fig. 6.16.

The results obtained are validated with the studies presented by the National

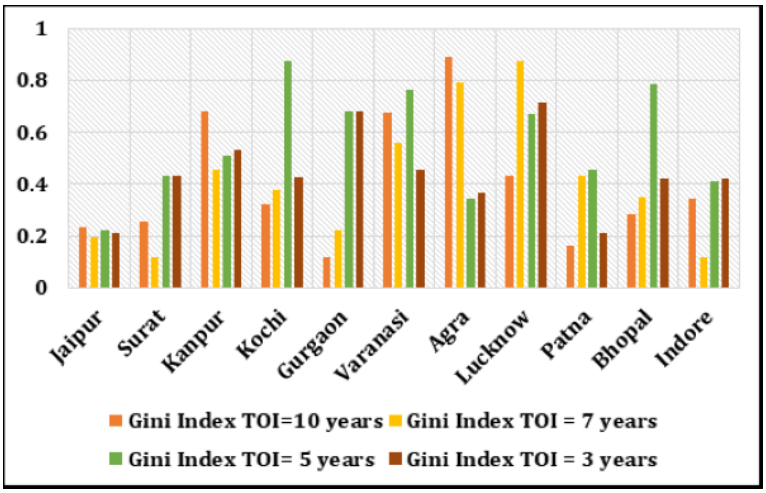

Figure 6.14: Comparison of Gini Index for Type Y cities for different TOIs

Institute of Urban Affairs, Government of India [148], and are relatively significant. The results of [148] claim high-growth cities as Pune, Ahmedabad, and Surat, which are par with the study presented. The dataset for the experiments are chosen based on the availability of ground truth.

6.6 Summary of the Chapter

The chapter presented an evaluative study of the decisive landscape metrics, which helps in identifying the changes that have happened in a landscape. After identifying the relevant landscape metrics, this chapter describes a hierarchical spatiotemporal metric miner to mine growth of regions of interest, which has occurred in different time of interest. The change pattern which has occurred over a period is parameterized using two growth indices, namely, inter-class growth index and intra-class growth index. The two growth indices are evolved through iterating with different landscape metrics and converging on relevant

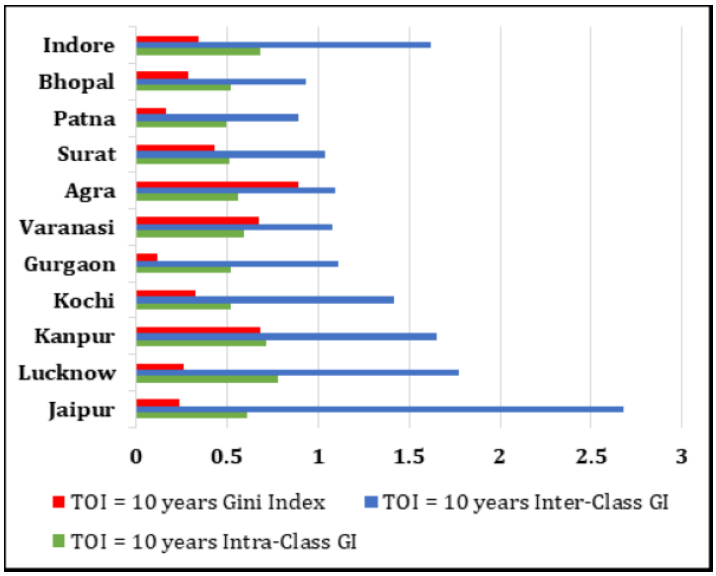

(a)

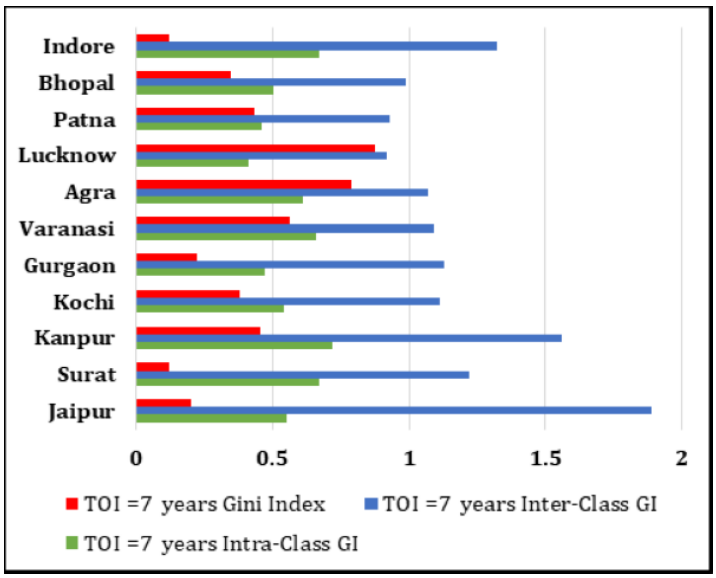

(b)

Figure 6.15: Comparison of Inter-Class Growth Index, Intra-Class Growth Index and average Gini Index values for Type Y cities for TOIs - 10 years and 7 years

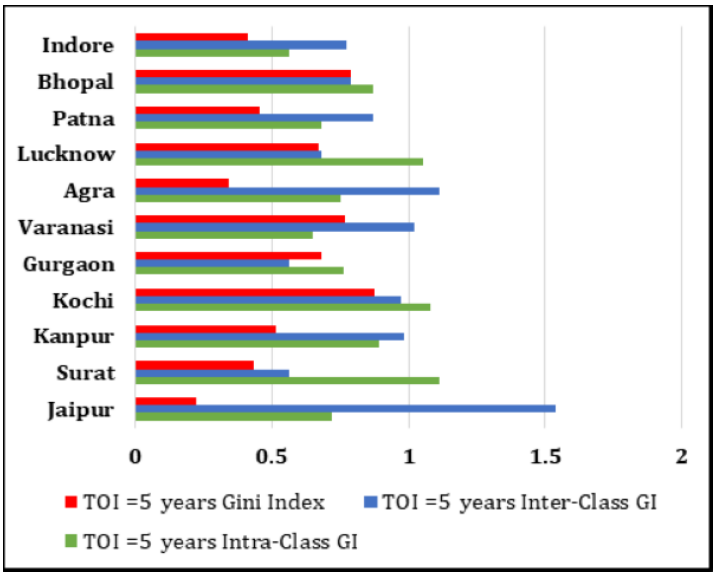

(a)

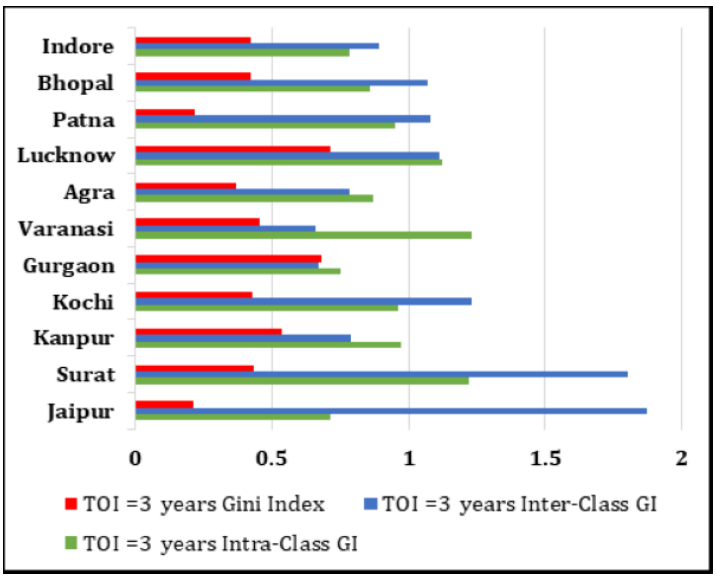

(b)

Figure 6.16: Comparison of Inter-Class Growth Index, Intra-Class Growth Index and average Gini Index values for Type Y cities for TOIs - 5 years and 3 years

metrics, which are termed as metrics of interest. The metrics of interest for analyzing inter-class growth index and intra-class growth index are found out by using weight-convergence methods. The images of Indian cities are used in the experiments. The study is more inclined towards the type-Y cities, which are analyzed in detail in terms of the growth indices. Different time of interest is chosen for the study. This miner yields us the knowledge of the different type-Y cities which are more inclined towards the type-X category. The relevance of the growth indices is also established through a comparison of the same with Gini index values.

To formalize the studies conducted in this thesis on change detection, the metrics contributing to change pattern analysis is conceptualized into an ontology. The study will help to quantify the growth or detainment of a region in an urban landscape, as detailed in the next chapter.

Chapter 7

Spatiotemporal Ontology for Change Detection

7.1 Introduction 134
7.2 Related Research 135
7.3 Design and Development of Spatiotemporal Ontology 136
7.3.1 Spatial Information 136
7.3.2 Temporal Information 138
7.3.3 Spatiotemporal Information 138
7.4 Reasoning of Spatiotemporal Ontology 138
7.5 Case Studies 141
7.5.1 Study Area 141
7.5.2 Discussion of results and Contributions 142
7.6 Summary of the Chapter 148

A spatiotemporal ontology to find the changes that have happened in a particular spatial region at different time periods is modeled in this chapter. The ontology formalizes the change detection of urban landscapes under study. The spatial and temporal aspects of the ontology are separately built and are analyzed in respect of certain case studies. By this attempt, the ontology helps

in conceptualizing the domain knowledge, thereby reducing the semantic gap between low-level image features and high-level spatiotemporal semantics.

7.1 Introduction

The conventional approach in the change detection method is to perform classification techniques on the pixel and perform an analysis on *changes/no changes* on the class label of the pixel. From this approach, the research has moved further away to understand the changes more semantically, than in terms of numeric values. It might also be interesting to see the evolution of changes on a time axis to govern or assess the driving factors. The chapter presents an ontology [149] model to understand the change patterns which has evolved on a temporal scale in a spatial region.

Ontology is a formal name for defining the types, properties, and relationships of entities that exist in a particular domain. Ontologies are generally created to limit complexity and organize information, and can then be applied to problem-solving. They can help to conceptualize the domain knowledge in the change analysis of a region. In this modeling, information of each region is obtained from the remote sensing satellite image. The remote sensing image of the region is assumed to be classified and is marked with appropriate class labels. Each satellite is associated with a spatial and temporal resolution, which will govern the extent to which the study can be mapped. The satellite image obtained at different time intervals are analyzed with respect to their class labels and associated features to understand the changes which have happened in the region. The ontology is modeled with semantics for the related features so that it bridges the gap between the low-level image features and

high-level spatiotemporal semantics. Thus the proposed ontology will help to understand the changes in a region more semantically in terms of features like morphology, shape and texture.

The research work related to spatiotemporal ontology is briefed in Section 7.2. The design and development of spatiotemporal ontology are described in detail in Section 7.3. The reasoning of spatiotemporal ontology is substantiated in Section 7.4. The rules and axioms obtained from the proposed ontology is also briefed in this section. Case Studies of Indian cities on the proposed ontology is presented in Section 7.5. The chapter is concluded in Section 7.6.

7.2 Related Research

The change detection techniques are now more formalized to bridge the semantic gap that arises from the analysis. It is noted that there are very few works in the literature that supports the modeling of change patterns semantically. Most of the traditional methods rely on post-classification analysis.

A SOWL was developed to model an ontology in the spatiotemporal domain [150]. The ontology handles both quantitative and qualitative information in the spatiotemporal mode. The associated query language supports a set of operators in the spatial and temporal domain. The work also incorporated rules for inferring spatiotemporal axioms in the existing domain. Likewise, a spatiotemporal ontology for change analysis for flood-affected regions using remote sensing images is described in [151]. The aim of the ontology is to query, detect, and analyze the disaster-affected region. This concept will help to analyze the temporal changes that have happened in flood-affected region.

7.3 Design and Development of Spatiotemporal Ontology

The design and development of spatiotemporal ontology is outlined in this section. This section also details the different concepts used in the ontology. As it is a spatiotemporal ontology, the information has to be encoded in the spatial and temporal domain.

7.3.1 Spatial Information

The spatial information of the region chosen for understanding change patterns has to be modeled in *classes*, *object properties*, *data properties* and *individuals* of the ontology. The entire ontology is built under *SpatiotemporalEntity* which is divided into subclasses like *SpatialEntity*, *TemporalEntity*, *ChangeModel*. The entire spatial information is modeled under *SpatialEntity*. The main sub concepts/classes of the spatial domain is *Regions*, *Labels* and *BoundingBox*. The *Regions* depict the spatial areas for the land under study. *Regions* are the subclasses of *Labels*. The *Labels* class is further divided into *Builtup*, *Baregrounds*, *Vegetation*, and *Water*. The boundaries of regions are marked through *BoundingBox*. The *BoundingBox* helps to mark the four corners of the region. The classes are connected through the object properties and associated data properties. A sample of object properties can be summarized as given in the following Table 7.1.

The *Region* class has the most important data property as *hasLabel*, which indicates the label on the region. The class is also associated with the property called *RegionFeatures*, which is further split into *ColorFeatures*, *TextureFeatures*, *ShapeFeatures*, *Indices* and *Metrics*. The *ColorFeatures* of the image has the Lightness, ‘a’ and ‘b’ components, and Near Infra Red features,

Table 7.1: Object properties, domain and range

Domain	Object Properties	Range
SatelliteImage	AcquireBy	Sensor
Sensor	InstalledIn	Satellite
Tile	BelongsToImage	SatelliteImage
Region	BelongsToTile	Tile
Tile	BelongsToImage	SatelliteImage
Region	BelongsToTile	Tile
Tile	ConsistsOfRegion	Region
SatelliteImage	ConsistsOfTile	Tile
BoundingBox	DirectionalRelation	BoundingBox
Region	hasBBox	BoundingBox
TemporalEntity	atTime	TemporalEntity

hence the data property—*ColorFeatures (mean_L, SD_L, mean_a, SD_a, mean_b, SD_b, mean_NIR, SD_NIR)*. Similarly the *TextureFeatures* is comprised of *(glcm_contrast, glcm_correelation, glcm_dissimilarity, glcm_entropy, glcm_homogenity, glcm_mean, glcm_second_moment, glcm_variance)*. The *ShapeFeatures* of the region has three components *Area, Elongation and Perimeter*. The indices under consideration are NDVI and SBI and hence the data property—*Indices(mean_ndvi, SD_ndvi, mean_sbi, SD_sbi)*. The relevant landscape metrics (which were deduced from Chapter 6) of the region are also taken into account in this ontology. Thus the data property *Metrics* can be written as *(hasClassArea, hasAWFractalDimension, hasCWEdgeDensity, hasContiguityIndex, hasIJIIndex, hasSDIIndex, hasSEIIndex, hasSplittingIndex)*.

7.3.2 Temporal Information

The entire temporal information is stored in the class *TemporalEntity*. The object property *atTime* binds the *Temporal Entity* to itself. The entity has the *TimeOfInterest* as the subclass which is further depicted as *TimeOfInterest (day, month, year)*. The temporal information provides the time at which the remote sensing image is acquired by the satellite.

7.3.3 Spatiotemporal Information

The *SpatiotemporalEntity* of the ontology models the *ChangeModel* from the *SpatialEntity* and *TemporalEntity*. The *ChangeModel* is associated with features like morphology, shape, position, and texture. The morphology property has individuals, namely, *strip* and *planar*. The individuals of the shape property are *regular* and *irregular*. The positional property has individuals *adjacent* and *disjoint*. The texture features are also described with individuals *rough* and *smooth*. The ontology is developed in Ontology Web Language –DL (OWL-DL) using Protégé and is available in *https://ontohub.org/repositories/spatiotemporal_ontology*. The ontology developed is able to perform spatiotemporal reasoning in the form of rules and axioms.

7.4 Reasoning of Spatiotemporal Ontology

Semantic Web Rule Languages (SWRL) Rules are modeled from the ontology to understand the change pattern of a region over a temporal scale. In the ontology, two different sets of *TimeOfInterest* is chosen, and a spatial region is being observed.

The SWRL rules is a subset of rules formulated from the proposed ontology. The rules help to find out the changes that have occurred in a spatial region at two particular instances of time. The rule reports the changes that have occurred in the region in terms of the class label and associated properties of the region. For example, Rule #1 describes the change pattern at two-time intervals, say t1 and t2, of a region r1 labeled as l1 at t1 has now changed to label l2 at t2. Similarly, Rules #2–3 describe the features of a region which has changed from time t1 to t2. These features include color, shape, indices, texture, and metric features, which has resulted in changes.

There are also inferred axioms, which resulted from the spatiotemporal ontology. A subset of the axioms is shown as Rules #4–9 in Table 7.2. The inferred axioms are modeled under *ChangeModel*. These axioms provide semantic information regarding changes rather than numeral values. It reports the evolution of changes in terms of morphology, shape, position, and texture. Rules #4–5 express the axioms which model the morphological change of a region as either a *strip* or a *planar* region.

Rules #6–7 depicts the shape change of a region in terms of a *regular* or an *irregular* polygon. Similarly, Rules # 8–9 express the change pattern in terms of position (*adjacent* and *disjoint*) and texture (*rough* and *smooth*). Closer examination of these rules point to the fact that the decisive factors on elaborating the semantics are generally the values associated with the different landscape metrics. This is the innovative contribution of the spatiotemporal ontology depicted.

Table 7.2: SWRL Rules and Inferred Axioms of the Spatiotemporal Ontology

Rule #	SWRL Rules/Inferred Axiom
1	atTime(?t1,?t2)^ hasBoundingBox(?r1,?b1)^ hasLabel(?l1,?t1) -> hasLabel(?l2,?t2)
2	atTime(?t1,?t2)^ hasBoundingBox(?r1,?b1)^ hasLabel(?l1,?t1)^ hasLabel(?l2,?t2) ->hasClassArea(?a1,?a2)^ hasElongation (?e1, ?e2)^ hasPerimeter (?p1, ?p2)
3	atTime(?t1,?t2)^ hasBoundingBox(?r1,?b1)^ hasLabel(?l1,?t1)^ hasLabel(?l2,?t2) ->hasCWEdgeDensity(?c1,?c2)^ hasIJIindex(?r12, ?iji_12)^ hasSDI(?sdi_1, ?sdi_2)
4	hasLabel(?l1,?t1)^ hasLabel(?l2,?t2)^ hasContiguityIndex(?r12,?ci_1) -> hasMorphology(?strip)
5	hasLabel(?l1,?t1)^ hasLabel(?l2,?t2)^ hasContiguityIndex(?r12,?ci_2) -> hasMorphology(?planar)
6	hasLabel(?l1,?t1)^ hasLabel(?l2,?t2)^ hasAWFractalDimension(?r12, ?aw_1)-> hasShape(?regular)
7	hasLabel(?l1,?t1)^ hasLabel(?l2,?t2)^ hasAWFractalDimension(?r12, ?aw_2)-> hasShape(?irregular)
8	hasLabel(?l1,?t1)^ hasLabel(?l2,?t2)^ hasIJIindex(?r12,?iji_1)-> hasPosition(?adjacent)
9	hasLabel(?l1,?t1)^ hasLabel(?l2,?t2)^ y hastexturefeature(?con_1, ?corr_1, ?diss_1, ?ent_1, ?homo_1, ?mean_1, ?sec_mom_1, ?var_1)-> hasTexture(?rough)

7.5 Case Studies

This section briefs about the study area analyzed with the help of modeled ontology. The change patterns in landscape metrics are analyzed in the next section to understand the growth of the regions under study.

7.5.1 Study Area

India is a land of diversities. The diversification of the country is attributed to many factors like the unique linguistic states, culture differences between northern and southern states, landscape patterns of the states, and population of the state. The diversification has evolved over the years. Of course, along these years, the landscape of the region also has undergone a drastic change. To study how the landscape has changed, two metropolitan cities, which have immensely contributed to the growth of the nation, namely, Mumbai and Bangalore, are taken as case studies.

Mumbai (formerly known as Bombay) is a metropolitan city situated on the west coast of India. It is one of the most populous cities in India. Over the past decade, Mumbai has grown as the financial and commercial center of India, thus supporting the nation's economy. Bangalore (officially known as Bengaluru), a metropolitan city of the Indian sub-continent and is accepted as a twin-town/sister city of many cities worldwide, including San Francisco, USA. It is the third most populous city in India and is located in southern India. The city is regarded as the Silicon Valley of India and is the leading IT exporter of the country. Bangalore city also accounts for the nation's development in terms of IT sector.

7.5.2 Discussion of results and Contributions

As mentioned in Section 7.5.1, the study area chosen is the two metropolitan cities of India (a) Mumbai and (b) Bangalore. The first step in this study is to apply the classification model to classify the remote sensing images. The second step is to use the spatiotemporal ontology on the classified images to observe the changes. The quantitative values resulting from the landscape metrics will aid in judging the landscape pattern evolution. It is to be noted that the features used for classification using Support Tensor Machines are intra-spectral and inter-spectral features, which are detailed in Chapter 3.

The landscape metric, Area Weighted Mean Fractal Dimension, is an indicator of the shape complexity associated with the region. The range of values for this metric is from 1 to 2. When the values approach 1, the shapes have a simple perimeter, and when the values approach 2, the shapes become more complex. Fig. 7.1 presents the shape complexity associated with Mumbai and Bangalore at different temporal resolutions. From the observations in the figure, each vertical line represents the highest and lowest value associated with that region. The marker in the vertical line is an indicator of the weighted average value of the fractal dimension. The graph of Mumbai points to the following facts (a) a drastic change in the shape complexity of the city is seen between 1999–2008 (b) the period between 1988–1999 does not exhibit a radical change, only a minor variation in the fractal dimension values are noted (c) the average value of 1999–2008 lies in the lower range of vertical line, thus indicating the presence of a large number of patches with simple shapes and (d) the change in the period 2008–2017 has happened in almost all patches as the average value has risen to 1.8. Similarly, an examination of Bangalore

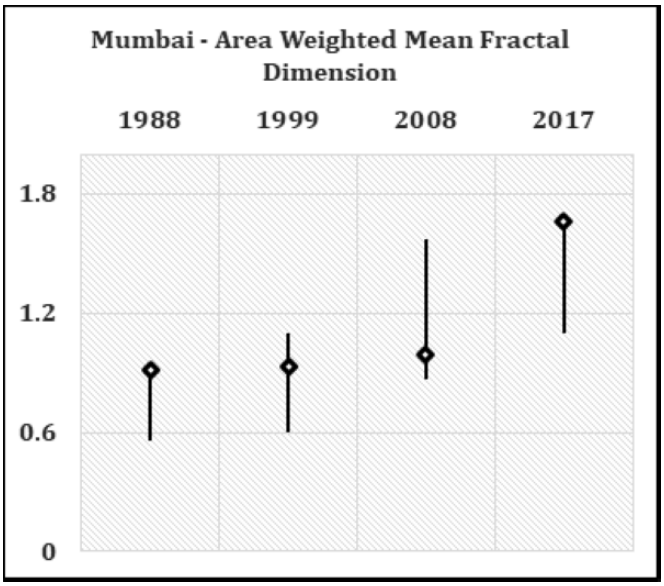

(a)

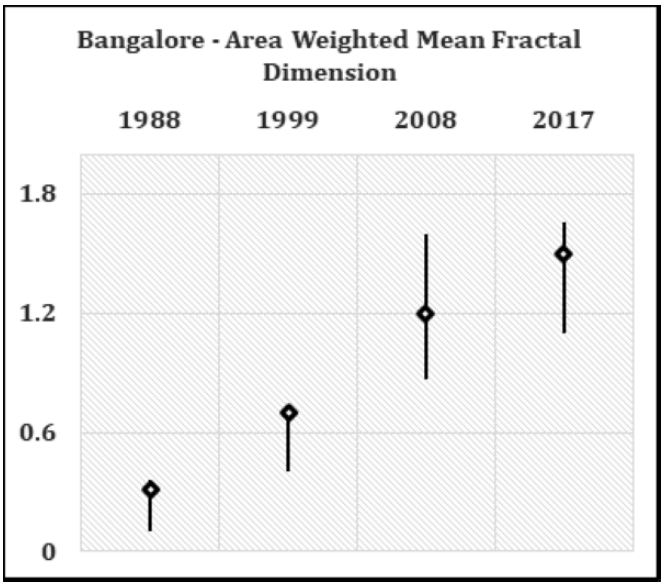

(b)

Figure 7.1: Area Weighted Mean Fractal Dimension—Shape Analysis

city points to the following notes (a) the change happened between the years 1988–1999 are appreciable as the average values in the two time ranges differ by 0.5 (b) almost all patches of Bangalore city has undergone changes in the period 1999–2008, thus indicating a mid-value average in the vertical line and (c) more regions have grown to complex shape in the time frame 2008–2017.

The morphological pattern associated with the regions of the landscape is given by the landscape metric called the contiguity index. It measures the elongation or compactness of a region, thus naming it as either strip or planar. The range of values is from 0 to 1. As the areas elongate, the value approaches zero, and as it becomes more compact, the value approaches 1. Fig. 7.2 depicts the study of the contiguity index for the two metropolitan cities. The two plots almost behave similarly, with the range of values in the same time slots is almost same, but with different averages. This leads to the conclusion that the way the structure of regions in two metropolitan cities has evolved is similar under the considered temporal resolutions.

To understand the texture composition of the region and also to understand the patch dispersion as adjacent or disjoint, the landscape metric Interspersion and Juxtaposition index comes into play. This is a relative index that indicates the level of interspersion as a percentage of maximum possible value for a given number of patch types. So the value is dependent on the number of patch types. The range of values is from 0 to 100. A higher value indicates a composition of smooth and adjacent same patch types, and as the value goes down, the texture becomes rough, and patches will be disjoint. Fig. 7.3 shows the Interspersion and Juxtaposition Index values for Mumbai and Bangalore cities.

On analysis of the indices, it is seen that for Mumbai city, considering the

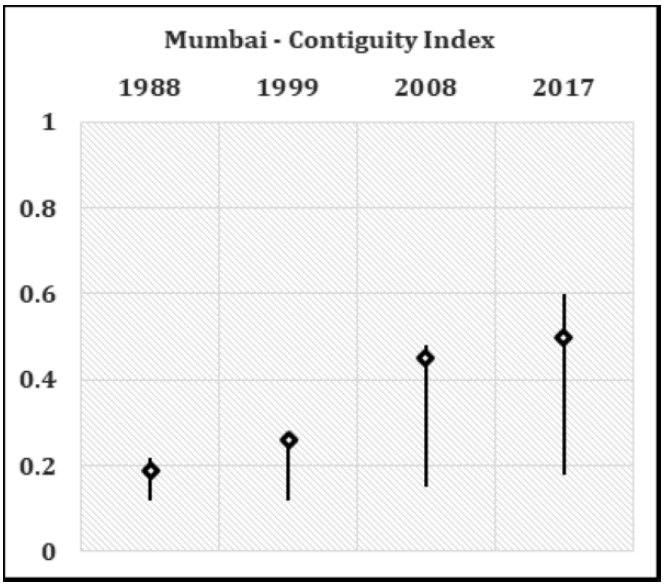

(a)

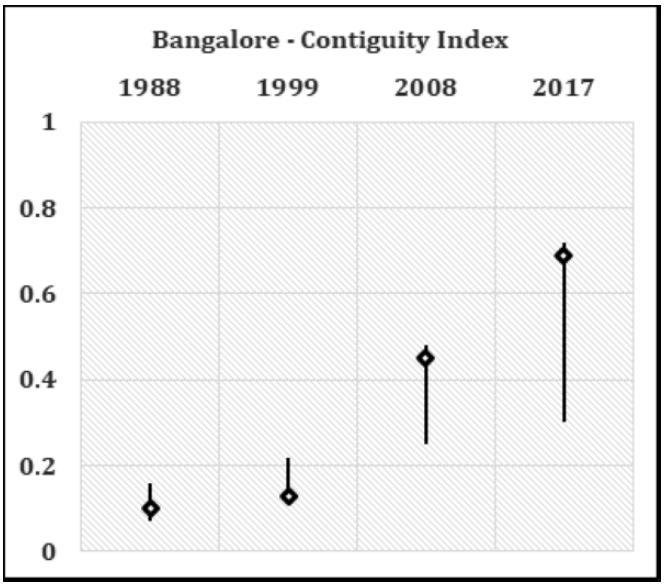

(b)

Figure 7.2: Contiguity Index—Morphological Analysis

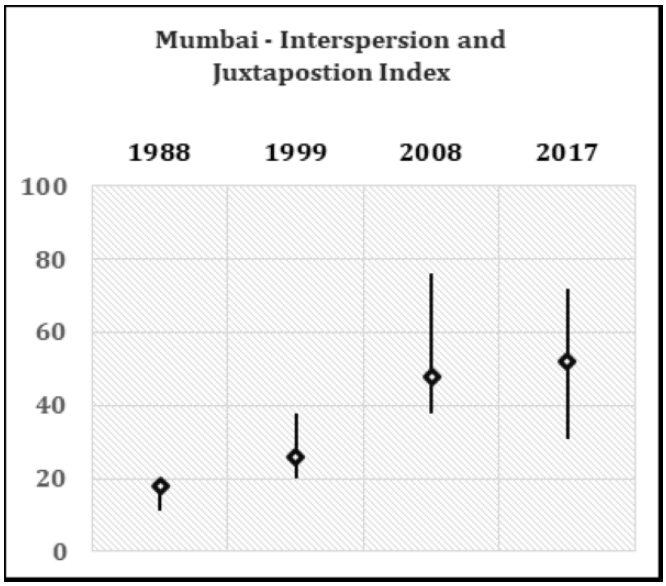

(a)

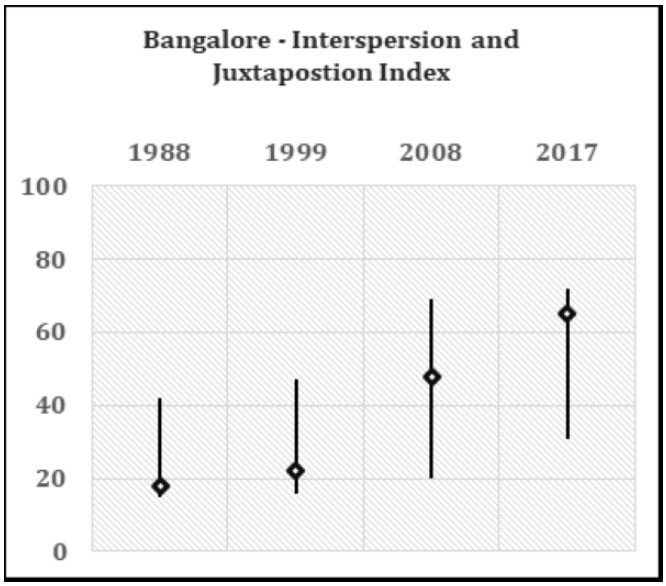

(b)

Figure 7.3: Interspersion and Juxtaposition Index–Texture Analysis

entire temporal resolution, in 2017, there is an equal number of rough and smooth patches as indicated by the average value. It has to be assumed that the urban structure contributing to this factor is equally spread in the region along with non-urban lands. Analyzing Bangalore city, the average value for the given number of patches is low in the first two temporal domains and high for the next two. This leads to the conclusion that the urban growth which has happened in 2008–2017 in Bangalore has been reflected in almost all the patches.

The three case studies reported are examples of the inferred axioms Rule #4 and Rule #5 for morphology analysis, Rule #6 and Rule #7 for shape analysis and Rule #8 for texture analysis.

From the case studies, it is evident that the spatiotemporal ontology proposed will give the opportunity to analyze the change pattern of a landscape in terms of shape, morphology, texture, and position of patches. The landscape metric values computed with the aid of ontology will help us to reach appropriate conclusions. The interpretation of the study can be summarized as follows

a. Mumbai and Bangalore city have grown tremendously in the period 1999 -2008 as evident from the landscape metrics given by the ontology.

b. Most of the regions in Bangalore city has moved to urban land, whereas in Mumbai, the development as an urban area in certain regions are more acute than others.

c. The shape patterns have grown more complex in the cities during the interval 2008 -2017, indicating urban growth at the borderlands.

d. The morphological structure of the regions in both the cities show synonymous behavior towards an elongated structure.

The analysis of this work is done using Google Earth Engine Python API.

7.6 Summary of the Chapter

The spatiotemporal ontology to understand the change pattern of the spatial region is presented in this chapter. The ontology modeled SWRL rules, which aided to understand the change which has happened to a region in terms of its class label. The inferred axioms of the ontology help to understand the changes evolved during the time of interest in terms of spatiotemporal semantics. The ontology presented can be further extended to model topological relationships between the regions, which is currently modeled only with the support of directional relationships. The ontology can also be extended to support the change analysis of a region to understand the dynamic events happening in a region like a flood, earthquake, and so on. This ontology can be used along with the model presented in the previous chapter to understand changes that have happened in a spatial region over a temporal tag.

Chapter 8

Conclusion and Future Perspectives

8.1 Conclusion **149**
8.2 Future Perspectives **153**

The thesis addressed the research problems in the field of spatiotemporal data mining. Spatiotemporal data mining, through its inherent characteristics, presented many challenges as well as opportunities, which was the basic motivation for the work in this thesis. In this chapter, a summary, which draws overall conclusions of the research work is outlined. The chapter also provides recommendation on the future perspectives.

8.1 Conclusion

The aim of the research is to design and develop algorithms for colocation pattern mining and semantic change detection through effective representation of spatiotemporal data. The thesis presented has made systematized efforts to accomplish the objectives set.

To comprehend the challenges and opportunities in the field of spatiotemporal data mining, an extensive literature review is attempted. The study included the different types of spatiotemporal data, representation methods of spatiotemporal data and the different data mining approaches. It is realized through the study and initial experiments that the tensor-based representation of spatiotemporal raster data opened up new avenues for pattern discovery. Experiments are done on remote sensing satellite images for the different representation techniques. Even though matrix representation is straight-forward, the spatial correlation information is not captured. The tensor-based representation preserves the spatial correlation and produces appreciable results in the classification task. Henceforth in the subsequent studies, the tensor representation of spatiotemporal data is adopted for the mining tasks to be performed.

From the literature review, it is observed that there is very few work in colocation pattern mining of images. The thesis is thus oriented to the colocation pattern mining problem. Colocation mining of the spatiotemporal data is attempted on the spatial as well as spatiotemporal context. The concept of tensor factorization forms the underlying principle of discovering colocation patterns. Algorithms are proposed for finding spatial and spatiotemporal colocation patterns in images, which yielded significant patterns. The algorithms proposed on the tensor-based approach for colocation pattern mining shows appreciable performance in terms of scalability and computational time, which is demonstrated by the sparse as well as dense spatiotemporal data sets. A new interestingness measure, called *spatial dominance*, is also defined in the study of spatial colocation mining. The proposed algorithm is compared with

relevant and similar work in the literature. It is observed that the algorithm finds spatial colocation patterns in less computational time. The colocation patterns mined contain patterns with more significance in terms of the containment of the number of image-objects as compared with the literature.

The success of spatial colocation mining using tensor-based approaches motivated to apply the concept to spatiotemporal colocation mining as well. An algorithm which is analogous to the earlier concept is proposed to yield spatiotemporal colocation patterns. As the component of time increases, the space to store the temporal tensors also increases. Hence, a modification to the algorithm in an incremental tensor factorization approach is also performed in this thesis. This algorithm performs the mining task based on the variance of the spatiotemporal data and stores only the variance tensor between two time periods. The incremental algorithm showed better performance in terms of convergence time when compared with the earlier approach. A new interestingness measure, called *spatiotemporal dominance*, is also defined in this study. The proposed algorithm is compared with the relevant work in literature in terms of the execution time. The execution time is analyzed in terms of two parameters (i) time slots and (ii) image-objects. It is observed that the proposed algorithms perform appreciably well when compared with the existing ones.

The spatiotemporal dominance value indicates the time prevalence the colocated pattern. This motivated to apply the above-said approach to detect changes in a landscape over a time period. Landscape metrics are modeled along with the spatiotemporal data to enhance the change detection problem with more semantics. This necessitated the need to do an elaborate and evaluative study of

the landscape metrics relevant for change detection in landscapes. The change detection algorithm proposed in this thesis discovers changes in the landscapes at different granularities of regions and time. Novel growth indices, namely, *Intra-class growth index* and *Inter-class growth index*, are defined in this study. Experimental results in detecting changes in Indian cities are quantified using growth indices and is also evaluated with the ground truth values. To formalize the studies on change detection, a spatiotemporal ontology is conceptualized. The low-level image features and the relevant landscape metrics identified for change detection forms the elements of the ontology. The study helped to understand the change pattern of the cities for a particular time period. The rules and axioms from the ontology helped to perform an assessment of the cities in terms of their morphological, texture, and shape patterns. Case studies on Indian cities (Mumbai and Bangalore) are attempted using the proposed spatiotemporal ontology. The growth patterns of the cities at different time periods are indicated by the rules and axioms from the ontology.

The research presented in this thesis has been focused on finding a representation method for spatiotemporal data. The tensor-based representation method evolved from the studies preserved the spatial relationships that exist between the entities, and are hence carried forward for the mining task. Algorithms are proposed for colocation pattern mining and change detection. The patterns mined are evaluated with the aid of new interestingness measures proposed in the thesis. The thesis also paved the way for semantic mining of patterns in spatiotemporal data. The algorithms proposed in this thesis contributes to applications like urban facility analysis, planning and management.

8.2 Future Perspectives

Tensorized representation of spatiotemporal data introduced in the studies can be carried to other application domains to find implicit patterns. More dimensions can also be introduced into the tensor data structure while incorporating multimodal data, as the proposed algorithms can accommodate the same without any changes. The possible lag in tensor factorization needs special attention. Application of convolutional functions in each mode of the tensor is promising in this direction.

In the proposed algorithms, patterns are derived from the whole set of colocation instances. Minimal set of colocation instances improve the computing speed. A technique to choose highly influential colocation instances need further investigation.

The proposed ontology can be extended to model changes for dynamic events like earthquake and flood. Features and SWRL rules specific to the events are to be incorporated into the ontology. Developing a query language for the proposed ontology is a future prospect.

The tensorized data proposed in the thesis can also be fed into new machine learning models like Support Tucker Machine, Polynomial Classifie and Higher Order Boltzmann Machiner for appropriate application. Nowadays, deep learning techniques are making footprints in the mining of spatiotemporal data like prediction [152]. This is because an accurate prediction relies on high quality features and deep learning models are powerful in feature learning. In contrast, works are still to be progressed in other areas like frequent pattern mining, change detection, and relationship mining of spatiotemporal data [153]. So it remains an open problem of how the deep learning models can

be integrated with the traditional models of frequent pattern mining for the broader application of spatiotemporal data mining tasks. The tensorization of spatiotemporal data proposed in this thesis is a stepping stone for the direct application of deep learning methodologies to the mining of spatiotemporal data.

Overall, the thesis had tried to contribute to the young field of spatiotemporal data mining and established promising avenues for work, in effervescent directions, as *"time and space are not conditions in which we live, but modes by which we think."*

Appendix A

Satellite Specifications

WorldView-2 Satellite Sensor Specifications

Launch Date	8 October 2009
Spatial Resolution	0.52 m
Orbit	705 +/- 5 km (at the equator) sun-synchronous
Orbit Inclination	98.2 +/- 0.15
Orbit Period	100 minutes
Grounding Track Repeat Cycle	1.1 days

Band # and Type	**Wavelength (μm)**	**Resolution (m)**
Band 1 Coastal	0.400 – 0.450	2
Band 2 Blue	0.450 – 0.510	2
Band 3 Green	0.510 – 0.580	2
Band 4 Yellow	0.585 – 0.625	2
Band 5 Red	0.630 – 0.690	2
Band 6 Red Edge	0.705 – 0.745	2
Band 7 Near Infrared 1	0.770 – 0.895	2
Band 8 Near Infrared 2	0.860 – 1.040	2

Landsat 7 ETM+ Satellite Sensor Specifications

Launch Date	15 April 1999
Spatial Resolution	15m Panchromatic, 30m VNIR/ SWIR
Orbit	705 +/- 5 km (at the equator) sun-synchronous
Orbit Inclination	98.2 +/- 0.15
Orbit Period	98.9 minutes
Grounding Track Repeat Cycle	16 days (233 orbits)

Band # and Type	Wavelength (μm)	Resolution (m)
Band 1 – Blue	0.45 – 0.52	30
Band 2 – Green	0.52 – 0.60	30
Band 3 – Red	0.63 – 0.69	30
Band 4 – Near Infrared	0.77 – 0.90	30
Band 5 – Shortwave Infrared 1	1.55 – 1.75	30
Band 6 – Thermal	10.40 – 12.50	60 * (30)
Band 7 - Shortwave Infrared 2	2.09 – 2.35	30
Band 8 - Panchromatic	0.52 – 0.90	15

LANDSAT 8 ETM+ Satellite Sensor Specifications

Launch Date	11 February 2013
Spatial Resolution	15 meters/30 meters/100 meters (panchromatic/multispectral/thermal)
Orbit	705 +/- 5 km (at the equator) sun-synchronous
Orbit Inclination	98.2 +/- 0.15
Orbit Period	98.9 minutes
Grounding Track Repeat Cycle	16 days (233 orbits)

Band # and Type	Wavelength (μm)	Resolution (m)
Band 1 Coastal	0.43 – 0.45	30
Band 2 Blue	0.45 – 0.51	30
Band 3 Green	0.53 – 0.59	30
Band 4 Red	0.63 – 0.67	30
Band 5 NIR	0.85 – 0.88	30
Band 6 SWIR 1	1.57 – 1.65	30
Band 7 SWIR 2	2.11 – 2.29	30
Band 8 Pan	0.50 – 0.68	15
Band 9 Cirrus	1.36 – 1.38	30
Band 10 TIRS 1	10.6 – 11.19	30 (100)
Band 11 TIRS 2	11.5 – 12.51	30 (100)

Appendix B

Landscape Metrics

Terms used in Landscape Metrics

Sl No	Terms	Explanation
1	TA	Total area in m^2
2	CA	Class area in m^2
3	N	Number of patches
4	E	Total length of edge in landscape
5	a_{ij}	Area of patch ij ('i' type 'j' number of patches) (in m^2)
6	p_{ij}	Perimeter of patch ij (in m)
7	m	Number of classes present in the landscape
8	n	Number of patches present in the landscape
9	p_i	Class i proportionate landscape
10	g_{ik}	Number of adjacencies between classes of type i and k
11	e_{ik}	Total length of edge in landscape between classes i and k
12	d_{ik}	Dissimilarity between patches i and k
13	c_{ijr}	Contiguity value for pixel r in patch ij
14	v	Sum of the values in a 3 by 3 cell template

Landscape Metrics

Sl No	Metrices	Mathematical Expression
1	Landscape Area (hectares)	$TA(\frac{1}{1000})$
2	Class Area (hectares)	$\sum_{j=1}^{n} a_{ij}(\frac{1}{1000})$
3	Mean Patch Size	$\frac{CA}{N}(\frac{1}{1000})$
4	Mean Perimeter-Area Ratio	$\frac{p_{ij}}{a_{ij}}$
5	Area Weighted Mean Fractal Dimension	$\sum_{i=j}^{m}\sum_{j=1}^{n}[(\frac{2ln(0.25p_{ij})}{lna_{ij}})(\frac{a_{ij}}{LA})]$
6	Mean Shape Index	$\frac{\sum_{i=1}^{m}\sum_{j=1}^{n}(\frac{0.25p_{ij}}{\sqrt{a_{ij}}})}{N}$
7	Contrast Weighted Edge Density	$\frac{\sum_{k=1}^{m} e_{ik}\cdot d_{ik}}{A}10000$
8	Contagion Index	$1+\frac{\sum_{i=1}^{m}\sum_{k=1}^{m}[\frac{p_i*g_{ik}}{\sum_{k=1}^{m} g_{ik}}]*[\ln\frac{p_i*g_{ik}}{\sum_{k=1}^{m} g_{ik}}]}{2\ln(m)}$ $[1+\frac{\sum_{i=1}^{m}\sum_{k=1}^{m}[\frac{p_i*g_{ik}}{\sum_{k=1}^{m} g_{ik}}]*[\ln(\frac{p_i*g_{ik}}{\sum_{k=1}^{m} g_{ik}})]}{2\ln(m)}]*100$
9	Interspersion and Juxtaposition Index	$-\frac{\sum_{i=1}^{m}\sum_{k=i+1}[(\frac{e_{ik}}{E})*\ln(\frac{e_{ik}}{E})]}{\ln(05[m(m-1)])}*100$ $-\frac{\sum_{i=1}^{m}\sum_{k=i+1}[(\frac{e_{ik}}{E})*\ln(\frac{e_{ik}}{E})]}{\ln(05[m(m-1)])}$
10	Contiguity Index	$\frac{\sum_{r=1}^{z}[\frac{c_{ijk}}{a_{ij}}]-1}{y-1}$
11	Shannon's Diversity Index	$-\frac{\sum_{i=1}^{m}(p_i)*\ln p_i}{\ln m}$
12	Shannon's Evenness Index	$-\frac{\sum_{i=1}^{m}(p_i)*\ln p_i}{\ln m}$

Appendix C

Sampled Indian Cities

Sampled Cities, ROIs, Latitude and Longitude

No.	City	ROI	Latitude	Longitude
1	Ahmedabad	Bavla	22.8928 N	72.3628 E
		Dholka	22.7428 N	72.4436 E
		Sanand	22.9913 N	72.3755 E
		Dhandhuka	23.3797 N	71.9816 E
2	Bangalore	Krishnarajapura	13.0040 N	77.6878 E
		Yeshwanthpur	13.0280 N	77.5409 E
		Nagarbhavi	12.9599 N	77.5083 E
		Banashankari	12.9255 N	77.5468 E
3	Chennai	Egmore	13.0732 N	80.2609 E
		Mylapore	13.0368 N	80.2676 E
		Mambalam	13.0387 N	80.2279 E
		Purasawalkam	13.0897 N	80.2541 E
4	Delhi	New Delhi	28.6139 N	77.2090 E
		Narela	28.8540 N	77.0918 E
		Dwaraka	28.5921 N	77.0460 E
		Daryaganj	28.6448 N	77.2404 E
5	Hyderabad	Amberpet	17.3923 N	78.5178 E
		Afzalgunj	17.3739 N	78.4702 E
		Cyberabad	17.3850 N	78.4867 E
		Masabtank	17.4037 N	78.4492 E

No.	City	ROI	Latitude	Longitude
6	Kolkata	North Parganas	22.6168 N	88.4029 E
		Hooghly	22.8963 N	88.2461 E
		Howrah	22.5958 N	88.2636 E
		South Parganas	22.1352 N	88.4016 E
7	Mumbai	Bandra	19.0607 N	72.8362 E
		Kurla	19.0600 N	72.8900 E
		Andheri	19.1363 N	72.8277 E
		Dadar	19.0213 N	72.8424 E
8	Pune	Pimpri	18.6298 N	73.7997 E
		Dapodi	18.5867 N	73.8316 E
		Bhosari	18.6385 N	73.8478 E
		Nigdi	18.6571 N	73.7659 E
9	Jaipur	Kotpuli	27.7046 N	76.2013 E
		Amber	26.9880 N	75.8610 E
		Sanganer	26.8061 N	75.7669 E
10	Lucknow	Ashiyana	26.7990 N	80.9710 E
		Aliganj	26.9041 N	80.9453 E
		Chinhat	26.8771 N	81.0400 E
11	Kanpur	Kidwai	26.4263 N	80.3276 E
		Jajmau	26.4234 N	80.4020 E
		Panki	26.4679 N	80.2473 E
12	Kochi	Ernakulam	9.9690 N	76.2910 E
		Thrikkakara	10.0327 N	76.3318 E
		Aluva	10.1075 N	76.3456 E
13	Gurgaon	Gurugram	28.4595 N	77.0266 E
		Kanahi	28.4521 N	77.0788 E
		Gurgaon Central	28.4795 N	77.0757 E
14	Varanasi	Cantt	25.3176 N	82.9739 E
		Sigra	25.3111 N	82.9864 E
		Bhelpur	25.3040 N	82.9900 E
15	Agra	KishanGarh	27.1766 N	78.0080 E
		Mohanpura	27.1713 N	78.0617 E
		Sadar Bhatti	27.1540 N	78.0146 E
16	Surat	Amber	21.1702 N	72.8311 E
		Sindhiwad	21.1855 N	72.8239 E
		Govalak	21.1596 N	72.8242 E

No.	City	ROI	Latitude	Longitude
17	Patna	Kumhrar	25.5928 N	85.1868 E
		Sheikpura	25.1417 N	85.8629 E
		Danapur	25.6207 N	85.0493 E
18	Bhopal	Govindpura	23.2472 N	77.4444 E
		Sonagiri	23.2485 N	77.4702 E
		Bhauri	23.2816 N	77.2736 E
19	Indore	Palasia	22.7244 N	75.8839 E
		South Tukoganj	22.7182 N	75.8749 E
		Chandan Nagar	22.7130 N	75.8236 E
20	Coimbatore	Puliakulam	11.0053 N	76.9917 E
		R S Puram	11.0104 N	76.9499 E
		Ukkadam	10.9902 N	76.9629 E

References

[1] Ranga Raju Vatsavai, Auroop Ganguly, Varun Chandola, Anthony Stefanidis, Scott Klasky, and Shashi Shekhar. Spatiotemporal data mining in the era of big spatial data: algorithms and applications. In *Proceedings of the 1st ACM SIGSPATIAL international workshop on analytics for big geospatial data*, pages 1–10. ACM, 2012.

[2] Shashi Shekhar, Zhe Jiang, Reem Ali, Emre Eftelioglu, Xun Tang, Venkata Gunturi, and Xun Zhou. Spatiotemporal data mining: A computational perspective. *ISPRS International Journal of Geo-Information*, 4(4):2306–2338, 2015.

[3] Nikos Mamoulis, Huiping Cao, George Kollios, Marios Hadjieleftheriou, Yufei Tao, and David W Cheung. Mining, indexing, and querying historical spatiotemporal data. In *Proceedings of the tenth ACM SIGKDD international conference on Knowledge discovery and data mining*, pages 236–245. ACM, 2004.

[4] Tammy M Thompson, Sebastian Rausch, Rebecca K Saari, and Noelle E Selin. A systems approach to evaluating the air quality co-benefits of us carbon policies. *Nature Climate Change*, 4(10):917, 2014.

[5] Pablo Samuel Castro, Daqing Zhang, and Shijian Li. Urban traffic modelling and prediction using large scale taxi gps traces. In *International Conference on Pervasive Computing*, pages 57–72. Springer, 2012.

[6] Yasuko Matsubara, Yasushi Sakurai, Willem G Van Panhuis, and Christos Faloutsos. Funnel: automatic mining of spatially coevolving epidemics. In *Proceedings of the 20th ACM SIGKDD international conference on Knowledge discovery and data mining*, pages 105–114. ACM, 2014.

[7] Gowtham Atluri, Angus MacDonald III, Kelvin O Lim, and Vipin Kumar. The brain-network paradigm: Using functional imaging data to study how the brain works. *Computer*, 49(10):65–71, 2016.

[8] Anuj Karpatne and Vipin Kumar. Big data in climate: Opportunities and challenges for machine learning. In *Proceedings of the 23rd ACM SIGKDD International Conference on Knowledge Discovery and Data Mining*, pages 21–22. ACM, 2017.

[9] Mark R Leipnik and Donald P Albert. *GIS in law enforcement: Implementation issues and case studies*. CRC Press, 2002.

[10] Gowtham Atluri, Anuj Karpatne, and Vipin Kumar. Spatio-temporal data mining: A survey of problems and methods. *ACM Computing Surveys (CSUR)*, 51(4):83, 2018.

[11] May Yuan. Use of a three-domain repesentation to enhance gis support for complex spatiotemporal queries. *Transactions in GIS*, 3(2):137–159, 1999.

[12] Alina Bialkowski, Patrick Lucey, Peter Carr, Yisong Yue, Sridha Sridharan, and Iain Matthews. Large-scale analysis of soccer matches using spatiotemporal tracking data. In *2014 IEEE International Conference on Data Mining*, pages 725–730. IEEE, 2014.

[13] Mohammad Taha Bahadori, Qi Rose Yu, and Yan Liu. Fast multivariate spatio-temporal analysis via low rank tensor learning. In *Advances in neural information processing systems*, pages 3491–3499, 2014.

[14] Dipti Verma and Rakesh Nashine. Data mining: Next generation challenges and futuredirections. *International Journal of Modeling and Optimization*, 2(5):603, 2012.

[15] Krzysztof Koperski, Junas Adhikary, and Jiawei Han. Spatial data mining: progress and challenges survey paper. In *Proc. ACM SIGMOD Workshop on Research Issues on Data Mining and Knowledge Discovery, Montreal, Canada*, pages 1–10. Citeseer, 1996.

[16] Martin Ester, Hans-Peter Kriegel, and Jörg Sander. Spatial data mining: A database approach. In *International Symposium on Spatial Databases*, pages 47–66. Springer, 1997.

[17] Donna J Peuquet and Niu Duan. An event-based spatiotemporal data model (estdm) for temporal analysis of geographical data. *International journal of geographical information systems*, 9(1):7–24, 1995.

[18] Sebastian Schutte and Karsten Donnay. Matched wake analysis: finding causal relationships in spatiotemporal event data. *Political Geography*, 41:1–10, 2014.

[19] Peter Revesz and Shasha Wu. Spatiotemporal reasoning about epidemiological data. *Artificial Intelligence in Medicine*, 38(2):157–170, 2006.

[20] Yu-Chiun Chiou and Chiang Fu. Modeling crash frequency and severity with spatiotemporal dependence. *Analytic Methods in Accident Research*, 5:43–58, 2015.

[21] Junghoon Chae, Dennis Thom, Harald Bosch, Yun Jang, Ross Maciejewski, David S Ebert, and Thomas Ertl. Spatiotemporal social media analytics for abnormal event detection and examination using seasonal-trend decomposition. In *IEEE VAST*, pages 143–152, 2012.

[22] Anthony C Gatrell, Trevor C Bailey, Peter J Diggle, and Barry S Rowlingson. Spatial point pattern analysis and its application in geographical epidemiology. *Transactions of the Institute of British geographers*, pages 256–274, 1996.

[23] Xiaolei Li, Jiawei Han, Jae-Gil Lee, and Hector Gonzalez. Traffic density-based discovery of hot routes in road networks. In *International Symposium on Spatial and Temporal Databases*, pages 441–459. Springer, 2007.

[24] Zhenni Feng and Yanmin Zhu. A survey on trajectory data mining: Techniques and applications. *IEEE Access*, 4:2056–2067, 2016.

[25] Yanchi Liu, Chuanren Liu, Nicholas Jing Yuan, Lian Duan, Yanjie Fu, Hui Xiong, Songhua Xu, and Junjie Wu. Exploiting heterogeneous human mobility patterns for intelligent bus routing. In *2014 IEEE International Conference on Data Mining*, pages 360–369. IEEE, 2014.

[26] Jian Dai, Bin Yang, Chenjuan Guo, and Zhiming Ding. Personalized route recommendation using big trajectory data. In *2015 IEEE 31st*

International Conference on Data Engineering, pages 543–554. IEEE, 2015.

[27] Anastasios Noulas, Salvatore Scellato, Neal Lathia, and Cecilia Mascolo. Mining user mobility features for next place prediction in location-based services. In *2012 IEEE 12th international conference on data mining*, pages 1038–1043. IEEE, 2012.

[28] Yingzi Wang, Nicholas Jing Yuan, Defu Lian, Linli Xu, Xing Xie, Enhong Chen, and Yong Rui. Regularity and conformity: Location prediction using heterogeneous mobility data. In *Proceedings of the 21th ACM SIGKDD International Conference on Knowledge Discovery and Data Mining*, pages 1275–1284. ACM, 2015.

[29] Siyuan Liu, Qiang Qu, and Shuhui Wang. Rationality analytics from trajectories. *ACM Transactions on Knowledge Discovery from Data (TKDD)*, 10(1):10, 2015.

[30] Huiji Gao, Jiliang Tang, Xia Hu, and Huan Liu. Modeling temporal effects of human mobile behavior on location-based social networks. In *Proceedings of the 22nd ACM international conference on Information & Knowledge Management*, pages 1673–1678. ACM, 2013.

[31] Anshul Gupta, Aurosish Mishra, Satya Gautam Vadlamudi, PP Chakrabarti, Sudeshna Sarkar, Tridib Mukherjee, and Nathan Gnanasambandam. A mobility simulation framework of humans with group behavior modeling. In *2013 IEEE 13th International Conference on Data Mining*, pages 1067–1072. IEEE, 2013.

[32] Thomas Liebig, Zhao Xu, Michael May, and Stefan Wrobel. Pedestrian quantity estimation with trajectory patterns. In *Joint European Conference on Machine Learning and Knowledge Discovery in Databases*, pages 629–643. Springer, 2012.

[33] Xuemei Liu, James Biagioni, Jakob Eriksson, Yin Wang, George Forman, and Yanmin Zhu. Mining large-scale, sparse gps traces for map inference: comparison of approaches. In *Proceedings of the 18th ACM SIGKDD international conference on Knowledge discovery and data mining*, pages 669–677. ACM, 2012.

[34] Bin Yang, Nicolas Fantini, and Christian S Jensen. ipark: Identifying parking spaces from trajectories. In *Proceedings of the 16th International Conference on Extending Database Technology*, pages 705–708. ACM, 2013.

[35] Andrzej Cichocki, Danilo Mandic, Lieven De Lathauwer, Guoxu Zhou, Qibin Zhao, Cesar Caiafa, and Huy Anh Phan. Tensor decompositions for signal processing applications: From two-way to multiway component analysis. *IEEE Signal Processing Magazine*, 32(2):145–163, 2015.

[36] Richard A Harshman et al. Foundations of the parafac procedure: Models and conditions for an" explanatory" multimodal factor analysis. 1970.

[37] Stephan Rabanser, Oleksandr Shchur, and Stephan Günnemann. Introduction to tensor decompositions and their applications in machine learning. *arXiv preprint arXiv:1711.10781*, 2017.

[38] Cyrus Shahabi, Liyue Fan, Luciano Nocera, Li Xiong, and Ming Li. Privacy-preserving inference of social relationships from location data: a vision paper. In *Proceedings of the 23rd SIGSPATIAL International Conference on Advances in Geographic Information Systems*, page 9. ACM, 2015.

[39] Banafsheh Rekabdar, Monica Nicolescu, Mircea Nicolescu, and Richard Kelley. Scale and translation invariant learning of spatio-temporal patterns using longest common subsequences and spiking neural networks. In *2015 International Joint Conference on Neural Networks (IJCNN)*, pages 1–7. IEEE, 2015.

[40] Philippe C Besse, Brendan Guillouet, Jean-Michel Loubes, and François Royer. Review and perspective for distance-based clustering of vehicle trajectories. *IEEE Transactions on Intelligent Transportation Systems*, 17(11):3306–3317, 2016.

[41] Soukaina Filali Boubrahimi, Berkay Aydin, Dustin Kempton, and Rafal Angryk. Spatio-temporal interpolation methods for solar events metadata. In *2016 IEEE International Conference on Big Data (Big Data)*, pages 3149–3157. IEEE, 2016.

[42] Nakarin Chaikaew, Nitin K Tripathi, and Marc Souris. Exploring spatial patterns and hotspots of diarrhea in chiang mai, thailand. *International Journal of Health Geographics*, 8(1):36, 2009.

[43] Jerry H Ratcliffe, Travis Taniguchi, Elizabeth R Groff, and Jennifer D Wood. The philadelphia foot patrol experiment: A randomized controlled

trial of police patrol effectiveness in violent crime hotspots. *Criminology*, 49(3):795–831, 2011.

[44] Timo Reuter, Symeon Papadopoulos, Giorgos Petkos, Vasileios Mezaris, Yiannis Kompatsiaris, Philipp Cimiano, Christopher de Vries, and Shlomo Geva. Social event detection at mediaeval 2013: Challenges, datasets, and evaluation. In *Proceedings of the MediaEval 2013 Multimedia Benchmark Workshop Barcelona, Spain, October 18-19*, 2013.

[45] Martin Kulldorff. A spatial scan statistic. *Communications in Statistics-Theory and methods*, 26(6):1481–1496, 1997.

[46] Emre Eftelioglu, Shashi Shekhar, Dev Oliver, Xun Zhou, Michael R Evans, Yiqun Xie, James M Kang, Renee Laubscher, and Christopher Farah. Ring-shaped hotspot detection: a summary of results. In *2014 IEEE International Conference on Data Mining*, pages 815–820. IEEE, 2014.

[47] Hamed Abdelhaq, Christian Sengstock, and Michael Gertz. Eventweet: Online localized event detection from twitter. *Proceedings of the VLDB Endowment*, 6(12):1326–1329, 2013.

[48] Yan-Tao Zheng, Zheng-Jun Zha, and Tat-Seng Chua. Mining travel patterns from geotagged photos. *ACM Transactions on Intelligent Systems and Technology (TIST)*, 3(3):56, 2012.

[49] Guangnan Zhang, Kelvin KW Yau, Xun Zhang, and Yanyan Li. Traffic accidents involving fatigue driving and their extent of casualties. *Accident Analysis & Prevention*, 87:34–42, 2016.

[50] Derya Birant and Alp Kut. St-dbscan: An algorithm for clustering spatial–temporal data. *Data & Knowledge Engineering*, 60(1):208–221, 2007.

[51] Guan Yuan, Penghui Sun, Jie Zhao, Daxing Li, and Canwei Wang. A review of moving object trajectory clustering algorithms. *Artificial Intelligence Review*, 47(1):123–144, 2017.

[52] Panos Kalnis, Nikos Mamoulis, and Spiridon Bakiras. On discovering moving clusters in spatio-temporal data. In *International Symposium on Spatial and Temporal Databases*, pages 364–381. Springer, 2005.

[53] Jacqueline K Faherty, John J Bochanski, Jonathan Gagné, Olivia Nelson, Kristina Coker, Iliya Smithka, Deion Desir, and Chelsea Vasquez. New and known moving groups and clusters identified in a gaia comoving catalog. *The Astrophysical Journal*, 863(1):91, 2018.

[54] Chloe Bracis, Keith L Bildstein, and Thomas Mueller. Revisitation analysis uncovers spatio-temporal patterns in animal movement data. *Ecography*, 41(11):1801–1811, 2018.

[55] Dongkuan Xu and Yingjie Tian. A comprehensive survey of clustering algorithms. *Annals of Data Science*, 2(2):165–193, 2015.

[56] Xiao Liu, Nanyin Zhang, Catie Chang, and Jeff H Duyn. Co-activation patterns in resting-state fmri signals. *NeuroImage*, 180:485–494, 2018.

[57] Dingxiong Deng, Cyrus Shahabi, Ugur Demiryurek, Linhong Zhu, Rose Yu, and Yan Liu. Latent space model for road networks to predict time-varying traffic. In *Proceedings of the 22nd ACM SIGKDD International Conference on Knowledge Discovery and Data Mining*, pages 1525–1534. ACM, 2016.

[58] YoungJoon Yoo, Kimin Yun, Sangdoo Yun, JongHee Hong, Hawook Jeong, and Jin Young Choi. Visual path prediction in complex scenes with crowded moving objects. In *Proceedings of the IEEE Conference on Computer Vision and Pattern Recognition*, pages 2668–2677, 2016.

[59] RA Gill, RH Kelly, WJ Parton, KA Day, RB Jackson, JA Morgan, JMO Scurlock, LL Tieszen, J Vande Castle, DS Ojima, et al. Using simple environmental variables to estimate below-ground productivity in grasslands. *Global ecology and biogeography*, 11(1):79–86, 2002.

[60] Zhiqiang Du, Linghu Bin, Feng Ling, Wenbo Li, Weidong Tian, Hailei Wang, Yuanmiao Gui, Bingyu Sun, and Xiaoming Zhang. Estimating surface water area changes using time-series landsat data in the qingjiang river basin, china. *Journal of Applied Remote Sensing*, 6(1):063609, 2012.

[61] Zhuoning Yuan, Xun Zhou, and Tianbao Yang. Hetero-convlstm: A deep learning approach to traffic accident prediction on heterogeneous spatio-temporal data. In *Proceedings of the 24th ACM SIGKDD International Conference on Knowledge Discovery & Data Mining*, pages 984–992. ACM, 2018.

[62] Yisheng Lv, Yanjie Duan, Wenwen Kang, Zhengxi Li, and Fei-Yue Wang. Traffic flow prediction with big data: a deep learning approach. *IEEE Transactions on Intelligent Transportation Systems*, 16(2):865–873, 2014.

[63] Zhidan Liu, Zhenjiang Li, Kaishun Wu, and Mo Li. Urban traffic prediction from mobility data using deep learning. *IEEE Network*, 32(4):40–46, 2018.

[64] Ridha Soua, Arief Koesdwiady, and Fakhri Karray. Big-data-generated traffic flow prediction using deep learning and dempster-shafer theory. In *2016 International joint conference on neural networks (IJCNN)*, pages 3195–3202. IEEE, 2016.

[65] Yan Huang, Shashi Shekhar, and Hui Xiong. Discovering colocation patterns from spatial data sets: a general approach. *IEEE transactions on knowledge & data engineering*, (12):1472–1485, 2004.

[66] Karthik Ganesan Pillai, Rafal A Angryk, and Berkay Aydin. A filter-and-refine approach to mine spatiotemporal co-occurrences. In *Proceedings of the 21st ACM SIGSPATIAL International Conference on Advances in Geographic Information Systems*, pages 104–113. ACM, 2013.

[67] Huiping Cao, Nikos Mamoulis, and David W Cheung. Mining frequent spatio-temporal sequential patterns. In *Fifth IEEE International Conference on Data Mining (ICDM'05)*, pages 8–pp. IEEE, 2005.

[68] Yan Huang, Liqin Zhang, and Pusheng Zhang. A framework for mining sequential patterns from spatio-temporal event data sets. *IEEE Transactions on Knowledge and data engineering*, 20(4):433–448, 2008.

[69] Florian Verhein. k-stars: Sequences of spatio-temporal association rules. In *Sixth IEEE International Conference on Data Mining-Workshops (ICDMW'06)*, pages 387–394. IEEE, 2006.

[70] Jaewon Yang and Jure Leskovec. Structure and overlaps of communities in networks. *arXiv preprint arXiv:1205.6228*, 2012.

[71] Jaewon Yang and Jure Leskovec. Defining and evaluating network communities based on ground-truth. *Knowledge and Information Systems*, 42(1):181–213, 2015.

[72] Manish Gupta, Jing Gao, Charu C Aggarwal, and Jiawei Han. Outlier detection for temporal data: A survey. *IEEE Transactions on Knowledge and Data Engineering*, 26(9):2250–2267, 2013.

[73] C-T Lu, Dechang Chen, and Yufeng Kou. Algorithms for spatial outlier detection. In *Third IEEE International Conference on Data Mining*, pages 597–600. IEEE, 2003.

[74] Charu C Aggarwal. An introduction to outlier analysis. In *Outlier analysis*, pages 1–34. Springer, 2017.

[75] Yingyi Bu, Lei Chen, Ada Wai-Chee Fu, and Dawei Liu. Efficient anomaly monitoring over moving object trajectory streams. In *Proceedings of the 15th ACM SIGKDD international conference on Knowledge discovery and data mining*, pages 159–168. ACM, 2009.

[76] Wei Liu, Yu Zheng, Sanjay Chawla, Jing Yuan, and Xie Xing. Discovering spatio-temporal causal interactions in traffic data streams. In *Proceedings of the 17th ACM SIGKDD international conference on Knowledge discovery and data mining*, pages 1010–1018. ACM, 2011.

[77] Elizabeth Wu, Wei Liu, and Sanjay Chawla. Spatio-temporal outlier detection in precipitation data. In *International Workshop on Knowledge Discovery from Sensor Data*, pages 115–133. Springer, 2008.

[78] James H Faghmous, Muhammed Uluyol, Luke Styles, Matthew Le, Varun Mithal, Shyam Boriah, and Vipin Kumar. Multiple hypothesis object tracking for unsupervised self-learning: An ocean eddy tracking application. In *Twenty-Seventh AAAI Conference on Artificial Intelligence*, 2013.

[79] Dan Xu, Rui Song, Xinyu Wu, Nannan Li, Wei Feng, and Huihuan Qian. Video anomaly detection based on a hierarchical activity discovery within spatio-temporal contexts. *Neurocomputing*, 143:144–152, 2014.

[80] Theodoros Lappas, Marcos R Vieira, Dimitrios Gunopulos, and Vassilis J Tsotras. On the spatiotemporal burstiness of terms. *Proceedings of the VLDB Endowment*, 5(9):836–847, 2012.

[81] Hamed Abdelhaq, Michael Gertz, and Christian Sengstock. Spatio-temporal characteristics of bursty words in twitter streams. In *Proceedings of the 21st ACM SIGSPATIAL international conference on advances in geographic information systems*, pages 194–203. ACM, 2013.

[82] Xun Zhou, Shashi Shekhar, Pradeep Mohan, Stefan Liess, and Peter K Snyder. Discovering interesting sub-paths in spatiotemporal datasets: A summary of results. In *Proceedings of the 19th ACM SIGSPATIAL international conference on advances in geographic information systems*, pages 44–53. ACM, 2011.

[83] Xun Zhou, Shashi Shekhar, and Reem Y Ali. Spatiotemporal change footprint pattern discovery: an inter-disciplinary survey. *Wiley Interdisciplinary Reviews: Data Mining and Knowledge Discovery*, 4(1):1–23, 2014.

[84] NA Quarmby and JL Cushnie. Monitoring urban land cover changes at the urban fringe from spot hrv imagery in south-east england. *International Journal of Remote Sensing*, 10(6):953–963, 1989.

[85] Philip J Howarth and Gregory M Wickware. Procedures for change detection using landsat digital data. *International Journal of Remote Sensing*, 2(3):277–291, 1981.

[86] Aaron Kim Ludeke, Robert C Maggio, and Leslie M Reid. An analysis of anthropogenic deforestation using logistic regression and gis. *Journal of Environmental Management*, 31(3):247–259, 1990.

[87] Emily Hoffhine Wilson and Steven A Sader. Detection of forest harvest type using multiple dates of landsat tm imagery. *Remote Sensing of Environment*, 80(3):385–396, 2002.

[88] R D Johnson and ES Kasischke. Change vector analysis: A technique for the multispectral monitoring of land cover and condition. *International Journal of Remote Sensing*, 19(3):411–426, 1998.

[89] Ofer Miller, Arie Pikaz, and Amir Averbuch. Objects based change detection in a pair of gray-level images. *Pattern Recognition*, 38(11):1976–1992, 2005.

[90] Irmgard Niemeyer, Prashanth Reddy Marpu, and Sven Nussbaum. Change detection using object features. In *Object-Based Image Analysis*, pages 185–201. Springer, 2008.

[91] Baudouin Desclée, Patrick Bogaert, and Pierre Defourny. Forest change detection by statistical object-based method. *Remote Sensing of Environment*, 102(1-2):1–11, 2006.

[92] Gregory Duveiller, Pierre Defourny, Baudouin Desclée, and P Mayaux. Deforestation in central africa: Estimates at regional, national and landscape levels by advanced processing of systematically-distributed landsat extracts. *Remote sensing of environment*, 112(5):1969–1981, 2008.

[93] Masroor Hussain, Dongmei Chen, Angela Cheng, Hui Wei, and David Stanley. Change detection from remotely sensed images: From pixel-based to object-based approaches. *ISPRS Journal of photogrammetry and remote sensing*, 80:91–106, 2013.

[94] Herbert Bay, Tinne Tuytelaars, and Luc Van Gool. Surf: Speeded up robust features. In *European conference on computer vision*, pages 404–417. Springer, 2006.

[95] Clement Farabet, Camille Couprie, Laurent Najman, and Yann LeCun. Learning hierarchical features for scene labeling. *IEEE transactions on pattern analysis and machine intelligence*, 35(8):1915–1929, 2012.

[96] Georgy L. Gimel'farb. Texture modeling by multiple pairwise pixel interactions. *IEEE Transactions on pattern analysis and machine intelligence*, 18(11):1110–1114, 1996.

[97] Juliang Shao and Wolfgang Foerstner. Gabor wavelets for texture edge extraction. In *ISPRS Commission III Symposium: Spatial Information from Digital Photogrammetry and Computer Vision*, volume 2357, pages 745–752. International Society for Optics and Photonics, 1994.

[98] Paolo Gamba, Fabio DellAcqua, Mattia Stasolla, Giovanna Trianni, Gianni Lisini, and X Yang. Limits and challenges of optical high-resolution satellite remote sensing for urban applications. *Urban remote sensing: Monitoring, synthesis and modeling in the urban environment*, pages 36–47, 2011.

[99] Qian Du. Modified fisher's linear discriminant analysis for hyperspectral imagery. *IEEE geoscience and remote sensing letters*, 4(4):503–507, 2007.

[100] DF Frey and RA Pimentel. Principal component analysis and factor analysis. 1978.

[101] Sibt Ul Hussain and William Triggs. Feature sets and dimensionality reduction for visual object detection. 2010.

[102] Yousef Rezaei, Mohammad Reza Mobasheri, MJ Valaddan Zoej, and Michael E Schaepman. Endmember extraction using a combination of orthogonal projection and genetic algorithm. *IEEE Geoscience and Remote Sensing Letters*, 9(2):161–165, 2011.

[103] Antonio Plaza, Pablo Martínez, Rosa Pérez, and Javier Plaza. Spatial/spectral endmember extraction by multidimensional morphological operations. *IEEE transactions on geoscience and remote sensing*, 40(9):2025–2041, 2002.

[104] Antonio Plaza, Pablo Martínez, Rosa Pérez, and Javier Plaza. A quantitative and comparative analysis of endmember extraction algorithms from hyperspectral data. *IEEE transactions on geoscience and remote sensing*, 42(3):650–663, 2004.

[105] Dengsheng Lu and Qihao Weng. A survey of image classification methods and techniques for improving classification performance. *International journal of Remote sensing*, 28(5):823–870, 2007.

[106] Piotr Dollár, Zhuowen Tu, Pietro Perona, and Serge Belongie. Integral channel features. 2009.

[107] Björn Fröhlich, Eric Bach, Irene Walde, Sören Hese, Christiane Schmullius, and Joachim Denzler. Land cover classification of satellite images using contextual information. *ISPRS Annals of the*

Photogrammetry, Remote Sensing and Spatial Information Sciences, 3(W1), 2013.

[108] http://data.satapps.org/dataset/worldview-2 Accessed on - 15 January 2014.

[109] Piotr Tokarczyk, Jan Dirk Wegner, Stefan Walk, and Konrad Schindler. Features, color spaces, and boosting: New insights on semantic classification of remote sensing images. *IEEE Transactions on Geoscience and Remote Sensing*, 53(1):280–295, 2014.

[110] Krzysztof Koperski and Jiawei Han. Discovery of spatial association rules in geographic information databases. In *International Symposium on Spatial Databases*, pages 47–66. Springer, 1995.

[111] Yasuhiko Morimoto. Mining frequent neighboring class sets in spatial databases. In *Proceedings of the seventh ACM SIGKDD international conference on Knowledge discovery and data mining*, pages 353–358. ACM, 2001.

[112] Shashi Shekhar and Yan Huang. Co-location rules mining: A summary of results. In *Proc. Spatio-temporal Symposium on Databases*, 2001.

[113] Rakesh Agrawal, Ramakrishnan Srikant, et al. Fast algorithms for mining association rules. In *Proc. 20th int. conf. very large data bases, VLDB*, volume 1215, pages 487–499, 1994.

[114] Jin Soung Yoo, Shashi Shekhar, John Smith, and Julius P Kumquat. A partial join approach for mining co-location patterns. In *Proceedings of*

the 12th annual ACM international workshop on Geographic information systems, pages 241–249. ACM, 2004.

[115] Jin Soung Yoo, Shashi Shekhar, and Mete Celik. A join-less approach for co-location pattern mining: A summary of results. In *Fifth IEEE International Conference on Data Mining (ICDM'05)*, pages 4–pp. IEEE, 2005.

[116] Seung Kwan Kim, Jee Hyung Lee, Keun Ho Ryu, and Ungmo Kim. A framework of spatial co-location pattern mining for ubiquitous gis. *Multimedia tools and applications*, 71(1):199–218, 2014.

[117] Bozhong Liu, Ling Chen, Chunyang Liu, Chengqi Zhang, and Weidong Qiu. Rcp mining: towards the summarization of spatial co-location patterns. In *International Symposium on Spatial and Temporal Databases*, pages 451–469. Springer, 2015.

[118] Xiaojing Yao, Ling Peng, Liang Yang, and Tianhe Chi. A fast space-saving algorithm for maximal co-location pattern mining. *Expert Systems with Applications*, 63:310–323, 2016.

[119] Roozbeh Mottaghi, Xianjie Chen, Xiaobai Liu, Nam-Gyu Cho, Seong-Whan Lee, Sanja Fidler, Raquel Urtasun, and Alan Yuille. The role of context for object detection and semantic segmentation in the wild. In *Proceedings of the IEEE Conference on Computer Vision and Pattern Recognition*, pages 891–898, 2014.

[120] Antonio Torralba, Kevin P Murphy, William T Freeman, et al. Sharing features: efficient boosting procedures for multiclass object detection. *CVPR (2)*, 3, 2004.

[121] Pauli Miettinen. Boolean tensor factorizations. In *2011 IEEE 11th International Conference on Data Mining*, pages 447–456. IEEE, 2011.

[122] Mete Celik, Shashi Shekhar, James P Rogers, and James A Shine. Mixed-drove spatiotemporal co-occurrence pattern mining. *IEEE Transactions on Knowledge and Data Engineering*, 20(10):1322–1335, 2008.

[123] Mete Celik. Partial spatio-temporal co-occurrence pattern mining. *Knowledge and Information Systems*, 44(1):27–49, 2015.

[124] Karthik Ganesan Pillai, Rafal A Angryk, Juan M Banda, Tim Wylie, and Michael A Schuh. Spatiotemporal co-occurrence rules. In *New Trends in Databases and Information Systems*, pages 27–35. Springer, 2014.

[125] Karthik Ganesan Pillai, Rafal A Angryk, Juan M Banda, Dustin Kempton, Berkay Aydin, and Petrus C Martens. Mining at most top-k% spatiotemporal co-occurrence patterns in datasets with extended spatial representations. *ACM Transactions on Spatial Algorithms and Systems (TSAS)*, 2(3):10, 2016.

[126] Berkay Aydin and Rafal A Angryk. Spatiotemporal event sequence mining from evolving regions. In *2016 23rd International Conference on Pattern Recognition (ICPR)*, pages 4172–4177. IEEE, 2016.

[127] https://tev-static.fbk.eu/DATABASES/objects.html Accessed on - 16 February 2016.

[128] Source—"Kochi" 9.9312^o N, 76.2673^o E GOOGLE EARTH, First and last day of all months from 2011 to 2016, December 18, 2017.

[129] Evelin Uuemaa, Marc Antrop, Jüri Roosaare, Riho Marja, and Ülo Mander. Landscape metrics and indices: an overview of their use in landscape research. *Living reviews in landscape research*, 3(1):1–28, 2009.

[130] Landsat on EarthExplorer, https://landsat.gsfc.nasa.gov Accessed on - 20 December 2016.

[131] Landsat on AWS s3://landsat-pds/c1/l8/139/ Accessed on - 18 January 2017.

[132] Kevin McGarigal and Barbara J Marks. Fragstats: spatial pattern analysis program for quantifying landscape structure. *Gen. Tech. Rep. PNW-GTR-351. Portland, OR: US Department of Agriculture, Forest Service, Pacific Northwest Research Station. 122 p*, 351, 1995.

[133] Stefan Lang, Ulrich Walz, Hermann Klug, Thomas Blaschke, and Ralf-Uwe Syrbe. Landscape metrics–a toolbox for assessing past, present and future landscape structures. *Geoinformation technologies for geocultural landscapes: European perspectives*, 207:207, 2008.

[134] A Benito-Calvo, A Pérez-González, O Magri, and P Meza. Assessing regional geodiversity: the iberian peninsula. *Earth surface processes and landforms*, 34(10):1433–1445, 2009.

[135] Mohammad N Alhamad, Mohammad A Alrababah, Rusty A Feagin, and Anne Gharaibeh. Mediterranean drylands: The effect of grain size and domain of scale on landscape metrics. *Ecological Indicators*, 11(2):611–621, 2011.

[136] Belinda Gallardo, Stéphanie Gascón, Xavier Quintana, and Franciso A Comín. How to choose a biodiversity indicator–redundancy and complementarity of biodiversity metrics in a freshwater ecosystem. *Ecological indicators*, 11(5):1177–1184, 2011.

[137] Evelin Uuemaa, Marc Antrop, Jüri Roosaare, Riho Marja, and Ülo Mander. Landscape metrics and indices: an overview of their use in landscape research. *Living reviews in landscape research*, 3(1):1–28, 2009.

[138] Chao Fan and Soe Myint. A comparison of spatial autocorrelation indices and landscape metrics in measuring urban landscape fragmentation. *Landscape and Urban Planning*, 121:117–128, 2014.

[139] Min Liu, Zhi-Ming Zhang, Ming-Yu Yang, Yu-Peng Geng, Xiao-Kun Ou, and Ding Song. Analysis of urban public greenspace pattern based on landscape metrics in kunming. In *Civil Engineering and Urban Planning IV: Proceedings of the 4th International Conference on Civil Engineering and Urban Planning, Beijing, China, 25-27 July 2015*, page 127. CRC Press, 2016.

[140] Yu Peng, Kai Mi, Fengting Qing, and Dayuan Xue. Identification of the main factors determining landscape metrics in semi-arid agro-pastoral ecotone. *Journal of Arid Environments*, 124:249–256, 2016.

[141] Hannes Taubenböck, Martin Wegmann, Christian Berger, Markus Breunig, Achim Roth, and Harald Mehl. Spatiotemporal analysis of indian megacities. *Proceedings of the international archives of the photogrammetry, remote sensing and spatial information sciences*, 10(Part B):75–82, 2008.

[142] Harini Nagendra, Suparsh Nagendran, Somajita Paul, and Sajid Pareeth. Graying, greening and fragmentation in the rapidly expanding indian city of bangalore. *Landscape and Urban Planning*, 105(4):400–406, 2012.

[143] Oleksandr Kit and Matthias Lüdeke. Automated detection of slum area change in hyderabad, india using multitemporal satellite imagery. *ISPRS journal of photogrammetry and remote sensing*, 83:130–137, 2013.

[144] Hannes Taubenböck, Martin Wegmann, Achim Roth, Harald Mehl, and Stefan Dech. Urbanization in india–spatiotemporal analysis using remote sensing data. *Computers, environment and urban systems*, 33(3):179–188, 2009.

[145] TV Ramachandra, HA Bharath, S Vinay, NV Joshi, Uttam Kumar, and K Venugopal Rao. Modelling urban revolution in greater bangalore, india. In *30th Annual In-House Symposium on Space Science and Technology, ISRO-IISc Space Technology Cell, Indian Institute of Science, Bangalore*, pages 7–8, 2013.

[146] http: //finmin.nic.in. Ministry of Finance , Government of India.Accessed on - 12 June 2016.

[147] Robert I Lerman and Shlomo Yitzhaki. A note on the calculation and interpretation of the gini index. *Economics Letters*, 15(3-4):363–368, 1984.

[148] https://smartnet.niua.org/content/ce67d809-eac2-4a2e-a487-f3cec9c097db. Accessed on - 2 February 2018.

[149] Deborah L McGuinness, Frank Van Harmelen, et al. Owl web ontology language overview. *W3C recommendation*, 10(10):2004, 2004.

[150] Sotiris Batsakis and Euripides GM Petrakis. Sowl: spatio-temporal representation, reasoning and querying over the semantic web. In *Proceedings of the 6th international conference on semantic systems*, page 15. ACM, 2010.

[151] Kuldeep R Kurte and Surya S Durbha. Spatio-temporal ontology for change analysis of flood affected areas using remote sensing images. In *JOWO@ FOIS*, 2016.

[152] Bowen Du, Hao Peng, Senzhang Wang, Md Zakirul Alam Bhuiyan, Lihong Wang, Qiran Gong, Lin Liu, and Jing Li. Deep irregular convolutional residual lstm for urban traffic passenger flows prediction. *IEEE Transactions on Intelligent Transportation Systems*, 2019.

[153] Senzhang Wang, Jiannong Cao, and Philip S Yu. Deep learning for spatio-temporal data mining: A survey. *arXiv preprint arXiv:1906.04928*, 2019.

Index

Aggregation Metrics, 101
Anomaly Detection, 29
Area Metrics, 100
Area Weighted Mean Fractal Dimension, 101
Axioms, 139

Boolean Tensor Factorization, 77

Change Detection, 30
Class Area, 100
Clustering, 25
Contagion Index, 101
Contiguity Index, 101
Contrast Metrics, 102
Contrast Weighted Edge Density, 101

Diversity Metrics, 102

Edge Metrics, 100
Event Data, 15

FRAGSTATS, 104
Frequent Pattern Mining, 28

Image-Object Tensorization, 60
Image-object, 53
Inter-Class Growth Index, 118
Inter-spectral Features, 35, 40
Interspersion and Juxtaposition Index, 101
Intra-Class Growth Index, 118
Intra-spectral Features, 35, 39

Landscape Metrics, 100

Mean Patch Size, 100
Mean Perimeter-Area Ratio, 101
Mean Shape Index, 101
Metric of Interest, 115

Patch Density, 101
Point Reference Data, 17
Predictive Learning, 27

Raster Data, 17
Region of Interest, 113

Shannon's Diversity Index, 102
Shannon's Evenness Index, 102
Shape Metrics, 101
Spatial Colocation, 50
Spatial Dominance, 62
Spatial Pattern Discovery, 56
Spatiotemporal Data, 13
Spatiotemporal Dominance, 80
Spatiotemporal Ontology, 136
Splitting Index, 102
STM-Miner, 117
SWRL Rule, 139

Tensor Factorization, 22
Tensors, 21
Time of Interest, 113
Trajectory Data, 16